5-3-2008

Effect of phosphorous poisoning on catalytic cracking of lipids for green diesel production

Stephen Thomas Dufreche

EFFECT OF PHOSPHOROUS POISONING ON CATALYTIC CRACKING OF LIPIDS FOR GREEN DIESEL PRODUCTION

By

Stephen Thomas Dufreche

A Dissertation
Submitted to the Faculty of
Mississippi State University
in Partial Fulfillment of the Requirements
for the Degree of Doctor of Philosophy in Engineering
in the Dave C. Swalm School of Chemical Engineering

Mississippi State, Mississippi

May 2008

Name: Stephen Thomas Dufreche

Date of Degree: May 2, 2008

Institution: Mississippi State University

Major Field: Chemical Engineering

Major Professor: Dr. Rafael Hernandez

Title of Study: EFFECT OF PHOSPHOROUS POISONING ON CATALYTIC CRACKING OF LIPIDS FOR GREEN DIESEL PRODUCTION

Pages in Study: 131

Candidate for Degree of Doctor of Philosophy

Biodiesel is one of the most widely used biofuels in the world, due in part to its simplicity of production, compatibility with existing engines, and reduction of green house gas emissions. However, technical difficulties with biodiesel include: (1) the need of highly refined oil for ASTM compliance, (2) incompatibility with the petroleum-diesel pipeline distribution system, and (3) a relatively small inventory of expensive feedstocks. Issues (1) and (2) could be overcome by the production of biofuels using chemical processes associated with petroleum refining. Catalytic lipid cracking could result in green diesel, a fuel chemically similar to conventional diesel but derived from a clean renewable feedstock.

The impact of phosphorus poisoning on catalytic cracking of lipids has been studied in this work using both homogeneous and heterogeneous catalysts. Catalytic cracking of model lipids was shown to occur in a homogeneous liquid phase with triflic acid, a superacid 100 times more acidic than sulfuric acid. Products obtained from the reaction were heavily oxygenated and generally unsuitable for fuel use, suggesting the

need for heterogeneous catalytic cracking. Reaction kinetics show a high linear dependence on Brönsted system acidity, with an overall reaction order of 3.

The affect of phosphorus on heterogeneous acid cracking was then studied. Since lipid feedstocks contain small amounts of phospholipids knowledge of the interactions between phospholipids and zeolites is crucial to a system-wide understanding of the lipid cracking process. Phosphorus-containing compounds were used to poison ZSM-5 (a solid zeolite catalyst) in order to simulate the cracking of phospholipids. Model compounds were then cracked over the poisoned zeolite, with differences in product distribution and kinetics based on phosphorus loading recorded. It was shown that phosphorous has a dramatic effect on both conversion and product distribution of cracking reactions. It is believed that phosphorous binds irreversibly to heterogeneous active sites, causing the majority of deactivation.

To address the issue of limited feedstock availability, research was also undertaken to find new lipids sources for biofuel use. It was determined that lipids extracted from microorganisms grown in a municipal wastewater treatment system could be suitable. However, any phosphorous must be removed before catalytic cracking of the extracted lipids.

DEDICATION

I would like to dedicate this research to my wife, Jasmine Dufreche. Her support throughout the years has enabled me to achieve more than I ever thought possible. I would also like to dedicate this to my parents, for encouraging my curiosity and learning from an early age.

ACKNOWLEDGEMENTS

The author would like to expresses his gratitude to the many people who gave their assistance on this project. Without their help this would not be possible. My first thanks go to Dr. Rafael Hernandez, for allowing me to continue my studies under his direction. His guidance was instrumental in the completion of my studies. Thanks are also due to Dr. Mark White, whose knowledge of catalytic systems was critical to the success of my research. Appreciation is also due to my other committee members, namely Dr. Todd French, Dr. Hossein Toghiani, Dr. Priscilla Hill, and Dr. Mark Zappi, for the aid and direction provided by their experience. The author would also like to recognize William Holmes for his technical expertise and guidance on analytical systems throughout his research. Coworkers Dr. Tracy Benson and Dr. Darrell Sparks also contributed greatly to this body of work.

TABLE OF CONTENTS

LIST OF TABLES

LIST OF FIGURES

CHAPTER I

INTRODUCTION

Throughout much of recorded history, renewable fuels were the major source of energy for the civilized and non-civilized worlds. Feedstocks such as wood, animal lipids, and various plant oils sustained man up until the mid-19th century [1]. At this time, the availability of cheap, plentiful fossil fuels began the decline of renewable energy. Recently, however, the production and consumption of renewable fuels has begun to increase, driven by rising costs and perceived scarcity of fossil fuels as well as a growing environmental movement [1]. Today, the renewables market contains fuels made from plant and animal sources. These biofuels are at the heart of a movement to displace and eventually replace petroleum sources.

1.1 Currently Available Biofuels

The United States currently uses over 20 million barrels of oil per day, 60% of which is imported [2]. As of October 15, 2007, oil was listed at $83 per barrel [3]. While a small percentage of the total volume goes to production of plastics and assorted materials the majority is appropriated to fuels. Within the category of transportation over 97% of energy used comes from fossil fuels [2]. In 2006 the U.S. used over 64 billion

gallons of petroleum diesel fuel and 142 billion gallons of gasoline, making the transportation sector the largest consumer of petroleum [4,5]. There are several biologically-based fuels that are currently being developed as an alternative to petroleum. These bio-fuels are clean burning, renewable, and can be produced locally to reduce dependence on foreign imports.

Some of the more common bio-fuels are ethanol, biodiesel, biogas, and hydrogen. These fuels all reduce the total amount of emissions released by internal combustion engines. The common theme is a reduction in compounds such as sulfur oxides (SO_X), carbon monoxide (CO), total unburned hydrocarbons (THC), and particulate matter (PM). This stems from the more complete combustion of these fuels, as well as the absence of atoms, such as sulfur, which is needed to create SO_X. The production of nitrogen oxides (NO_X), however, either remains the same or increases slightly. Neat biodiesel showed a 13% increase in NO_X over petroleum diesel [6]. This is an unavoidable side effect of combustion in a nitrogen-containing atmosphere. While carbon-based bio-fuels produce lower emissions than petroleum they still produce carbon dioxide. CO_2 is a known greenhouse gas and may contribute to global warming. Of all the currently researched bio-fuels only hydrogen produces no CO_2 when burned, releasing only gaseous water and NO_X [7]. Due to the higher temperature of combustion NO_X levels may be greater than that of conventional fuels. However, while the burning of other renewable fuels produces carbon dioxide there is no net addition of CO_2 to the biosphere like that of fossil fuel combustion. This is due to the carbon content in biofuels coming from the atmosphere during plant growth, instead of reservoirs far underground.

Quick adoption of bio-fuels requires an infrastructure capable of handling supply and demand. Ethanol and biodiesel have been widely accepted as an alternative fuel since the current equipment in vehicles can run on these fuels with little to no modification. Straight vegetable oil can be used as a substitute for petroleum diesel with minor engine modification. Hydrogen and biogas can also be used to fuel conventional internal-combustion engines (ICEs) with minor changes to the fuel system. The overall principle remains the same, with a combustion reaction occurring inside an engine block to produce usable power. This allows an energy conversion efficiency of around 30% [2].

1.1.1 Hydrogen

Hydrogen fuel involves the use of elemental hydrogen and is either burned in an internal combustion engine or used to power an electric fuel cell. In both cases the products are power, either electrical or mechanical, waste heat, and water vapor. While the use of hydrogen as a fuel is one of the most environmentally friendly and thermodynamically efficient at the point of end use, over 95% of hydrogen used today is produced from conversion of fossil fuels [8]. This means that use of hydrogen is still a major consumer of nonrenewable fuels. Work is currently being done on hydrogen production from the fermentation of biomass and the splitting of water through solar power. However, both of these methods have technological hurdles to overcome before widespread use [9]. Hydrogen fuel also suffers from lack of a national distribution

system, leading to higher costs as fuel must be trucked across the country for consumption.

1.1.2 Ethanol

Ethanol enjoys the largest market share of any renewable transportation fuel, due in no small part by support received from industry and government [10]. Today, it is produced almost exclusively by the fermentation of simple sugars. It is then blended with petroleum gasoline and designated as an E blend, with E85 representing 85% ethanol by volume. FlexFuel vehicles can burn gasoline with up to 85% ethanol while conventional vehicles are limited to 10%. Current problems with ethanol revolve around the use of food-grade feedstock for its production. Most ethanol in the U.S. is produced from locally grown corn, driving up the market for all corn-related products. New technologies for ethanol production are being developed to use complex and C_5 sugars in the fermentation process, which would allow efficient use of feedstocks such as cellulosic biomass and other sugars. Research is this area has focused on industrial production of enzymes which convert the complex feedstocks into the simple sugars needed by microorganisms for fermentation.

The ethanol production cost is dependent on both enzyme production and feedstock cost of the sugars used. Ethanol also suffers from lack of a national distribution network, where its tendency to absorb water into solution corrodes piping and damages equipment. Thus, it cannot be shipped through the existing national petroleum pipeline, consequently increasing distribution costs.

1.1.3 Vegetable Oil

Vegetable oil is another alternative to displace petroleum derived fuels. The use of vegetable oil to run diesel engines dates back to the first diesel engine, which Rudolf Diesel demonstrated at the 1900 world's fair using peanut oil for fuel [11]. It was not until the availability of cheap petroleum that the switch away from renewable was made. While straight plant oils can be run in a diesel, there are several problems associated with using it in a modern engine. The viscosity of vegetable oil is several times higher than that of petroleum diesel, leading to pumping problems in the fuel system. Vegetable oil can also leak past seals to contaminate and thicken engine oil, leading to premature component failure. According to the Engine Manufacturers Association, straight vegetable oil can cause: "(i) piston ring sticking; (ii) injector and combustion chamber deposits; (iii) fuel system deposits; (iv) reduced power; (v) reduced fuel economy and (vi) increased exhaust emissions" [12]. The low cloud-point of vegetable oils (the temperature at which solidification begins) also precludes its use in colder environments unless fuel heaters are employed.

1.1.4 Biodiesel

Biodiesel has the second largest market share of renewable biofuels behind ethanol, and is a displacement alternative for petroleum diesel fuel. The ASTM specification for biodiesel defines it as "the mono alkyl esters of long chain fatty acids derived from vegetable oils or animal fats, for use in compression-ignition (diesel)

engines" [13]. The feedstocks used for biodiesel production can be any animal or plant lipid source. It has similar properties to petroleum diesel and allows one to bypass many of the drawbacks inherent to straight vegetable oil [6]. It is commonly sold as blends with petroleum diesel from 2 to 100 percent designated B2, B100, and so on. All vehicles can burn up to a B20 blend without modification [14]. The most common feedstock in the U.S. is soybean oil although rendered animal fat, used fry grease, and other plant oils are also used. Compared to petroleum diesel, biodiesel produces lower levels of unburned hydrocarbons, particulate matter, and carbon dioxide. It generally gives higher levels of NO_X emissions due to the higher combustion temperature [15]. Since biodiesel contains oxygen in the molecule, the energy density is less than petroleum diesel, giving about 11% less gas mileage [16]. Biodiesel also suffers from the inability to transport it through existing petroleum pipelines. One reason for this is the ability of biodiesel to loosen and dissolve deposits left by petroleum diesel. This and other factors increase the end cost per gallon.

1.2 The Future of Biofuels

While current interest in renewables is bringing their use into the media focus there are still several problems left to solve before biofuels can replace significant amounts of petroleum fuel. Examining the current industrial environment and researching new feedstocks will allow biofuels to continue advancing.

1.2.1 New Feedstocks

The foremost issue with current feedstocks is limited availability in the face of increasing demand. A common theme is the use of food crops to produce fuel, a non-sustainable long-term model. Large amounts of corn grown in the heartland are turned into ethanol, and most surplus soybean oil is converted to biodiesel [17]. Replacement feedstocks are therefore needed that will not place unreasonable demands on the nation's foodstuffs. New technologies are currently being developed to augment the feedstocks used today. Processes such as fermentation of cellulosic sugars for ethanol production are expanding the pool of available feedstocks to materials which were previously ignored by industry. For diesel replacement, new plant oil sources are constantly evaluated on their properties as a transesterified product. These range from trees, such as the Chinese Tallow tree, to plants such as Castor.

Microbial sources have also caught the attention of several researchers as a new feedstock. Work on farming algae for lipids was started during the oil crunch of the 70's, but declined after the drop in crude oil prices. While interest has recently picked up in using harvested lipids as biodiesel feedstock, problems still exist regarding the cost of raising the algae since they must be grown for harvest [18].

One of the most novel and promising feedstocks, however, involves the use of readily available microorganisms as a lipid source. Municipal wastewater treatment facilities (MWWTF) in the USA produce 6.2×10^6 tons (dry basis) of microbial sludge annually [19]. This sludge is composed of a variety of organisms which consume organic matter in wastewater. The content of phospholipids in these cells have been estimated at

24% to 25% of dry mass [20,21]. Since phospholipids can be transesterified they could serve as a ready source of biodiesel. The sludge produced is currently viewed as a waste product and disposed of through landfills, land application on farms, or incineration. Since the sludge is produced through an established, necessary process, there is no extra cost associated with raising the microorganisms.

1.2.2 Industry Requirements

Current attempts at displacement of petroleum diesel involve switching to biodiesel. Although biodiesel is made from a renewable source, the national infrastructure needed to convert large amounts of lipids into biodiesel currently does not exist. This has resulted in a frenzy of new construction, bringing plants online every year. In addition, biodiesel suffers from the same fate as most other biofuels in that it cannot be transferred through the existing national petroleum pipeline. This results in higher per gallon costs since the fuel must be trucked across country to the end user. Since most biodiesel is produced in the Midwest and consumed in the coastal states this could be a significant portion of the final cost. The inability of biodiesel to run in stock engines at more than a B20 blend is also a limiting factor in its final acceptance.

In comparison to constructing new production plants, a method which uses lipids to make biodiesel in a conventional refinery would be more economical and practical. However, the chemistry regarding biodiesel production is vastly different from petroleum refining. A method which creates a biofuel compatible with petroleum diesel while allowing production in a traditional refinery would therefore be beneficial. One promising method involves the cracking of lipids via acid catalysis to produce non-polar

long-chain hydrocarbons, known as Green Diesel. Lipids would be fed into the head of a refinery and passed over a bed of acid catalyst similar to the catalytic cracking units already used in petroleum refining. The resulting hydrocarbons would continue throughout the plant as if derived from a petroleum source, resulting in an increased fraction of petroleum diesel fuel. This fuel would be chemically similar to conventional diesel fuel, but derived from a renewable feedstock.

Thermal cracking of oils, known as pyrolysis, has been the focus of research for several years. This process uses thermal energy to break bonds in the feedstock, creating many different products. Research has shown that the products consist mainly of C_4-C_6 aromatic and aliphatic hydrocarbons, C_2-C_4 olefins, hydrogen, and a fraction similar to that of petroleum diesel [22]. However, this still requires high temperatures in the range of 300-500°C with no control over the final products [22,23]. The use of acid catalysis in production of diesel-range compounds allows for temperature reduction to 150-400°C and a more controlled cracking than pyrolysis [24].

1.3 Overcoming Catalysis Challenges

Silica / Alumina (SiAl) catalysts have played an important part in the research and development of many organic reactions over the years, and most have been well characterized with regard to structure and properties. Along with modifiers added to the crystal structure they can be used for chemical reactions ranging from cracking to alkylation [25]. However, not all aspects of SiAl catalysts have been completely studied. One area lacking research is the cracking of microbial oils to produce biofuels. While

some work has been performed on cracking of vegetable oil there is a lack of data on the effects of various heteroatoms, such as phosphorous, on the catalyst. Since phosphorous present in microbially-extracted oil could have a negative effect on cracking performance knowledge of how phosphorous interacts with catalyst active sites would allow for better process modeling of refinery operations.

One of the goals of this project is to achieve a better understanding of phosphorous poisoning mechanisms and effects through deactivation of catalyst with phosphorous-containing molecules. If the level of phosphorous required to deactivate a catalyst is found process control can be modified to keep the amount of phosphorous low enough to minimize poisoning. Knowing the effect phosphorous poisoning will have on reactant conversion and product distribution will allow for better process optimization in an industrial setting.

CHAPTER II

LITERATURE REVIEW

2.1 Green Diesel from Lipids

Biodiesel is produced through esterification or transesterification of lipids, converting them to a fuel which is partially similar to the properties of petroleum diesel. Although some properties are similar the molecular structure is vastly different. While this is good enough for blending with petroleum diesel in small quantities, blends higher than 20% require engine modification [26]. In contrast, a fuel made from renewable feedstocks but with the same molecular structure as petroleum diesel would be a much better match. Green diesel fits this role by being chemically identical to petroleum diesel. The green in its name comes from the renewable nature of its feedstock. It is produced through cracking of lipids, the products of which are chemically very similar to petroleum diesel. In addition, it may be possible to crack non-lipid feedstocks and produce a fuel with the qualities of green diesel.

2.1.1 Upgrading of Pyrolysis Products

Previous work has concentrated on products obtained from thermal catalytic cracking (pyrolysis) of biomass. Such product is often referred to as bio-oil, and contains

compounds such as organic acids, alcohols, aldehydes, ethers, esters, ketones, furans, phenols, hydrocarbons, and other non-volatile components [27]. Overall, bio-oil is considered a poor substitute for conventional fuels due to its low BTU value and incompatibility with existing engines [24]. Of concern is the large amount of entrained water, in some cases higher than 20% by weight. Thermal cracking also requires high temperatures that increase production cost. One reason for the large variety of products obtained from biomass pyrolysis is the complex structure of the feedstock.

In contrast, oils obtained from plants, animals, and microorganisms are of a fairly consistent composition. Consisting of long hydrocarbon chains terminated with esters and carboxylic acids, cracking of renewable oils could produce a variety of long-chain hydrocarbons chemically similar to petroleum diesel [28]. Research on thermal cracking of natural oils has shown that the products consist mainly of C_4-C_6 aromatic and aliphatic hydrocarbons, C_2-C_4 olefins, hydrogen, and a fraction similar to that of petroleum diesel [22]. However, this still requires high temperatures in the range of 300-500°C with no control over the final products [22,23]. Selectivity of the cracking process is therefore limited, possibly reducing final yields.

It has been discovered that catalytically cracking bio-oil after production through pyrolysis dramatically improves the product quality [24]. The use of several catalysts has been explored in this situation. The Silica / Alumina catalyst ZSM-5 is widely used in laboratory experiments due to its simplicity and ease of use, but is not widely used in commercial processes due to low stability. Other catalysts include H-Y, mordenite, silicalite, and silica-alumina [29]. Adjaye and Bakhshi [29,30] performed cracking of

maple wood bio-oil over the five catalysts listed above and discovered significant differences in the product distribution. Between temperatures of 210 – 400°C ZSM-5 gave the highest yield of hydrocarbons, with 27.9 wt% [30]. This was followed in descending order by H-Y, silica-alumina, silicalite, and mordenite. The majority of hydrocarbons produced by ZSM-5 and mordenite were aromatic while the others gave more aliphatics. Aromatics are a preferred product due to the higher octane obtainable versus aliphatics. ZSM-5 also produced the least amount of coke byproducts, with 370°C giving the optimal yield of total hydrocarbons [29,31]. In all cases studied, the use of ZSM-5 showed little deoxygenation of bio-oil, acting more as a cracking catalyst than anything else [27,32]. A finishing step with specialized catalysts may be necessary to achieve high quality diesel fractions.

Other catalysts which operate in the temperature range of 150 – 200°C have been used such as sulfated zirconia, which has seen use for the production of gasoline alkylates and cracking reactions [33]. Cracking of pyrolytic bio-oil from pine sawdust over sulfated zirconia results in an aqueous phase rich in phenolics at 300°C, but a drop in temperature to 200°C gives a product with up to 20% methanol [24]. Aromatics and related compounds are preferred for fuel over low alcohols and paraffins due to the higher octane available [25].

2.1.2 Catalytic Cracking of Lipids

The use of catalysts to catalytically crack lipids was first brought to the attention of scientists in 1979 by researchers at Mobil [34]. The use of superacids to produce

diesel-range compounds allows for temperature reduction to 150-200°C and a more controlled cracking than pyrolysis [24]. This gives a product with better characteristics than bio-oil, although solid biomass such as wood scraps could not be used. In comparison to bio-oil, however, the cracking of lipids offers a smaller range of products than that obtainable through pyrolysis. This comes at the trade-off of larger molecular weights. Proposed reaction mechanisms show the cracking of lipids to follow fairly linear path, with few possible branches [27]. It begins with acids and esters undergoing either decarboxylation or deoxygenation, then continuing toward completion. A sample of the proposed mechanisms is shown in Figure 2.1. Studies have shown that temperature plays a vital role in product distribution with the use of superacid catalysts, with lower temperatures producing larger amounts of aliphatic hydrocarbons [28,35].

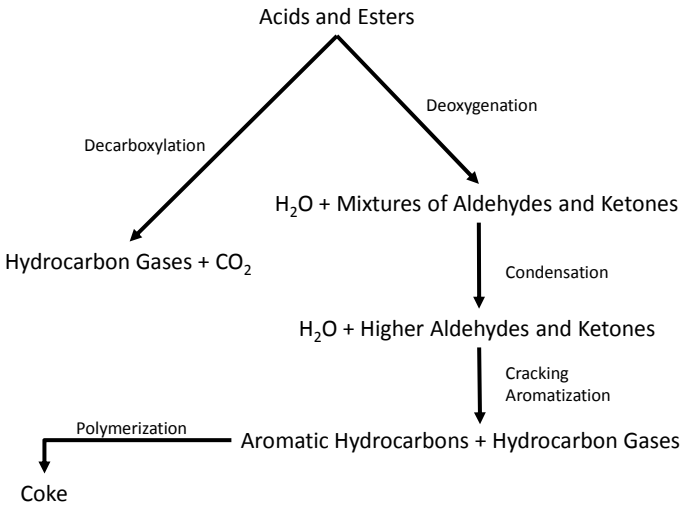

Adapted from Adjaye [27]

Figure 2.1 Reaction Pathway for Cracking of Acids and Esters Over Heterogeneous ZSM-5 Catalyst

As mentioned earlier all the lipids have a similar structure, especially compared to the wide range of compounds in bio-oil. This translates to a cracking product stream that is remarkably similar across different lipid sources [36]. The majority of research on catalytic lipid cracking, detailed below, concentrates on cracking of the most common lipid source, canola oil. This was reacted over various microporous catalysts such as ZSM-5, mordenite, H-Y, silicalite, and silica-alumina; as well as mesoporous catalysts like MCM-41/SBA-15.

Billaud [23] studied the cracking of octanoic acid over activated alumina and an amorphous silica-alumina catalyst. Since fatty acids are thought to be an intermediate in triglyceride cracking this would give information about possible reaction mechanisms. He showed that the optimal reaction temperature was 400°C. Activated alumina produced 54.6% of liquid organic product (LOP) by mass and 1.8% coke, with the remainder as gas. The silica-alumina gave 37.1% LOP and 11.2% coke by mass, inverting the quantities of liquid and gas. This was explained by the silica-alumina having a higher acidity than activated alumina, and thus favoring heavy cracking reactions [23].

Conversion of canola oil over heterogeneous catalysts such as ZSM-5 is perhaps the most studied aspect of lipid conversion. Prasad and Bakhshi [37] studied the effects of varying weight hourly space velocity (WHSV) and temperature on ZSM-5, as applied to a statistical analysis. The results show that canola oil is easily converted to liquid hydrocarbons rich in aromatics, comprising 48 – 78% of total hydrocarbon fraction heavier than pentane. Gas products were heavy in C_3 and C_4 paraffinic hydrocarbons,

with higher reaction temperatures favoring gas yield over liquid hydrocarbons. This data is similar to that reported by others [38,39]. Other catalysts were also studied with Canola Oil, including mordenite, H-Y, silicalite, aluminum pillared clay, and silica-alumina catalysts. Comparison of results show that ZSM-5 has the highest selectivity toward liquid hydrocarbons and the amount of aromatics contained therein, giving around 40% total liquid hydrocarbons by weight [38,40]. ZSM-5 also produced the least amount of coke formation. Silica-alumina has the highest selectivity for aliphatics, while Al-pillared clay gives the highest levels of gas phase olefins. In all cases, the crystalline pore structure of catalysts such as ZSM-5 resulted in larger amounts of liquid products; while amorphous catalysts facilitate secondary cracking, giving higher selectivity toward aliphatic hydrocarbons [39]. Co-injection of steam into the cracking process has also been reviewed. Addition of steam into the cracking process decreases coke formation in the system but increases selectivity toward olefins going from an average of 31.5% weight percent to 75.5% [35].

Palm oil has also been a recipient of research due to its availability in tropical locations. The cracking of palm oil over ZSM-5 results in similar products to canola oil. An optimization routine carried out by Ooi found that 450°C and a WHSV of 3.5 – 4.5 h^{-1} gave a gasoline fraction of 41.5% by weight [41]. This is comparable to the 40% given for canola oil. Experiments on other catalysts also mirror results obtained for canola oil. Twaiq [42] evaluated ZSM-5, zeolite-β, and ultrastable Y zeolites (USY) for their performance in palm oil cracking. As before, ZSM-5 produced the largest yield of gasoline range organics and lower coke formation. USY and zeolite-β, however, showed

higher selectivity towards the diesel range organics and lower production of gaseous products [42]. ZSM-5 produced a maximum of 4.8% diesel range organics by weight, while zeolite-β and USY gave 10.7 and 14.4%, respectively.

Several researchers have modified the structure of various catalysts in an effort to increase yield of specific products. Katikaneni added potassium to the structure of ZSM-5, which poisoned the active catalyst sites [28]. The experiments utilized similar conditions to reactions detailed above; temperatures of 400 – 500°C and 1.8 – 3.6 h^{-1} WHSV. Potassium was impregnated into the ZSM-5 at 0, 0.5, 1, and 2% by weight. The reduction in acidity switched the product distribution from aromatic hydrocarbons to aliphatics. Total organic liquid and gas products were also reduced, while coking increased [28].

Most research in this area focuses on the use of micro and mesoporous catalysts in a packed bed reactor due to the expense and difficulty of larger systems. However, there are some research groups examining larger systems. Dupain has cracked rapeseed oil using a common fluidized cracking catalyst (FCC), with both pure vegetable oil and rapeseed mixed with conventional petroleum feedstock [43]. The temperatures used were from 485 to 585°C. Initial thermal cracking of the triglycerides gives rise to fatty acids, which are then cracked catalytically. Coke production is high, similar to conventional FCC units. Aromatics remain in the range of 30 – 40% weight percent within the gasoline fraction. The organic products are heavily deoxygenated, with water being the major oxygenate product [43].

2.2 Poisoning and Modification of HZSM-5

While there has been a large amount of literature published on the subject of ZSM-5 modification and poisoning, little of it has to do with phosphorous and phosphorous containing compounds. The University of Petroleum in east China modified HZSM-5 with triethyl phosphate in an effort to increase the zeolite stability to steam [44]. Triethyl phosphate was added to the zeolite in liquid phase at 0.8% by weight. This was then calcined for a total of three hours. This resulted in the formation of both Si-P-Si and Si-P-Al bonds in the crystal lattice. The addition of phosphorous to the framework decreased the activity from 0.79 to 0.69 mmol / gram of heptane cracked. However, steam treatment of the catalyst resulted in an activity drop to 0.00 mmol / gram for plain ZSM-5, while phosphorous treated catalyst retained an activity of 0.18 mmol / gram. It is explained that the higher electronegativity of phosphorous leads to a more stable framework, and decreases the dealumination during steam treatment. Molecular mechanics simulations showed that heat of formation for phosphate containing framework is -63.0 kJ / mol, while heat of formation for regular zeolite framework is -22.6 kJ / mol. The result is that phosphorous modified zeolite is in a more stable configuration, leading to greater resistance of dealumination.

Pruski, from Iowa State University, has led a study regarding the modification of HZSM-5 zeolites with phosphorous [45]. ZSM-5 was impregnated with phosphoric acid in an aqueous state, and then calcined at 600°C for 1 hour. Samples were prepared with 0, 2, 5, 7.5, 13, and 15 weight percent phosphorous. Samples were then analyzed by temperature programmed desorption, as well as NMR and IR spectra. Analysis of NMR

spectra shows that tetrahedral framework aluminum, responsible for catalyst activity, decreased with increasing phosphorous levels; although this only occurred after steaming of the catalyst. A species of aluminum in a highly distorted octahedral formation was seen, but remained relatively constant throughout all phosphorous levels. A new species of aluminum was also identified as octahedral aluminum phosphate. This compound did not appear to have any activity in cracking reactions, but may impede reactions by tetrahedral framework aluminum by blocking pore access. In continuing experiments it was determined that phosphorous was more likely to form polyphosphates with phosphorous-oxygen-phosphorous bonds as opposed to phosphorous-oxygen-aluminum [46]. The situation was reversed, however, when the samples were steamed. Their data shows that modification of ZSM-5 with phosphoric acid did not significantly reduce the amount of framework aluminum in the samples, even at high loadings of phosphorous. Catalyst activity was significantly reduced, but was attributed to polyphosphate complexes blocking pores, as well as small amounts of aluminum phosphate species. This resulted in larger occurrences of low molecular weight olefin production as larger molecules could no longer fit in the crystalline framework.

Mobil Oil Corporation also looked at the effect of phosphorous on zeolite catalysts by deactivating the surface with bulky organophosphates [47]. The compounds used were butyltriphenylphosphonium bromide, tetraphenylphosphonium bromide, tetraphenylphosphonium hydroxide, triphenylphosphate, and methyldiphenylphosphine. These compounds are too large to enter the pores of ZSM-5 and only react on the surface. All compounds showed a deactivation of total acid sites between 2.7 and 17%. Two

probe reactions were carried out on the samples, dealkylation of 1,3,5-tri-*tert*-butylbenzene and polymerization of propylene. All compounds except 2,6-DTBP showed zero activity for dealkylation, with 2,6-DTBP showing a reduction of 96%. Polymerization of propylene decreased from "very active" to "active" for all compounds.

Kaliaguine's group from the Université Laval in Québec also looked at modification of HZSM-5 by phosphorous complexes [48]. A loading of 2.44 weight percent triphenylphosphine was deposited onto the catalyst through gas-phase adsorption, and then calcined in air at 500°C. The activity was evaluated using a methanol-to-gasoline test (MTG) and while conversion was complete in both cases, showed significant differences in the products obtained. The amount of olefins generated in the reaction increased from 2.7 weight percent of total hydrocarbons to 45.1% after phosphorous modification. Total C_5^+ compounds decreased by 5%, while the percentage of hydrogen in hydrocarbons remained relatively constant. The results show that phosphorous was an efficient compound for the poisoning of Brønsted active sites, giving a wide range of changes to product composition.

2.3 Renewable Fuels from Microbial Lipids

It has been known for some time that various plants, animals, and microorganisms could be harvested for their oils [49]. These oils are usually an energy storage device for the organism in question, leading to cells which contained relatively large droplets of oil. The practice of harvesting microorganisms for energy production, however, was often

overlooked by those looking to extract oil from easily accessible sources such as phytomaterial.

2.3.1 Lipids in Wastewater Sludge

All municipal wastewater treatment plants (MWWTF) function through the use of microorganisms in one form or another. In 1914, Arden and Lockett discovered what is known as the activated sludge process [50]. This was the beginning of wastewater treatment facilities, which allowed for the removal of organic contaminants in a timeline of hours instead of days. At first a theory on how the process worked was unavailable, but research built up until workable models were developed in the 1950s and 60s.

2.3.2 Lipid Origins

It has always been known that municipal, and even some industrial wastewater contains lipids. A cursory glance at wastewater entering a plant allows one to see oil and grease floating on top of the influent wastewater. This is due to the influent water bringing free lipids into the plant in the form of vegetable or animal wastes. An often overlooked source of lipids, however, is the microorganisms which inhabit the treatment plant. Like all animal cells, the microbes in a MWWTF are surrounded by a cell wall composed of lipids. Some of these cells also store energy in the form of lipids. Although some information was known about modeling of MWWTFs, the demand for a more complete operational picture called for increased model complexity. For example, it was found that long-chain fatty acids produce various toxic effects during anaerobic digestion [51,52]. Anaerobic digestion refers to the reduction of sludge mass through bacterial

metabolism in the absence of oxygen. Bacteria produce methane gas as a metabolic waste product, which leaves the digester in the gas phase. Due to this and other pressing reasons there have been several attempts to document the amount and composition of lipids in the entire treatment process.

A typical MWWTF consists of several different sections working in sequence to take large amounts of organic waste and reduce it to manageable levels for release back into the environment. The standard measure of how much effect wastewater will have if released into the environment is the Biochemical Oxygen Demand (BOD). This is the amount of oxygen needed by organisms to degrade organics in the water. Figure 2.2 shows a standard MWWTF. Raw influent wastewater typically enters at the headworks, where large debris is removed to avoid clogging the system. The water then travels to primary clarification, where the majority of influent Biochemical Oxygen Demand (BOD) is removed through settling out of solids from the water. The primary solids are then thickened and dewatered for anaerobic digestion. The clarified water enters the activated sludge process, where aerobic microorganisms degrade organics in the water. These organisms conglomerate to form clusters of microbial mass which remove the organic load, converting it to lipids and other cellular material [53]. They are not a single species, but rather a consortium of different microbes. A delicate balance must be maintained between types filamentous organisms and those which remove nitrogen and phosphorous [54,55].

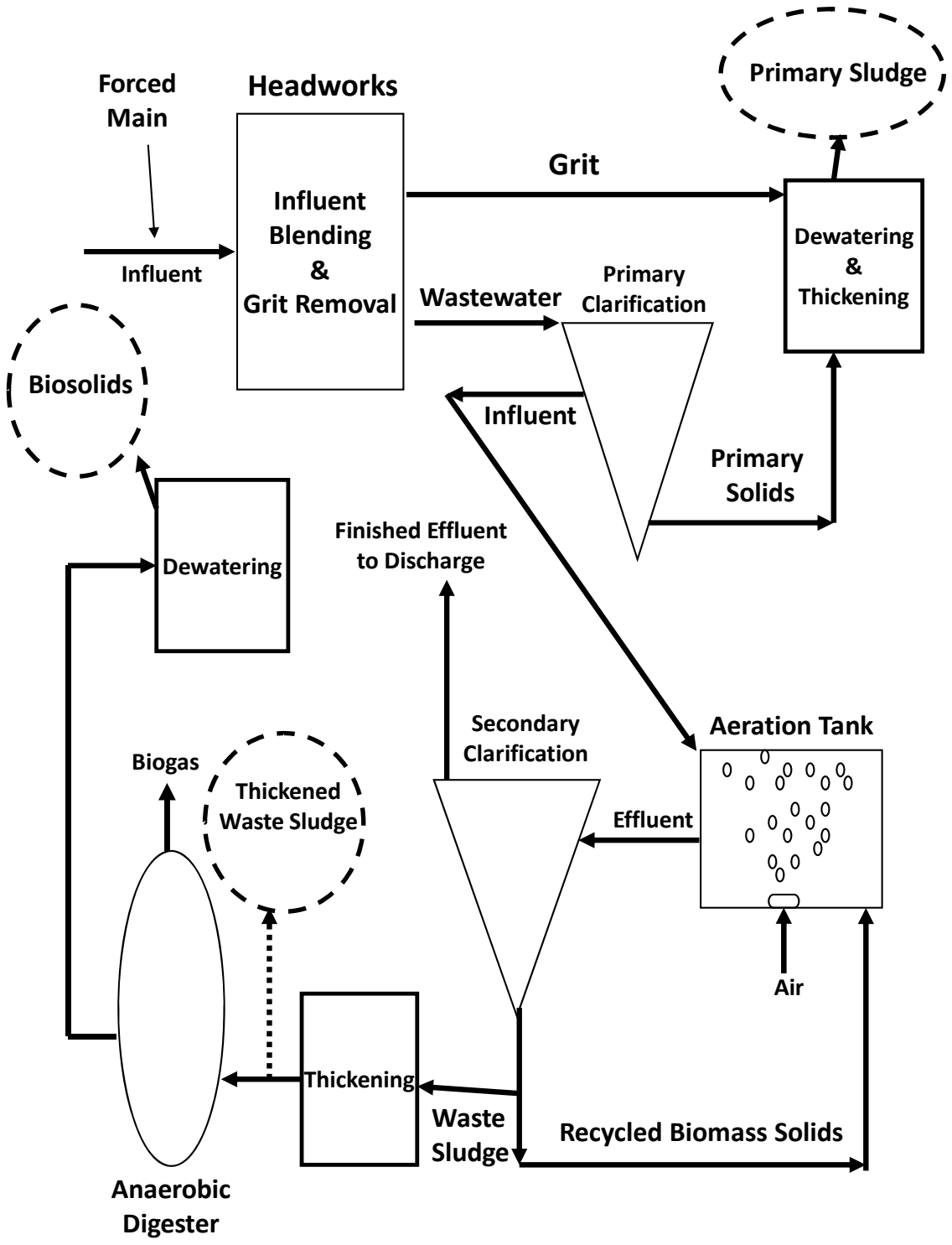

Figure 2.2

Standard Municipal Wastewater Treatment Plant

The water is passed through a secondary clarifier to remove the microbial cells, with the clarified water being clean enough for discharge in most cases. Part of the settled material is recycled back into the activated sludge process to maintain a steady state concentration of microorganisms, while the remainder is either disposed of or digested anaerobically. Both primary and secondary sludge are often digested anaerobically to reduce the mass of sludge which must be disposed of. In the aerobic process of activated sludge treatment, organisms remove BOD and convert it to energy and cellular material, as well as residual solids. This generates a large amount of biomass. In the anaerobic digestion process organisms convert waste microbial cells to energy and small molecules such as methane and hydrogen. This has the effect of reducing the mass of sludge left after digestion. Any remaining sludge is then dewatered for disposal.

It has been reported by Barttelbort and others that MWWTF influent is over 50% organic material, and composed of 20 to 25% lipids by mass [56,57]. Of these, kitchen waste is responsible for 14 to 36% of the total [58]. Feces themselves contain between 4 to 23% lipids by mass [59]. In an average plant 45% of the total influent lipid content is derived from feces, while 55% is from kitchen wastes [60]. The overall goal of a treatment plant is to reduce the organic load exiting after treatment. This removal process takes place at several stages throughout the treatment plant, where organisms consume the lipids and other organic matter for energy [61].

The types of lipids, or lipid profile, also changes as influent material travels through the treatment plant. Lipids in raw wastewater are composed mainly of

triglycerides, the dominant lipid type in animal and plant oils. This composition continues into the primary clarification step. As the treatment process moves toward the activated sludge tank, the lipid profile changes to include more phospholipids, glycolipids, and sterols [62]. This reflects the change from free lipids in solution to cellular lipids which were created by microorganisms feeding on organic matter in the waste. A major part of cells within the activated sludge system is the extracellular polymeric system (EPS). The EPS helps to bind organisms together and form flocs, to increase settling of the sludge. EPS varies between species of microorganisms, but normally contains carbohydrates, proteins, and lipids [53]. One significant difference is that pure bacterial cultures produced an EPS high in carbohydrates, while samples take in MWWTFs are higher in protein [63]. Martinez analyzed variations of carbohydrate, protein, and lipids over long periods; finding that while protein fluctuated from 7 - 40%, the levels of carbohydrate and lipids remained constant at 40% by weight for lipids [64]. A byproduct of the activated sludge process is foam created by the microorganisms. This foam was also found to be a source of lipids, with some plants showing a concentration of up to 29% [65]. The wastewater lipid profile changes once again when aerobic microorganisms are replaced with anaerobic in the digester. The digester contains lower amounts of lipids than other parts of the process, but the lipids present have a much different composition than those found elsewhere in the plant [66]. Bacteria which inhabit an anaerobic digester contain specialized fatty acids, such as branched-chain fatty acids, which are not found in aerobic processes such as that of the activated sludge process.

2.3.3 Lipid Extraction and Analysis

Most research on lipids in wastewater focus on extraction for laboratory work rather than commercial utilization. In microbiology, scientists often identify bacterial cultures by the types of fatty acids in their cells. The procedure required to prepare lipids for analysis, however, is the same chemical reaction used to produce crude biodiesel from lipids. In this sense, researchers are creating biodiesel every time they analyze a sample. The standard method consists of lysing the cells through physical or mechanical means [67,68]. The extraction of lipids is then performed through use of a solvent, followed by conversion to fatty acid methyl esters (FAMEs). Solvent used can range from hexane to toluene, isopropyl alcohol, methanol, and benzene [69-71]. In an experiment performed by Casado [68], the cells were mechanically lysed using sonication and extracted with methylene chloride. Others use the method of Bligh and Dier which involves extracting lipids in a single-phase system, then separating it into two phases [70,72,73]. The extracted lipids were transesterified with a solution of BF_3 in methanol and analyzed through mass spectrometry [68]. One can substitute sulfuric acid or sodium hydroxide for BF_3 without significant changes in lipid profiles or conversion efficiencies, but the chromatograms obtained have larger amounts of byproducts [74]. It is also possible to use other alcohols besides methanol in deriving lipids, although the products will not be methyl esters. A common alternative is isopropyl alcohol (IPA). Werker analyzed microbial communities in MWWTFs using sulfuric acid and IPA [75]. Dried cells were lysed in IPA with sulfuric acid, and then extracted with hexane for analysis. Table 2.1 shows common values for lipid composition in sewage sludge as reported in literature.

In a sample without large numbers of microorganisms the lipids can be extracted from the sample without any lysing steps. When analyzing lipid concentrations in foam produced from the activated sludge process, Fahmy extracted free lipids with a combination of water washing and solvent extraction [65]. Work has also been performed on extracting lipids and other chemicals from biomass using supercritical fluids [76]. The use of supercritical fluids allows for easily tuning the extraction to maximize the yield of desired products.

Table 2.1 Comparison of Fatty Acid Distribution of Wastewater vs. Microalgae

Fatty Acid	Percent Total Lipid Fraction	
	Wastewater	Microalgae
C14	9.3	10.1
C16	22.1	41.7
C18	46.3	11.4
C20	1.2	22.6
C22	1.2	8.4
Others	19.9	5.8

Wastewater Data from Casado [68]
Microalgae Data from Grima [77]

2.3.2 Lipids in Other Microorganisms

There are other sources of microbial lipids than just sewage sludge. Algae, for example, have often been harvested for their oil production; although it was not always for fuel use. From 1978 to 1996 the U.S. Department of Energy conducted a study on obtaining microbial oil from various algal species with the intent of biodiesel production [18]. This study spawned a 328 page report detailing advances made in algae to fuel conversion over two decades of research. Researchers worked on over 3,000 different

algae species, trying to find oil producers able to thrive in various conditions. The final organisms showed high growth rates and oil levels of up to 50% by weight [18]. Unlike organisms in a MWWTF, modifying the amounts of available nitrogen did not seem to have a significant effect on increasing the amount of oil produced. Although great breakthroughs were made in the large-scale production of oil from algae, including the use of CO_2 as a carbon source, the cost of production remains too high for fuel use. Even using assumptions of photosynthetic efficiency near the theoretical limit, the projected cost of oil is twice that of petroleum derived fuel. Most of the cost was attributed to maintaining the organisms and pond systems required for large-scale production. The county of San Francisco conducted its own research into the problem, growing algae on municipal wastewater. This removed the requirement of feeding the algae expensive feedstock to produce oil. While oil production was favorable problems were still encountered with environmental conditions [78]. In both cases, the amount of land required to produce significant amounts of oil is still prohibitive to national replacement of petroleum fuel.

Other companies have grown algae for oil harvesting purposes other than fuel production. Martek Biosciences Corp. is a commercial company which grows algae for the purpose of extracting nutritional fatty acids such as docosahexaenoic acid (DHA) and arachidonic acid (ARA) [79]. Their organisms produce around 20% lipids by weight, only 25% of which are nutritional fatty acids of commercial interest for their market. When using corn syrup as the carbon source in industrial fermenters, the operating cost are high. However, the market for DHA and ARA is so strong that the company is

consistently meeting profit goals. This is partly due to the FDA announcing in 2004 that adding omega-3 fatty acids to one's diet may reduce the risk of coronary heart disease [80]. Interestingly enough, after extracting DHA and ARA Martek disposes of most remaining oil, which may be suitable for fuel production.

Extraction of lipids is often carried out through simultaneous saponification and extraction of the oil using ethanol, with some researchers adding hexane as a cosolvent [81]. Purities of up to 97% have been reported using this method when combined with urea fractionation [82]. Chloroform can also be used alone or in a Bligh-Dyer extraction, but chlorinated solvents are not regularly used in industry [77,83]. Lysing the algae cells through sonication or grinding increases extraction yield of lipids, as it does for sewage sludge [84]. Care must be taken, however, to keep lipid degradation to a minimum.

To date, research in alternative oil production is fairly active. However, the involvement of commercial backers and large-scale production plants for lipid-based renewable fuels will not occur until fundamental problems with production are solved. These include production of the lipid containing material, plants or microorganisms, as well as extraction and transportation of the final lipid product.

2.4 Summary

Due to the cost and scarcity of petroleum-based fuels interest in renewable biofuels has increased dramatically in the past few years. However, most of the attention in this field has focused on fuels with similar properties, but different molecular structures, than the fossil fuels being displaced. This leads to difficulties in production,

transportation, and use of renewable fuels as compared to conventional petroleum. Green diesel fits this role by being chemically identical to petroleum diesel, but made from a renewable lipid feedstock. Experiments on canola oil cracking show that ZSM-5, a zeolite catalyst, has high selectivity toward liquid hydrocarbons and the amount of aromatics contained therein, giving around 40% total liquid hydrocarbons by weight [38,40].

Another source of concern is the availability of sufficient renewable feedstock to keep pace with demand. This can be lessened with the addition of microbial lipids to the feedstock pool. Lipids extracted from microorganisms contained in wastewater treatment plants could supply a novel source of renewable feedstock for fuel production. While this lipid source could be used to create green diesel, the effects of heteroatoms such as phosphorous on cracking are unknown. Available data shows that modification of ZSM-5 with phosphoric acid did not significantly reduce the amount of framework aluminum in the samples, even at high loadings of phosphorous; although catalyst activity was significantly reduced, attributed to polyphosphate complexes blocking catalyst pores [46]. Further research shows that phosphorous is an efficient compound for the poisoning of Brønsted active sites, giving a wide range of changes to product composition when cracking compounds [85].

Phosphorous impregnation work has taken place regarding zeolite catalysts such as ZSM-5, but none of them have looked at poisoning in a gas-phase cracking reaction such as would occur in an industrial setting. In conclusion, research on the effect of phosphorous on catalytic cracking of lipids to produce a renewable green diesel fuel has

not been reported previously. This study reports the effect of phosphorous on the cracking of lipids to produce green diesel.

CHAPTER III

RESEARCH HYPOTHESIS AND PROJECT OBJECTIVES

In light of the rapidly expanding biofuels market, it is imperative that new sources of renewable feedstock be discovered and commercialized. One overlooked source of renewable feedstock is lipid extraction from microorganisms. It is hypothesized that microorganisms present in sewage sludge will provide a ready source of lipids from which biofuels, such as green diesel could be produced. This can be performed through cracking of lipid feedstocks to smaller molecules. In the case of microbial extraction, however, the lipid extract will also contain phospholipids, an integral part of bacterial cells. It is hypothesized that phosphorous present in the phospholipids of microbial oils will have a negative impact on catalyst performance, in both conversion of reactants and product distribution. In limited work on poisoning of catalyst, phosphorous was shown to form covalent bonds with the active sites [46]. The feasibility of catalyst regeneration is unknown, but thought to be possible.

The objective of this project is as follows:

- Examine the behavior of lipids in a liquid phase cracking reaction through use of triflic acid. Simplicity of the Triflic acid system could allow for prediction of

cracking products and rates. Results could then be used to plan for experiments in solid acid cracking.

- To evaluate the performance of HZSM-5, a silica/alumina zeolite, with regard to the conversion and product distribution of cracked reactants.
- Evaluate the performance at different levels of phosphorous poisoning, achieved through a phosphorous-containing lipid substitute. The catalyst would be tested after poisoning for activity change and regeneration ability.
- Determine the phosphorous loading required to deactivate the catalyst. Results could be applied to reactor models for process simulation.
- Evaluate the ability of microbial lipid sources to produce a quality biofuel. This includes yield of extractable oil and economics relating to feedstock generation for green diesel production.

CHAPTER IV

METHODS AND MATERIALS

4.1 Triflic Acid Reactor System and Operation

The experiments with triflic acid were all performed in an argon atmosphere to remove the risk of reaction with oxygen or water in the environment. Moving samples into or out of the dry box required two purges to remove oxygen and moisture from the outside as well as hazardous fumes from the inside.

4.1.1 Chemicals

Methyl palmitate, chloroform, sodium bicarbonate, 1,3-dichlorobenzene, 99% trifluoromethanesulfonic acid, and trifluoroacetic acid were purchased from Fisher Scientific, Atlanta, GA, USA. These chemicals were used as received. High-purity argon was provided by NexAir, Memphis, TN, USA.

4.1.2 Sample Preparation

Methyl palmitate was first melted at 60°C, and 0.250 g dispensed into a 40 mL amber I-Chem vial. A disposable stirbar was added before insertion into the drybox

containing an argon atmosphere. Preparation of mixtures with varying acidity was performed in the drybox using amounts shown in Table 4.1.

4.1.3 Acidity Dependence

To determine the effect of acid strength on conversion of methyl palmitate, 0.250 g samples were reacted with 1.0 mL of each acid mixture. The reactions were performed in triplicate with Hammett acidities of –14.1, -13, -12.2, and –11.9. Hammett acidity (Ho) is a measure of the acid strength of a system, expressed on a log scale with a decreasing number indicating increasing acidity. It is used for highly acidic and superacidic systems since it relies on indicator compounds instead of the hydronium ion. Samples were reacted for 10 minutes at 50°C, then neutralized with a 10% solution of sodium bicarbonate and water. 5.0 mL of chloroform were then added and the sample vortexed to promote mixing. A 1.0 mL aliquot of organic phase was then removed and further diluted with chloroform to 0.5 mg / mL for analysis on a GC-FID.

4.1.4 Kinetics

Experiments were performed to determine the kinetic rate of disappearance of methyl palmitate and the reaction order. Vials containing 0.250 g methyl palmitate prepared as described in Section 4.2.2 were reacted with a TFA/Triflic mix of Ho = -11.9. The reaction was performed in triplicate at 50°C and time intervals of 5, 10, 15, 20, 30, 45, and 60 minutes. After the specified time interval, the mixture was neutralized with a 10% w/v solution of sodium bicarbonate and water. 5.0 mL of chloroform was then added and the sample vortexed to promote mixing. A 1.0 mL aliquot was then removed

and further diluted to 0.5 mg / mL for analysis on a GC-FID, as described in Section 4.1.5.1.

4.1.5 Triflic Acid Reactant and Conversion Products

The data were analyzed with commercially available software from Varian, Inc. The Varian MS Workstation suite allowed review of ion data, while a spectra library provided by NIST allowed for matching of unknown compounds.

4.1.5.1 Methyl Palmitate Analysis

Analysis of the remaining unreacted methyl palmitate was performed on an Agilent gas chromatograph (Model 6890; Palo Alto, CA) with a flame-ionization detector, as described in section 4.3.7. The method consisted of injecting a 1 µl sample into the GC with a split ratio of 100:1. The temperature program began at 140 °C, holding for 2 minutes. It then increased by 10 °C per minute to 160 °C where it was held for 4 minutes. After 9 minutes of total run time, the temperature increased 2 °C per minute until reaching 240 °C. The temperature was then held constant for 1 minute giving a total run time of 40 minutes.

4.1.5.2 Reaction Product Identification

Analysis of unknown reaction products in the liquid phase was performed on a Varian Star 3600 GC with helium as a carrier gas passing through a Phenomenex ZB5 column (30 M x 0.25 mm x 0.25 µm) coupled with the Varian Saturn 2000 GC/MS with wave board technology. The NIST library was used for identification. A volume (2.0

µL) of sample was injected into a splitless injection port at 280°C. The initial GC oven temperature of 50°C was held for 3 minutes and then ramped to 150°C at 10°C/minutes. It was then raised to 280°C at 1°C/min and held at 280°C for 2 minutes. Electron impact ionization (EI) or chemical ionization (CI) of the analytes with isobutene was achieved using the Saturn 2000, with a scan range of 100-450 m/z and scan time of 0.45 scan/sec.

Analysis of unknown gas phase products was performed by injecting 150 µL of headspace gas into a Varian Star 3600 CX chromatograph coupled to a Saturn 3 quadrapole GC/MS with ion trap. Helium was used as the carrier gas, with a RXI-1MS column from Resteck (Bellefonte, PA). The column size was 30 m x 0.25 mm with a 0.25 µm film thickness. The temperature profile consisted of -20°C for 3 minutes, then ramping at 5°C/min to 10°C. This was immediately followed by a ramp of 25°C/min to 50°C, then 10°C/min to 320°C. The temperature was then held at 320°C for 4.4 minutes.

To determine the amount of product released to the gas phase, a 15 mL vial was charged with 2.0 mL of undiluted chloroform extract and placed in a Zymark TurboVap LV (Fisher Scientific, Atlanta, GA, USA). The vials were suspended in a water bath at 40°C and dried under a stream of nitrogen for 30 minutes. After drying, the vials were weighed using an Ohaus analytical balance. A mass balance was then performed to determine the amount of material that escaped into the gas phase.

4.2 Quatra C Design and Operation

4.2.1 Chemicals

Triethyl phosphate and hexafluorobenzene were purchased from Fisher Scientific, Atlanta, GA, USA. 1,2-Dipalmitoyl-*sn*-Glycero-3-Phosphoethanolamine and 1-Palmitoyl-2-Hydroxy-sn-Glycero-3-Phosphoethanolamine were purchased from Avanti Polar Lipids, Inc., Alabaster, AL, USA**.** These chemicals were used as received. High-purity helium was provided by Airgas, Columbus, MS, USA. Analytical gas standards were provided by Restek, Bellefonte, PA, USA.

4.2.2 Instrument Design

The Quatra C unit consists of a Varian 3600x series GC modified for this project. Figure 4.1 shows an overall schematic of the system. Injector B was connected in line with injector A and the column. The body of injector B is used to hold a catalyst bed filled with the compound required by the current experiment. The tail of injector B is connected to a column splitting nut manufactured by Restek, which allows the products from cracking to be analyzed on two different columns and detectors. Column one is a Restek Rxi-1ms (30m x 0.535mm, with a 1.50 μm film). This leads to a Saturn 3 mass spectrometer with ion trap capabilities, manufactured by Varian Inc., Palo Alto, CA. Due to the nature of the column and the mass spectrometer range this column is used for identification and quantization of compounds containing more than six atoms of carbon. Column two is a Restek RT-QPLOT (30m x 0.53mm, DVB Plot Column). This column

feeds a thermal conductivity detector and is used for low molecular weight gasses and compounds. Injector A can be modified with the Chromatoprobe accessory from Varian which enables it to accept solid samples in addition to standard liquid and gas. Injector A was also fitted with liquid CO_2 influent lines to allow cryogenic cooling of the reactant. This allows a sample in injector A to be heated from -40°C to 400°C at up to 180°C per minute. Solid samples loaded into the Chromatoprobe were always less than 0.50 mg for both 1,2-Dipalmitoyl-*sn*-Glycero-3-Phosphoethanolamine (DPPE) and 1-Palmitoyl-2-Hydroxy-sn-Glycero-3-Phosphoethanolamine (LPE).

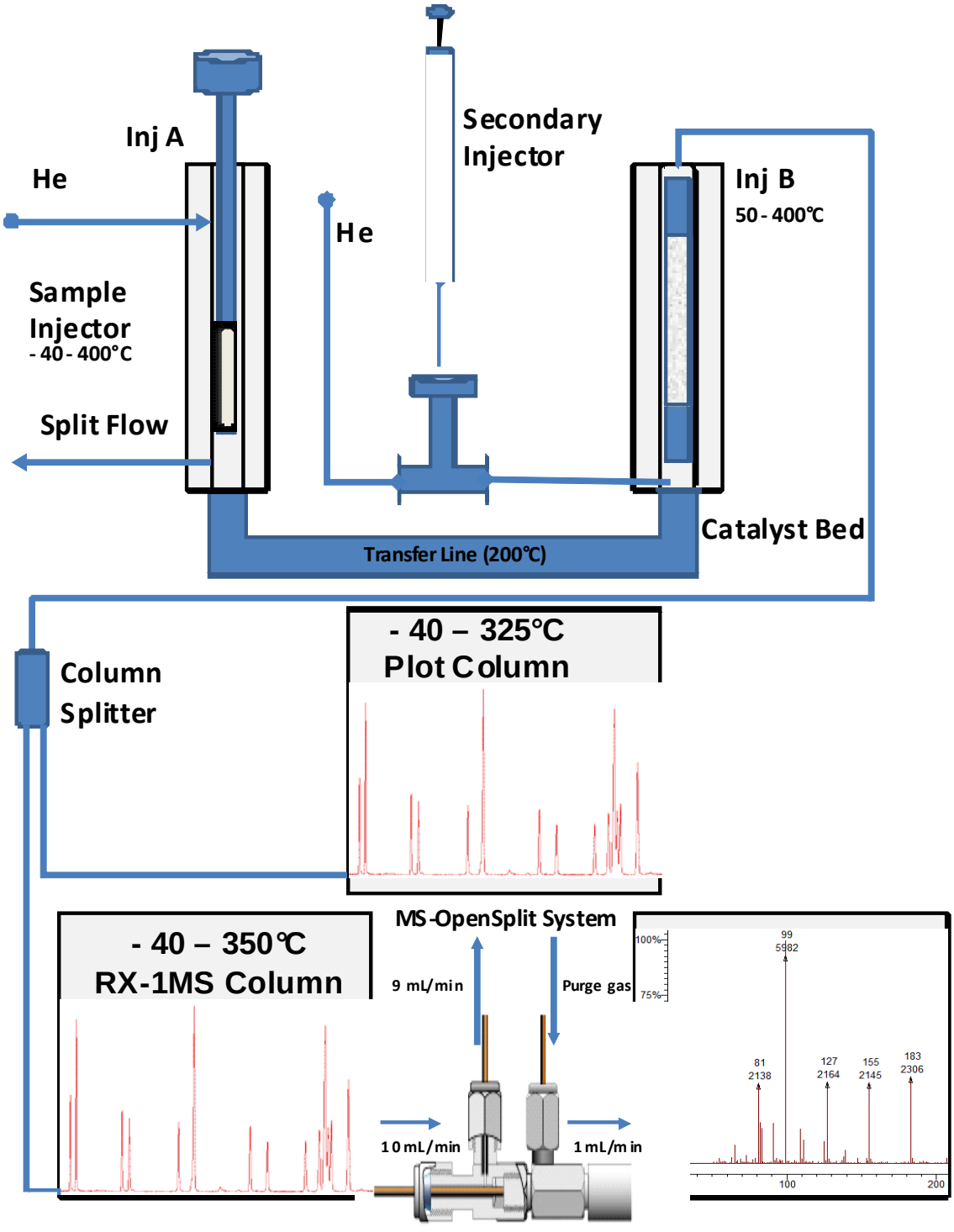

Figure 4.1

Design Diagram of Quatra C

The oven used on the Varian 3600x also has cryogenic capabilities, allowing the use of column temperatures below ambient to assist with compound retention and separation. This was used extensively in the beginning phases of this project when the Quatra C had only one column. Cryogenic cooling was no longer necessary after the addition of the second column.

4.2.3 HZSM-5 Reaction Products

The data were analyzed with commercially available software from Varian, Inc. The Varian MS Workstation suite allowed review of ion data, while a spectral library provided by NIST allowed for matching of unknown compounds.

4.2.3.1 DPPE and LPE

Analysis of reaction products varied as required by the reaction of different starting compounds. Initial experiments concerned with cracking DPPE and LPE were performed using the Chromatoprobe accessory from Varian, Inc. Injector A was in splitless mode and chilled to 30°C then ramped at 180°C per minute to temperatures from 200° to 300°C depending on the experimental conditions required. Injector B was held constant at 200° to 400°C. The GC oven contained one column, a RX-1ms megabore from Restek (Bellfonte, PA, USA). The column dimensions were 30 m x 0.53 mm, with a 1.50 µm film. Oven temperature was held at -20°C for 3.0 minutes then ramped at 5°C per minute to 10°C. It was then ramped at 25°C per minute to 50°C followed by a 10°C

ramp to 320°C, which was held for 4.4 minutes. This gave a total run time of 40.0 minutes. Total column flow was 10.0 mL / min. at -20°C.

The mass spectrometer was set to run two different methods due to the wide range of products under analysis. For the first 10 minutes the scanned mass range was 10 to 85 atomic mass units at 300 milliseconds. After 10 minutes on the scanned masses were 50 to 650 mass units at 1000 milliseconds. This allows for increased sensitivity of low molecular weight products which come out in the beginning of the chromatogram. The second scan also activated the Ion Trap function on the MS to eject problematic ions associated with breakdown of the column's siloxane backbone. This allowed for a relatively flat baseline at elevated temperatures.

4.2.3.2 Hexane and Triethyl Phosphate

For analysis of liquid samples, injector A was configured for normal operation in splitless mode at a constant temperature of 300°C. Injector B was held constant at 400°C. The GC oven initially contained one column, a RX-1ms megabore from Restek, which is detailed in section 4.4.2.1. Both hexane and triethyl phosphate were analyzed with the same analytical methods to minimize error and downtime in the experiments. During the course of experiments, a second column was added through the use of a two column adapter nut. This allows the catalyst effluent to be split between two columns, and subsequently analyzed by two different detectors. The column was a RT-QPlot column made by Restek (Bellfonte, PA, USA), and was 30 m x 0.53 mm. The setpoints when the system contained a single column were as follows: Oven temperature was held

at -40°C for 3.0 minutes then ramped at 5°C per minute to 10°C. It was then ramped at 25°C per minute to 50°C followed by a 10°C ramp to 204°C. This gave a total run time of 30.0 minutes. Total column flow was 10.0 mL per minute at -20°C. When the system was modified to hold two columns, there was no longer a need to separate the products with cryogenic cooling. Therefore, the oven temperature was held at 40°C for 1.0 minute then ramped at 8°C per minute to 300°C. This was held for 6.5 minutes giving a run time of 40.0 minutes. Total column flow was 10.0 mL per minute at -20°C.

Originally the mass spectrometer was set to run two different methods on each sample due to the wide range of products under analysis. For the first 10 minutes, the scanned mass range was 10 to 85 atomic mass units at 300 milliseconds. After 10 minutes, the scanned masses were 50 to 200 mass units at a rate of 500 milliseconds. After the addition of a second column, the MS only analyzed higher weight compounds, while the TCD handled the low MW molecules. The method was therefore switched to a single segment, with the scan range set from 40 to 300 mass units with a scan rate of 700 milliseconds.

Chemical ionization was also used with the MS to help identify products. The ionization gas was acetonitrile (ACN), and gave results of m+1. Settings for CI mode were a scan range of 40 to 300 mass units with a scan rate of 700 milliseconds.

4.2.4 Thermogravimetric Analysis

Analysis was performed with a Versa Therm HS Thermogravimetric Analyzer (TGA) manufactured by Thermo Cahn Inc. (Waltham, MA, USA). This instrument

allowed the measurement of the amount of coking produced in the cracking reaction as well as reduction in acidity of the catalyst. The setup also included an FT-IR, but the sample cell was too large for the sample to give an accurate reading. Data were analyzed with the ThermalAnalyst software bundled with the TGA.

4.2.4.1 Coke Removal

Removal of coke was performed at elevated temperatures in the presence of air to facilitate burnoff. A sample of coked material approximately 2 – 10 mg was placed in the sample boat and the machine closed. Flow rates were set to 35 mL per minute helium to keep the balance cool and isolated, while the air stream passing over the catalyst was set to 30 mL per minute. After flow rates were set, the balance was allowed to equilibrate for at least 10 minutes. The sample was then heated from ambient to 600°C at a rate of 10°C per minute and held there for 10 minutes. It was then allowed to cool at a maximum of 10°C per minute. The air passing over the catalyst reacted with coke on the surface and in pores to produce CO_2 which left the system. After the sample had cooled to its starting temperature, the experiment was repeated on the same sample to produce a blank run. As the inert gas surrounding the sample was heated during a run, the gas density changes depending on the temperature profile used. Known as a buoyancy effect, it can change the weight recorded by the instrument. The blank run was used to correct for buoyancy effects in the system by subtracting the weight change of the sample experiencing weight loss. Plots of weight vs. time and weight vs. temperature show an

initial drop for loss of water formed during the reaction and absorbed into the catalyst since its removal. A second drop was indicative of coke burnoff.

4.2.4.2 Hoffmann Reaction

Determination of acidity reduction was performed by a Hoffmann elimination reaction with the HZSM-5. The Hoffmann reaction is used to measure the number of acidic active sites left on a catalyst through desorption of a base from the active sites. If a coked sample was to be analyzed it was first decoked using the method described previously. A sample of coked material approximately 2 – 10 mg was placed in the sample boat and the machine closed. Flow rates for the TGA were set to 35 mL per minute helium to keep the balance cool and isolated while the inert nitrogen stream passing over the catalyst was set to 30 mL per minute. After setting the flow rates, the balance was allowed to equilibrate for at least 10 minutes to ensure a stable reading. If the sample was of fresh catalyst, then a run would be performed to remove any water absorbed onto the catalyst while in storage. If the sample had just been decoked, then one could assume no water was present in the sample. After the drying run, the sample was exposed to n-propylamine in one of two ways.

First, a glass bubbler filled with n-propylamine was connected in-line with the inert nitrogen stream and the vapor was allowed to flow over the catalyst. Second, the sample was removed from the TGA and suspended in a capped vial above a layer of liquid n-propylamine. In both cases, the vapors were allowed to adsorb onto the catalyst until the weight was constant. The sample was then placed back in the TGA (if

removed), and the weight allowed to stabilize once more. The sample was then heated from ambient to 500°C at a ramp rate of 10°C per minute and held for 20 minutes. Plots of weight vs. both time and temperature showed two main drops in mass. The first due to physical desorption and the second due to chemical reactions as the n-propylamine decomposes into propylene and ammonia. The weight loss of the sample was then used to calculate the number of active sites on the catalyst.

4.3 Extraction of Lipids from Sewage Sludge

Several different methods were used to collect and process sludge used in this study, depending on origin and type of material.

4.3.1 Chemicals

Methanol, acetone, 1,3-dichlorobenzene, sulfuric acid, sodium chloride, and *n*-hexane were purchased from Fisher Scientific, Atlanta, GA. Industrial grade carbon dioxide was provided by NexAir, Memphis, TN. These chemicals were used as received.

4.3.2 Sewage Sludge

Secondary sewage sludge was collected from a municipal wastewater treatment plant (MWWTP) located in Tuscaloosa, AL. It was collected from the aerobic waste sludge line, which fed into the anaerobic digester.

4.3.3 Sample Preparation

Upon collection at the facility, the sludge flocks were allowed to gravity settle. Separation of the clarified water resulted in a sludge containing 2% solids. This sludge was dewatered by centrifugation or pressure filtration. Centrifugation was performed with a Marathon 3000 centrifuge, manufactured by Fisher Scientific, and operated at 3000 rpm for 20 minutes. Removal of the free water resulting from this step gave a sludge containing 7-8% solids. Pressure filtration was conducted with a Millipore 1.5 L pressure filter pressurized in 69 kPa increments from 103-517 kPa. Sludge was first filtered using an 80 μm nylon filter with the filter cake collected for later use. The filtrate was then filtered again with a 20 μm nylon filter and the cake combined with that from the 80 μm run. The remaining sludge cake contained 12-14% solids.

4.3.4 Organic Solvent Extraction

Prior to organic solvent extraction, dewatered sludge was mixed with Hydromatrix (manufactured by Varian, Inc., Palo Alto, CA) and loaded into a steel sample vessel. The Hydromatrix absorbed residual free water in the sample and competed for bound water during extraction. Hydromatrix was added until the sample formed small pellets and flowed freely. Solvent extraction was conducted using a 200 Series Accelerated Solvent Extraction system (ASE) (manufactured by Dionex, Sunnyvale, CA), which included a multi-solvent control system. The system was operated at 10.3 MPa and 100 °C for 1 hour per extraction. Single or sequential (2 or 3 times) extractions were examined using the following solvent mixtures (% by volume) or pure solvents:

1. 60% hexane/20% methanol/20% acetone (HMA) (same mixture 3 times)
2. Pure methanol followed by pure hexane (MH)
3. Pure hexane (single extraction)
4. Pure methanol (single extraction)

After extraction, the sample vessel was drained into a glass collection vial followed by a solvent flush equal to 50% of the sample vessel's volume. The lipid-containing solvent vial was then stored at -15°C until further analysis. Each experiment was performed in duplicate except for extraction with pure hexane, which was a singlet.

4.3.5 In Situ Transesterification

A fluidized bed drier was used in the same manner as the supercritical CO_2 extraction unit to achieve a sample with 5% moisture content. The dried sludge was then ground in a mortar and pestle until a fine powder was obtained. A screw-top vial was then charged with 1 mL of 1% sulfuric acid in methanol and 200 mg of powdered sample. The vial was then capped and heated overnight at 50 °C. Then, a 5 mL aliquot of 5% NaCl (w/v) in water was added and the FAMEs were extracted with hexane (2 x 5 mL), vortexing the vial between extractions to provide efficient mixing. The hexane phase was washed with 2% sodium bicarbonate and dried over sodium sulfate. The experiment was performed in duplicate.

4.3.6 Analysis of Fatty Acid Methyl Esters

After extraction, the lipid-containing solvent phase was removed under vacuum in a Büchi R205 Rotary Evaporator (rotovap) at 40 °C and 15-30 kPa of vacuum. The resulting liquid oil was weighed using an Ohaus analytical balance. The yield of extracted material was then determined and expressed as grams of extractable lipid per gram of dry solid.

Conversion of the lipids to FAMEs for extraction with organic solvents was carried out through acid catalysis using a modified version of Christie's method [86]. 20 mg of lipids were dissolved in 1 mL of hexane containing 1,3-dichlorobenzene as an internal standard and added to a vial with 2 mL of 1% sulfuric acid in methanol. The vial was then capped and heated overnight at 50 °C. Then, a 5 mL aliquot of 5% NaCl in water was added and the FAMEs were extracted with hexane (2 x 5 mL), vortexing the vial between extractions to provide efficient mixing. The hexane phase was washed with 2% sodium bicarbonate and dried over sodium sulfate.

Transesterification of lipids from SC-CO_2 extractions was performed in an Erlenmeyer flask. The flask was charged with 0.1-0.2 g of lipid and 10.0 mL of *n*-hexane. 4.0 mL of 0.5 N sodium methoxide was then added and the mixture refluxed for 10 minutes. The flask was allowed to cool and 5.0 mL of 14.0% BCl_3 was added. The mixture was refluxed for 10 minutes and was dried by filtering through sodium sulfate.

The FAMEs produced by transesterification were analyzed on an Agilent gas chromatograph (Model 6890; Palo Alto, CA) with a flame-ionization detector. Helium was used as the carrier gas. The separation was achieved with a fused silica capillary

column composed of stabilized 90% polybiscyanopropyl/10% cyanopropylphenyl siloxane (SP-2380; Supelco, Bellefonte, PA). The dimensions of the column were 100 m x 0.25 mm with a phase thickness of 0.2 μm. A calibration curve was prepared by injecting known concentrations of an external standard mixture comprised of 37 fatty acid methyl esters (47885-U, 37 Component FAME Mix, Supelco, Bellefonte, PA). All calibration curves were linear with a correlation coefficient of 0.99 or better. 1,3-Dichlorobenzene was used as an internal standard. The method consisted of injecting 1 μl of sample into the GC with a split ratio of 100:1. The temperature program began at 110 °C, holding for 2 minutes. It then increased by 10 °C per minute to 140 °C, where it was held for 4 minutes. After 9 minutes of total run time, the temperature increased 2 °C per minute until reaching 240 °C. The temperature was then held constant until a total run time of 99 minutes was achieved. Concentration data obtained from GC runs were used to calculate the amount of saponifiable material in extracted lipids. Only compounds with a concentration greater than 1% were counted toward the total FAME. Software bundled with the instrument was used to analyze the data.

4.4 Heterogeneous Catalysts

The heterogeneous catalyst chosen for this project was a Silica / Alumina zeolite catalyst called ZSM-5. It is a highly ordered, small pore zeolite catalyst, which has been well characterized by industrial and academic sources. However, the low hydro and thermal stability preclude its widespread use in petroleum refining. ZSM-5 is composed of a SiO_2 framework with molecules of Al_2O_3 inserted into the 3-dimensional structure.

The crystals are grown in liquid phase systems, the constituents of which include SiO_2, Al_2O_3, Na_2O, H_2O, and tetrapropyl ammonium hydroxide (TPA-OH) in different ratios, depending on the desired catalyst properties [87,88]. This is heated at 150 to 175 °C for 12 hours to 8 days, then allowing the mixture to cool. Water is then driven off at elevated temperature to dry the catalyst. The resulting crystal structure is composed of tetrahedral silica and aluminum atoms in the form of SiO_4 and AlO_4. Aluminum that is attached to 4 other framework sites in the crystal structure is called framework aluminum. Other types of aluminum bonding exist, and are defect sites in the crystal where Al is attached by at least one covalent bond. While silica is neutral in the tetrahedral state, aluminum acquires a negative charge which is balanced during formation by bonding of the TPA-OH. After the zeolite is grown and dried, it can be calcined at 500°C which converts the aluminum-bound ammonium to ammonia and an H^+ [89]. The ammonia then leaves the catalyst in the gas phase resulting in an acidic site on the framework. This site is characterized as a Brønsted acid site, and is responsible for the major catalytic activity of ZSM-5. Brønsted acids are defined as proton donors, while Lewis acids are defined as electron acceptors. Once the zeolite has been calcined, the name can be written as HZSM-5 to denote the acidic site form. In contrast, steam treatment of HZSM-5 results in the removal of aluminum from the framework. This switches the active sites from Brønsted to Lewis acid sites, held on the non-framework aluminum. A sample of HZSM-5 with no Lewis acid sites, and hence no defects, is considered one of the strongest solid acid catalysts [90].

Due to the ability of crystal structures to share and transfer charges between atoms in the lattice, the acidity of an aluminum site increases as the distance between neighboring aluminums increases. This creates a tradeoff between the acidic strength of a catalyst and the number of active sites it can have per unit volume. A sample of ZSM-5 is considered a superacid if the ratio of Si/Al_2 is greater than 10 – 12. This is important since saturated hydrocarbons require superacid-strength sites to initiate carbocations [91]. Two different strengths of catalysts were used in the experiments, with Si/Al_2 ratios of 23 and 280. The ZSM-5 23 catalyst has a much lower acidity than the ZSM-5 280 due to its higher aluminum content, which means the active sites are closer together. While this reduces the strength of active sites, it leaves many more active sites available for reaction. When referring to a zeolite's Si/Al_2 ratio, the number given is usually obtained by elemental analysis. However, only the aluminum atoms which reside in the crystal framework and have a tetrahedral configuration provide active Brønsted acid sites. The ratio of active aluminum atoms is therefore larger than that given through elemental analysis. The catalysts used were purchased from the commercial supply company, Zeolyst Inc.

The catalysts used in this study were crushed to a particle size of approximately 5 μm, and have a surface area of 300 m^2 / g. Pore size is on the order of 5.5 angstroms. Zeolite catalyst will retain moisture from the air if left exposed to ambient conditions. This can be removed by heating the catalyst in a stream of dry nitrogen or helium. When constructing catalyst beds for insertion into the Quatra C, it was necessary to know the percent moisture of the sample in order to make calculations based on activity. To do

this, samples of the catalyst were dried in a thermogravimetric analyzer as described in Chapter IV. A sample trace of ZSM-5 280 is shown in Figure 4.2. The equilibrium moisture content for ZSM-5 23 was found to be 6.80% while ZSM-5 280 was 2.79% by weight. The catalyst beds were constructed of fire-polished glass tube, packed with glass wool and catalyst. Their construction is detailed in Chapter IV.

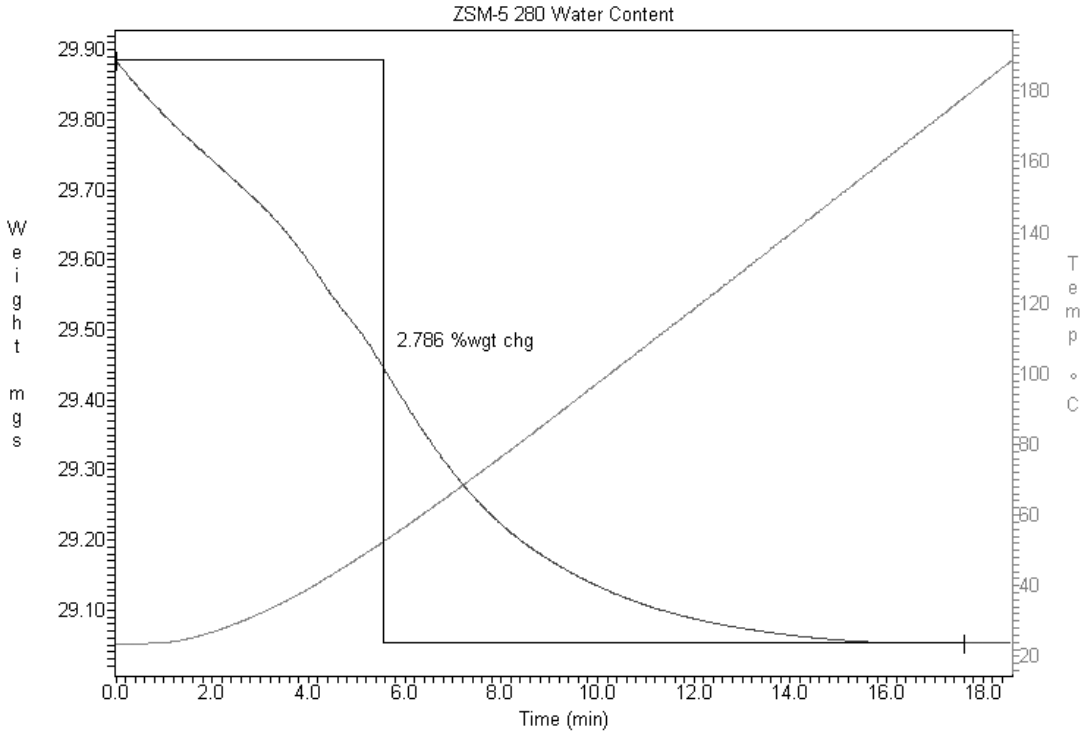

Figure 4.2

TGA Trace Showing Entrained Water Removal in a Zeolite Sample

CHAPTER V

HOMOGENEOUS CATALYTIC CRACKING OF LIPIDS WITH TRIFLIC ACID

This phase of the project focused on superacid cracking of methyl palmitate with trifluoromethanesulfonic acid (TFMSA). Methyl palmitate was used as a model compound of a simple glyceride. The use of TFMSA allows for cracking at lower temperatures than heterogeneous zeolite catalysts such as ZSM-5. TFMSA also contains only Brönsted acid sites, while zeolites may contain a mixture of Brönsted and Lewis acid sites. This makes it easier to model reaction pathways and interpret results. Performing cracking reactions in the liquid phase could therefore allow for prediction of products formed in heterogeneous reactions. TFMSA is also resistant to oxidation and reduction, and does not act as a source of fluoride ions [92]. Finally, the reaction with homogeneous catalyst will not suffer any pore diffusion effects that may be present in heterogeneous catalysts.

5.1 Methyl Palmitate

5.1.1 Effect of Acidity

In initial attempts to determine the reaction rate, it became apparent that the rate was so fast accurate measurements were difficult or impossible to achieve. At lower temperatures, the methyl palmitate solidified, and no solvent could be found which would not react with triflic acid. It was decided that diluting the triflic acid with a weaker acid, which was incapable of cracking lipids on its own, would allow calculation of the reaction order and rate. Trifluoroacetic acid (TFA) was chosen due to its similarity to TFMSA and the ability to create an acid system with Hammett acidities of ⁻14.1 to ⁻2.7 [93,93]. Analysis of methyl palmitate after reaction with TFA for one hour showed no statistical difference from the initial reactants. Table 5.1 gives compositions of acid mixtures employed in mixing the acids.

Table 5.1 Hammett Acidity of Trifluoroacetic Acid and Triflic Acid Mixtures

Ho	Mol Fraction		Mass Fraction		Volume %	
	TFA	Triflic	TFA	Triflic	TFA	Triflic
-14.1[a]	0.000	1.000	0.000	1.000	0.000	1.000
-13.0[b]	0.248	0.752	0.200	0.800	0.216	0.784
-12.2[a]	0.535	0.465	0.466	0.534	0.490	0.510
-11.9[a]	0.631	0.369	0.565	0.435	0.589	0.411

[a] Data obtained from [94]
[b] Data obtained from [95]

Experiments to determine the effect of acidity on conversion of methyl palmitate were carried out as described in Chapter IV. The results are shown in Figure 5.1. Using a fixed temperature and time period, the fractional conversion of methyl palmitate

demonstrated a linear dependence on the Hammett acidity of the reaction medium. Since TFMSA is a Brönsted acid, this is strong evidence that the cracking mechanisms of methyl esters are dependent on the Brönsted acidity. This is an important link in modeling the cracking behavior of lipid compounds on heterogeneous catalysts. Heterogeneous catalysts, such as ZSM-5, are composed of active sites which are predominately characterized as having Brönsted acidity. These catalysts are used in industry cracking reactions to produce many valuable products. A cracking reaction which is linear with respect to the Hammett acidity allows the formation of models which could predict conversion at different levels of system acidity.

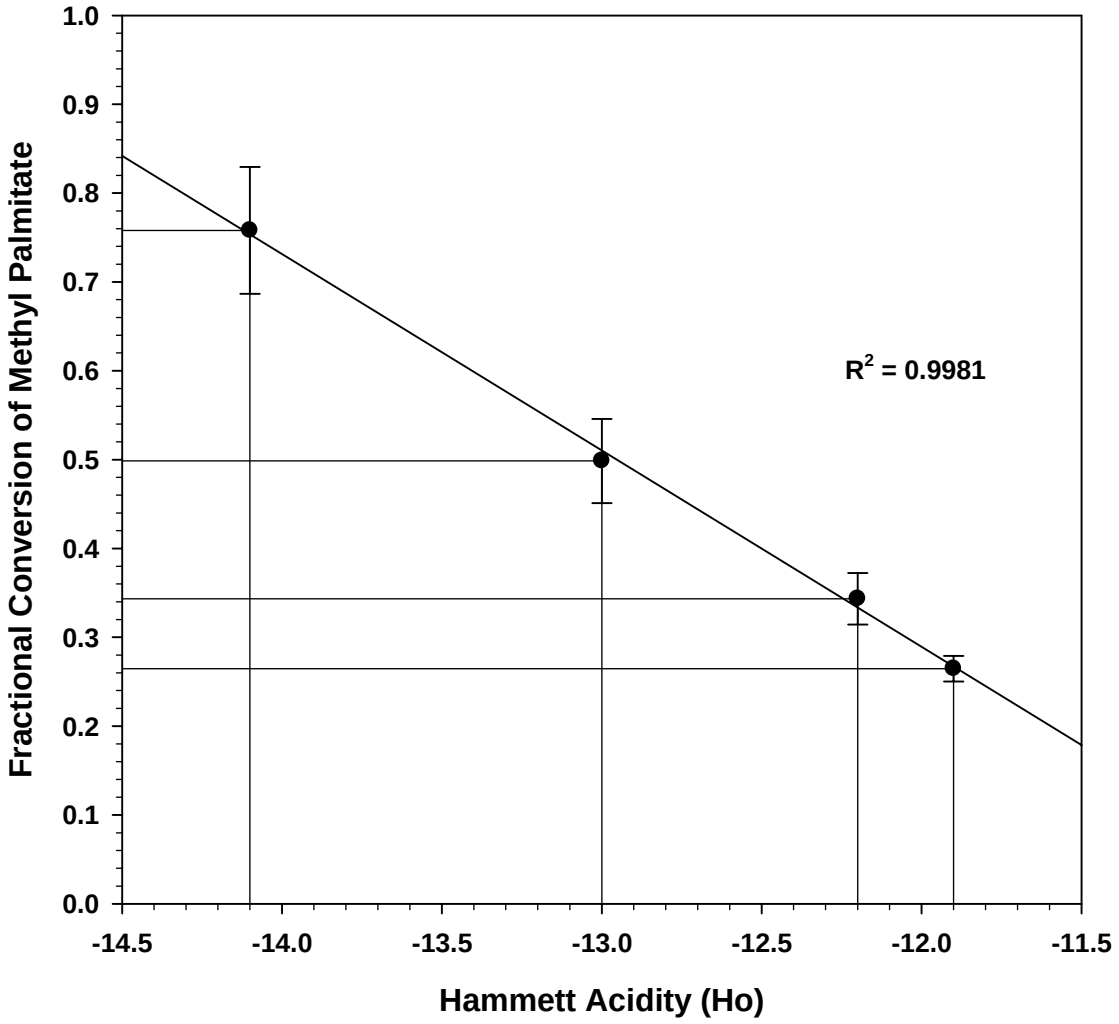

Figure 5.1

Conversion of Methyl Palmitate vs. Ho at 50°C for 10 Minutes

Palmitic Acid

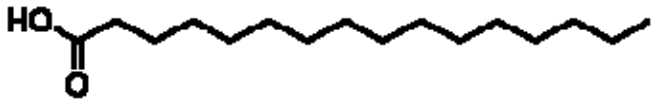

Palmitic Acid Methyl Ester

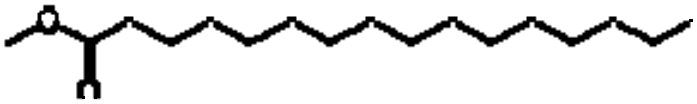

Phosphatidylethanolamine

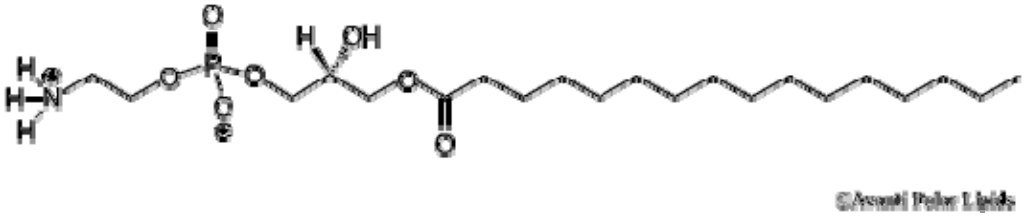

Di- phosphatidylethanolamine

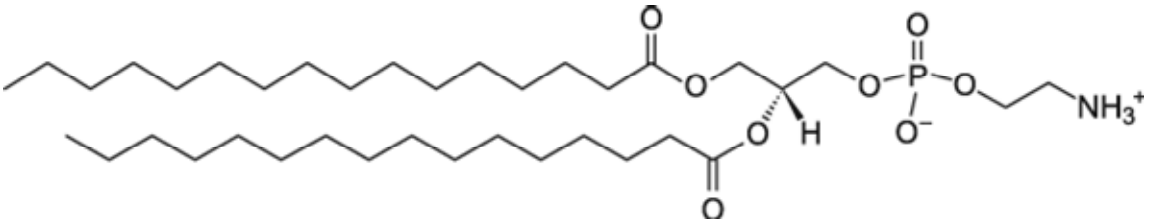

Figure 5.2

Model Compounds Used in Reaction Studies

5.1.2 Reaction Pathways

The original experimental plan was to crack both palmitic acid and methyl palmitate, followed by 1-Palmitoyl-2-Hydroxy-sn-Glycero-3-Phosphoethanolamine (LPE). The reaction products would then be compared. This would give an indication of products and pathways as the substrate increased in complexity, shown in Figure 5.2. However, it was found during experiments performed by other researchers in the group that palmitic acid showed no detectable reaction with triflic acid. This is in contrast to the reaction of methyl palmitate, which proceeds readily even at sub-ambient temperatures.

In an effort to explain the difference in observed reaction outcomes the two systems were modeled using Spartan Molecular Modeling Software (Wavefunction, Inc., Irvine, CA). In simulating the lowest energy configuration of the two systems, it was found that the palmitic acid and triflic acid formed an acid dimer with either a hydrogen and oxygen or hydrogen and fluorine of TFMSA. Methyl palmitate was attacked by TFMSA on either the carbonyl or ester oxygen. The formation of a dimer is common in systems containing organic acids, and represents a lower energy state than the monomer. Quantitative simulation results give the palmitic acid – TFMSA dimer a molecular strain of 46.8 kcal / mol, with a heat of formation of -446.5 kcal / mol. The methyl palmitate – TFMSA simulation had a molecular strain of 76.9 kcal / mol, and heat of formation of -434.5 kcal / mol. This suggests that the palmitic acid – TFMSA dimer represents a stable low-energy configuration, which requires a large amount of available energy to escape the potential well and produce a reaction.

5.1.3 Kinetic Determination

Methyl palmitate was reacted with a TFA/TFMSA acid mixture having a Hammett acidity of ¯11.9 for 5, 10, 15, 30, 45, and 60 minutes at 50°C. The samples were then analyzed according to Chapter IV, Section 4.1.5.1. The data were imported into Polymath where conversion of methyl palmitate was fit to the rate law $-r_a = k'[Ca]^{\propto}$. Regression was used to determine that $\alpha = 3$. The rate law was then substituted into the equation for a batch reactor, $C_{A0}(dX/dt) = k' \cdot C_A^3$. The value for conversion (X) was obtained from Figure 5.1 using linear regression and is defined as $X = -0.221 \cdot \text{Ho} - 2.363$, where Ho is the Hammett acidity of the system. This allows for the determination of k' for any value of Ho, where k' [=] $\text{L}^2/(\text{mol}^2 \cdot \text{min})$.

$$k' = \frac{11.16}{(C_{A0}^2 \cdot t + 0.5)\,(15.217 + \text{Ho})^2}$$

The data was then fit to the equation $k' = k(-Ho)_0^{\beta}$. The activity of the catalyst is assumed to be constant due to the 12:1 molar excess of acid. After substitution, the main rate equation becomes

$$N_{A0}\frac{dX}{dt} = k(-Ho)_0^{\beta'} C_A^{\alpha} \cdot V$$

The final calculated values are $k = 2.95x10^{-20}$, $\beta = 16.93$, and $\alpha = 3$.

The calculated values of k' for the Hammett acidities used in the experiment are shown in Table 5.2. Using the calculated the relationship of $k' = k(-Ho)_0^{\beta}$, one can also calculate concentration vs. time data and compare them to experimental results, this is shown in Figure 5.3. As expected, the rate of reaction increased with increasing acidity

of the system. However, it does not follow the same linear trend as conversion when compared to the Hammett Acidity.

Table 5.2 Calculated Values of k' Based on Hammett Acidity of Trifluoroacetic Acid and Triflic Acid Mixtures

Ho	Conversion	k'
-14.1	0.7531	0.9014
-13.0	0.5100	0.1852
-12.2	0.3332	0.0731
-11.9	0.2669	0.0504

k' [=] $\mathrm{L}^2/(\mathrm{mol}^2 \cdot \mathrm{min})$

5.1.4 Product Distribution

The liquid phase products of methyl palmitate reacted with triflic acid were analyzed as described in Chapter IV. Figure 5.4 shows a standard chromatogram for the liquid phase. The large peak at 34 minutes is the initial reactant, methyl palmitate. The second large peak at 38 minutes is ethyl palmitate, formed during the reaction. Between the two is a small peak of palmitic acid at 35.5 minutes. There are also a large number of smaller peaks at the low end of the time scale which represent products formed during reaction.

The majority of compounds in the sample are isomers of fatty acid methyl and ethyl esters with small amounts of the corresponding acid. Ethers, ring structures, and hydrocarbons were also seen in small amounts. Due to the large number of compounds present in the liquid the products were grouped according to isomer carbon number and compound class.

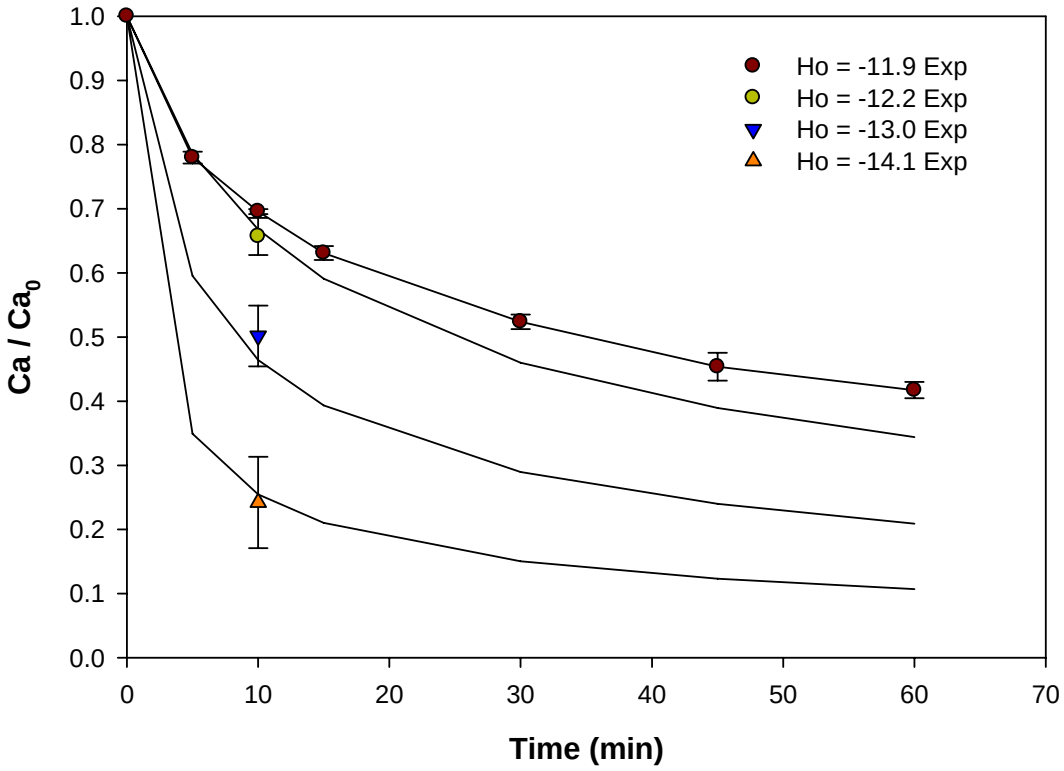

Figure 5.3

Experimental and Calculated Conversion of Methyl Palmitate vs. Time at 50°C
(TFMSA/TFA Catalyzed with 12:1 Molar Ratio Acid:Reactant)

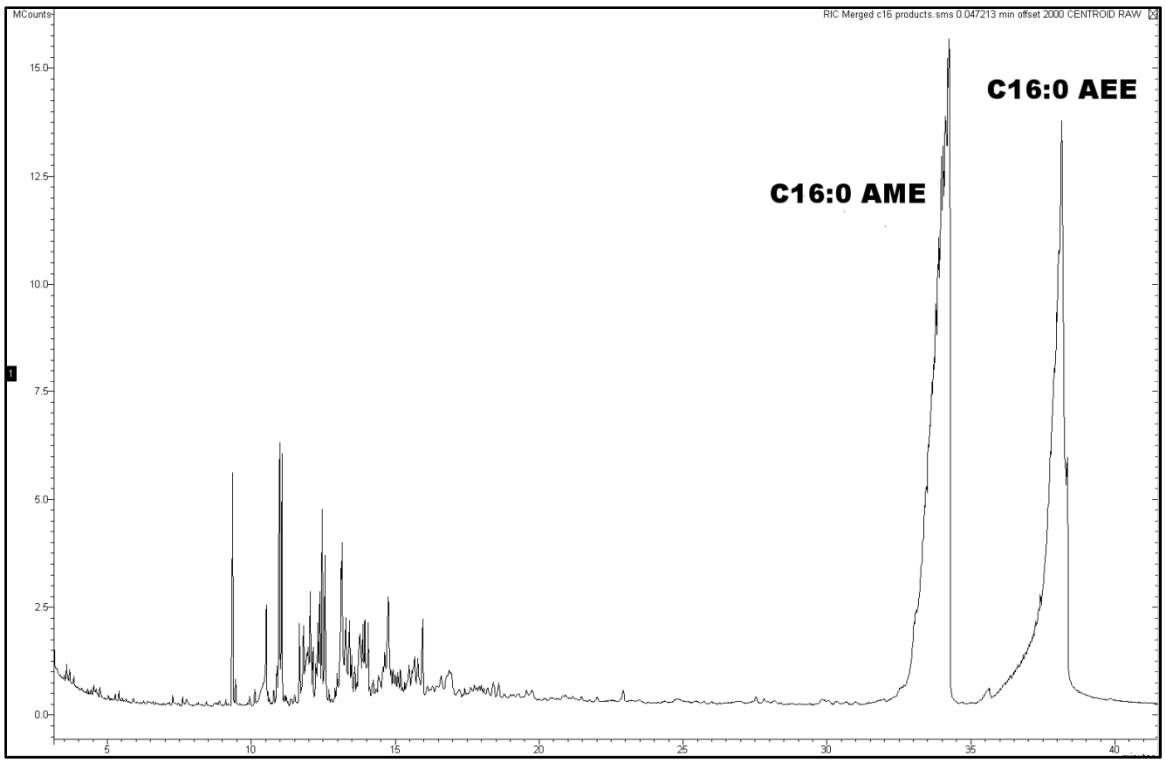

Figure 5.4

Total Ion Chromatogram of Liquid Phase Methyl Palmitate Cracking Products
(TFMSA/TFA Catalyzed with 12:1 Molar Ratio Acid:Reactant)
(10 minute Reaction @ 50ºC)

Table 5.3 lists the percent area of products, excluding the methyl and ethyl palmitate. An examination of the data shows that most ester isomers contain nine or ten carbons tails. Although the octanoic isomers were lower in total area, there was only one isomer product compared to the others, which contain four or more. Trace amounts of fatty acid isomers were also detected down to propanoic AME (C3:0). The largest amounts of hydrocarbons were seen in ten-carbon chains, with trace amounts of lower molecular weight species. It is hypothesized that the low MW compounds escape to the gas phase. A gravimetric mass balance on the liquid phase shows that 74.5% of the

starting mass remained after a reaction. Aromatics and naphthenes attached to an ester remnant tend to form ring structures near the ester end of the molecule. Since no evidence was found of pentadecanoic AME (C15), it is thought that the cracking process starts with the β-scission of two or three carbons from the tail of methyl palmitate to give tetradecanoic or tridecanoic AME. The primary cation would then collapse to a double bond, or remain as a cation and migrate closer to the alkyl end of the molecule. Remaining carbons in the tail could then undergo molecular rearrangement to form highly branched compounds. Isomerization of alkanes is a known effect of TFMSA systems and has been shown to follow first order kinetics [96]. Once branching has occurred, β-scission could take place at secondary or tertiary carbons, resulting in further cracking of the compound. Ethyl esters could be formed by substitution of the methyl group by ethane from β-scission.

The gas phase products were analyzed as described in Chapter IV, Section 4.1.5.2. Due to lack of standards, only the relative area percentages could be reported. These data are shown in Table 5.4. The majority of identified products are straight-chain alkanes and branched-chain isomers with six to seven carbons atoms. There is also a considerable amount of cyclopropane.

Table 5.3 Liquid Phase Composition of Triflic / TFA Reaction Products

Chemical Group		Area %
Ester Isomers		64.35%
Octanoic	C8	8.61%
Nonanoic	C9	26.01%
Decanoic	C10	26.09%
Undecanoic	C11	17.91%
Dodecanoic	C12	13.69%
Tridecanoic	C13	6.06%
Tetradecanoic	C14	1.63%
Carboxylic Acids		16.54%
Ethers		8.09%
Ring Structures		12.16%
Hydrocarbons		4.71%
Unknowns		3.22%

Table 5.4 Gas Phase Composition of Triflic / TFA Reaction Products

Compound	Area %
Cyclopropane	13.21%
2,2-dimethyl butane	8.88%
2,3-dimethyl butane	11.42%
2-methyl pentane	28.18%
3-methyl pentane	16.22%
n-Hexane	3.67%
2,2-dimethyl pentane	1.28%
2,4-dimethyl pentane	6.70%
3,3-dimethyl pentane	0.91%
2-methyl hexane	5.64%
3-methyl hexane	3.90%

Farcasiu has shown that hexane catalyzed by TFMSA will isomerize to 2,2-dimethyl butane, 2,3-dimethyl butane, 2-methyl pentane, and 3-methyl pentane [93]. All of these products were found in the gas phase as shown in Table 5.4, as well as five isomers of heptane: 2,2-dimethyl pentane, 2,4-dimethyl pentane, 3,3-dimethyl pentane, 2-

methyl hexane, and 3-methyl hexane. The presence of isomers with six and seven carbon molecules fits well with the data collected for the liquid phase, where the majority of products were nine- or ten-carbon esters. This suggests that while removal of one or two carbons at a time is occurring in the reaction, there is also a significant amount of cracking at the ninth or tenth carbon due to β-scission.

5.2 Phospholipids

For the second phase of homogeneous catalysis, phospholipids were cracked with TFMSA with hopes of obtaining the same data as for methyl palmitate. The experimental objective was to evaluate the effect of phosphorus on the rate and product distribution of lipid cracking. Unfortunately, this was not possible due to experimental complications regarding the physical properties of the phospholipids chosen for the experiment. The phospholipids used were 1-Palmitoyl-2-Hydroxy-sn-Glycero-3-Phosphoethanolamine (LPE) and 1,2-Dipalmitoyl-*sn*-Glycero-3-Phosphoethanolamine (DPPE). As shown in Figure 5.2, DPPE is identical to the LPE except that it has an extra palmitic acid tail in place of the hydroxyl group at position 2. Both of these compounds are very insoluble in pure solvents, requiring solvent mixtures to dissolve fully. Calibration curves were obtained for DPPE and LPE using an LC/MS as described in Chapter IV, with correlation coefficients of 0.99 or higher. Due to the nature of the experimental setup and analysis, however, the use of multi-solvent systems in the reaction was not possible. This meant that it was not possible to evaluate kinetic rate parameters since accurate conversion versus time data were unattainable. However, most

products formed were soluble in single-component systems. Thus, it was possible to collect information on initial products from the cracking reaction. Cracking of both LPE and DPPE were performed at the same experimental conditions as the methyl palmitate reactions; a 12:1 molar ratio of TFMSA to reactant at 50°C for 10 minutes.

Results from the cracking of LPE are shown in Figure 5.5. Although there are several compounds at the high end of the chromatogram, the majority of products are smaller molecules, eluting from three to twenty minutes. The products formed are highly cyclic, including tri- and tetramethyl benzene, phenols, hexatrienes, and xylenes. Remnants of the carboxylic acids were also found, such as 2-hexanoic acid ethyl ester. In comparison, cracking of DPPE showed that a single compound accounts for the majority of products. This is shown in Figure 5.6. The large peak at 30 minutes was identified as having a molecular weight of 256 as given by CI analysis. The EI identification shows that it has a good match to either heptadecanol or hexadecane-1,2-diol, as shown in Figure 5.7. This molecule can be formed by removal of the two palmitic tails from the glycerol backbone. The chromatogram also contains other higher molecular weight compounds, including nitrogen containing compounds from the ethanolamine, and the original reactant. From these results, it would appear that phospholipids with all glycerol bonds filled tend to split near or at the glycerol backbone, with the resulting compounds degrading to intermediates. These intermediates then slowly crack into lower molecular weight compounds. Phospholipids with a hydroxyl group in one position are degraded more completely, perhaps due to attack of the hydroxyl group at the middle glycerol position by TFMSA. In order to rule out degradation effects due to GC analysis, a

standard was created and analyzed using the same method as LPE and DPPE. This chromatogram of DPPE is detailed in Figure 5.8, and showed only minor thermal degradation.

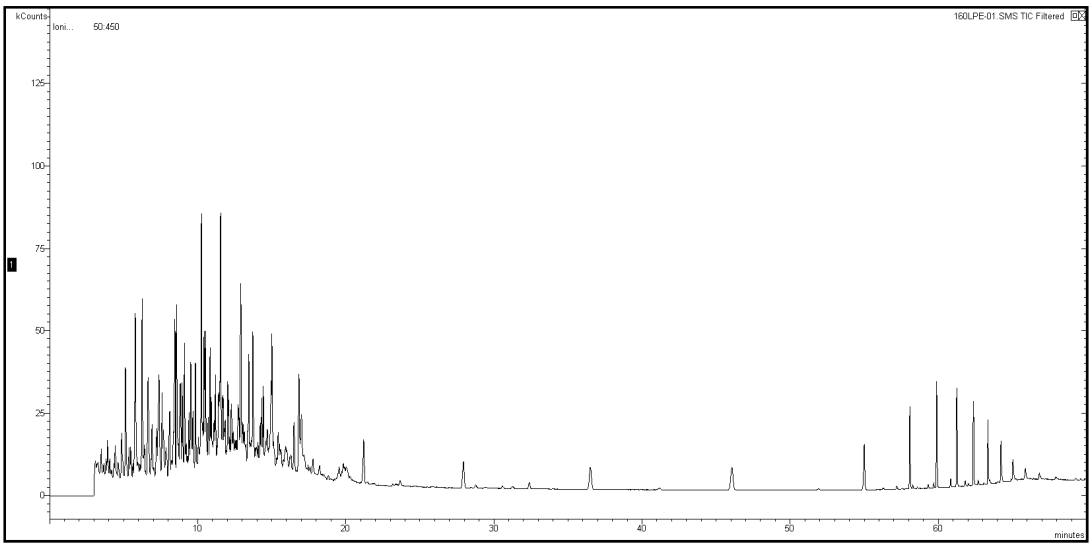

Figure 5.5

Total Ion Chromatogram of LPE Liquid Phase Cracking Products
(TFMSA/TFA Catalyzed with 12:1 Molar Ratio Acid:Reactant)
(10 minute Reaction @ 50ºC)

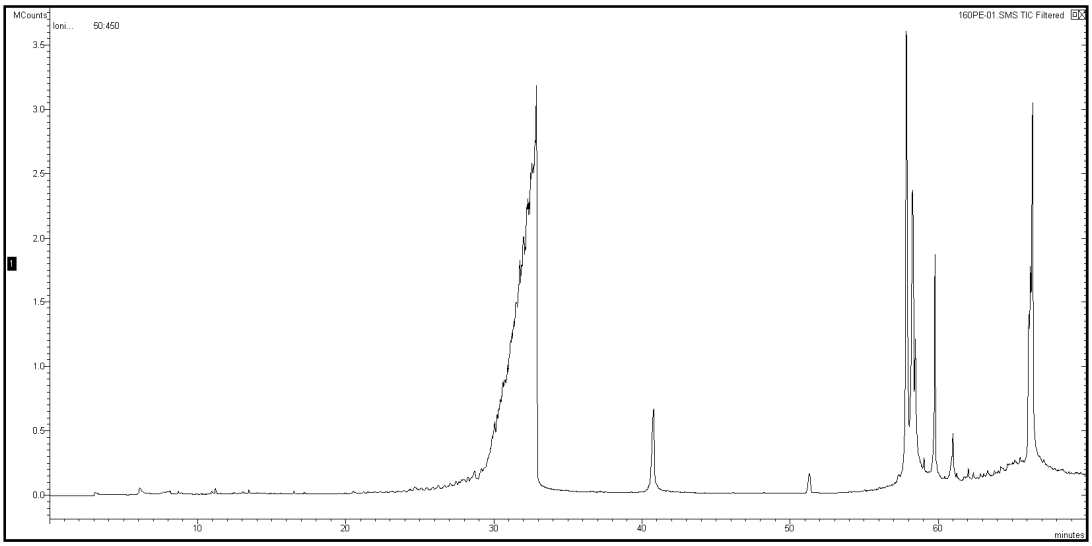

Figure 5.6

Total Ion Chromatogram of DPPE Liquid Phase Cracking Products
(TFMSA/TFA Catalyzed with 12:1 Molar Ratio Acid:Reactant)
(10 minute Reaction @ 50ºC)

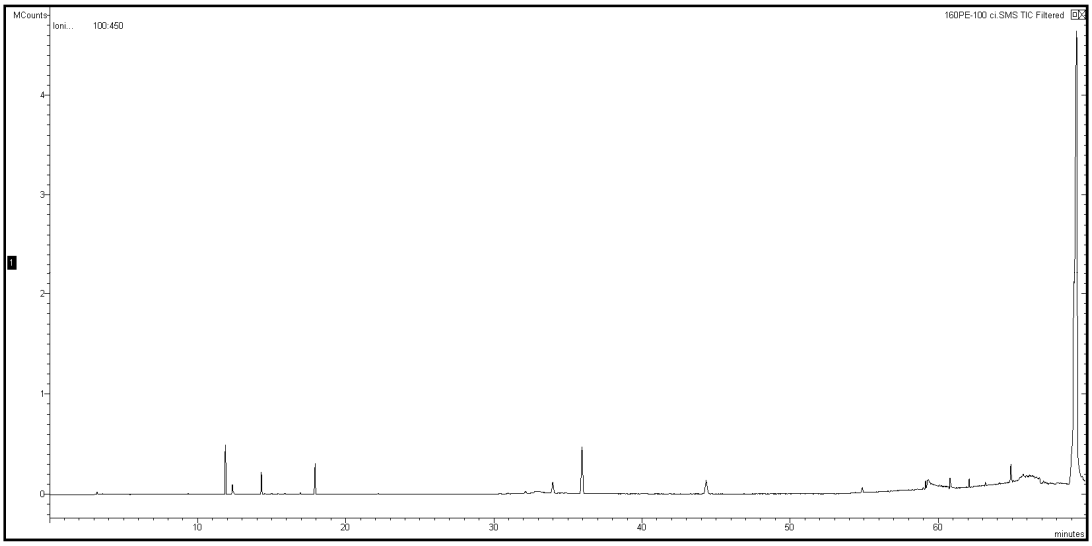

Figure 5.7

Total Ion Chromatogram of DPPE Standard Thermal Decomposition
(100 ng / µL DPPE in Chloroform)

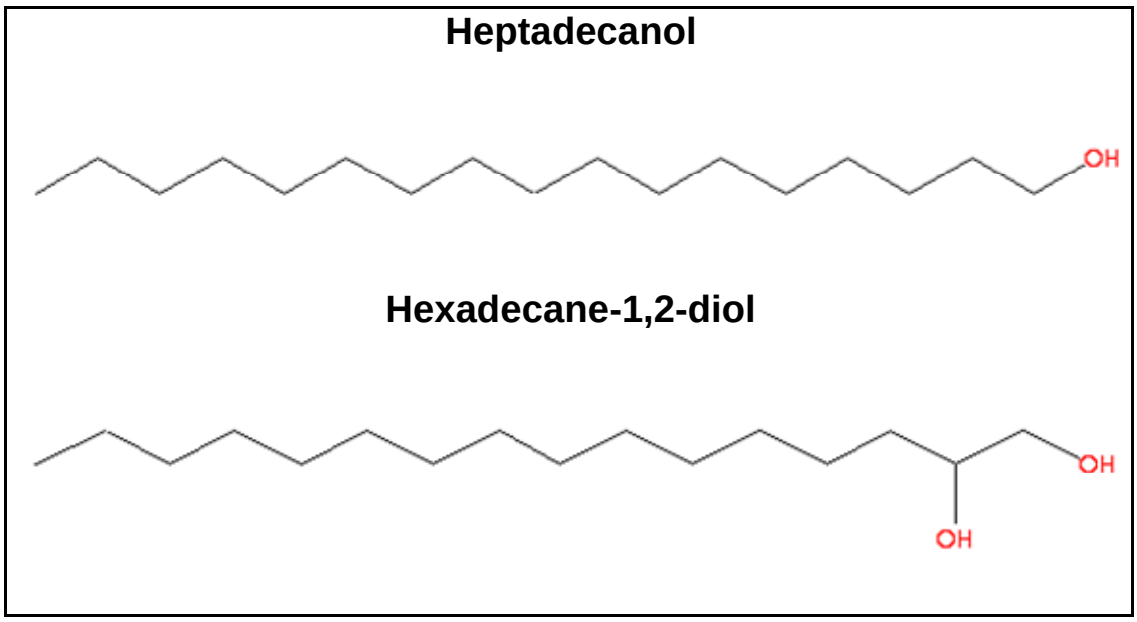

Figure 5.8

Possible Reaction Products of Phospholipid Cracking with Triflic Acid

5.3 Summary

Methyl palmitate was used as a simple molecule that comprises parts of the larger phospholipids found in bacterial sources. Cracking of this molecule allows for modeling of how it may react in heterogeneous catalyst systems used in industry. Methyl palmitate was cracked with mixtures of trifluoromethanesulfonic acid (TFMSA) and trifluoroacetic acid (TFA). Conversion was linearly dependent on the Hammett acidity of the system, with higher acidity giving faster conversions. The overall reaction order was found to be 3 with reaction rate being proportional to the system acidity. Major products are isomerized esters of shorter chain length than methyl palmitate. Ethers, ring structures, and hydrocarbons were also seen in small amounts. The reaction headspace was composed of C_6 - C_7 hydrocarbon isomers with a small amount of cyclopropane. In the

cracking reaction, β-scission on the ninth or tenth carbon gave the most common products. A mass balance on the liquid phase puts 25% of the starting mass in the headspace after reaction. The large amount of esters formed indicates that transition metal catalysts may be required to completely decarboxylate the reactant. Results on cracking of phospholipids with TFMSA show that they are easily reacted, giving a wide range of products. Initial cracking occurs near the phosphorous atom and may continue throughout the molecule depending on the configuration of functional groups on the glycerol backbone.

Phospholipids with a hydroxyl group in one position are degraded more completely, perhaps due to attack of the hydroxyl group at the middle glycerol position by TFMSA. No phosphorous was detected in compounds identified by GC/MS, suggesting that phosphorous was converted to water soluble compounds and removed during the water washing step.

CHAPTER VI

HETEROGENEOUS CATALYTIC CRACKING OF LIPIDS VIA ZSM-5

The processing of lipid sources via heterogeneous catalysis to create biofuels is not uncharted territory. Indeed, ConocoPhillips recently signed a deal with Tyson foods to "create a new type of diesel fuel made from beef, pork, and poultry fat" [97]. Although some work has been done on cracking of lipids for fuel production, there is a lack of literature regarding how different heteroatoms may affect catalyst performance. When examining the process of lipid extraction from microorganisms, such as algae or wastewater sludge, it becomes obvious that non-trivial amounts of phospholipids will be extracted with any oil obtained. It is therefore pertinent to establish what effects the cracking of such compounds will have on the catalyst and overall process in general.

6.1 Poisoning

The objective of this project was to measure the change in both activity of the catalyst and product distribution from cracking. It was decided to pass phospholipids over the catalyst and allow them to poison the ZSM-5. This would simulate poisoning of the catalyst in a commercial setting. Hexane would then be cracked as a probe reaction to determine how the phosphorous affected the catalyst, if at all. The reactions were

performed on a modified GC/MS, which could accept solid, liquid, or gas samples passing over a catalyst bed in vapor phase. This system is described in detail in Chapter IV.

6.1.1 Poisoning Through Phospholipids

Initially, only 1-Palmitoyl-2-Hydroxy-sn-Glycero-3-Phosphoethanolamine (LPE) was to be used in the cracking experiments, but 1,2-Dipalmitoyl-*sn*-Glycero-3-Phosphoethanolamine (DPPE) was also tried after a quantity was ordered for the homogeneous cracking experiments in Chapter VI. Structures of these molecules are shown in Figure 6.1. Since both LPE and DPPE are solids at room temperature the Chromatoprobe accessory was used on the Quatra C to allow injection of solid samples. However, when experiments were started we were unable to get the phospholipids into the vapor phase without severe and sometimes complete thermal degradation. Although compounds such as triglycerides can be partially volatilized in this manner with minimal degradation, addition of phosphorous to the molecule seems to greatly decrease the thermal stability.

Several experimental conditions were tried to minimize the thermal degradation. The injector temperature responsible for vaporizing the phospholipids (Injector A) was varied between 50° and 180°C per minute, with final temperatures of 250°, 275°, and 300°C. The injector's split ratio was also varied from 24, 44, or 200 mL per minute. Finally, the catalyst bed temperature was varied from 200° to 400°C. Even though thermal degradation was seen with an empty catalyst chamber, the set point of 400°C was higher than the upper limit of Injector A (InjA) and may cause further cracking. Figure

6.2 shows the result of slowly increasing the temperature of InjA to determine when DPPE started to decompose and vaporize. The initial decomposition started at 250°C, while the melting point of DPPE is only 200°C. This is shown in Figure 6.3 where the final ramp temperature was varied from 250 to 300°C. At 300°C the amount of total and cracked material are much larger than at 250°C. The first major peak, at 28 minutes, has been identified as hexadecanenitrile. This was followed by the dominant product peak at 30 minutes. This peak is a mixture of hexanoic acid and hexanoic acid methyl ester. Varying the split ratio changed the speed at which material was swept out of the injector bed. This turned out to have a pronounced effect on the products of thermal cracking, as shown in Figure 6.4. The split ratio of 24 mL / min showed a major product peak followed by two smaller product peaks trailing off of it. As the split ratio increases to 200 mL / min the major product peak changes as a function of residence time in the injector, with the dominant ion switching from 239 to 265. Changing the catalyst bed temperature from 400 to 200°C greatly reduced the amount of degradation observed. Figure 6.5 is normalized for scale, and shows a much larger peak for the main product at 200°C. The timescale has been shifted for easier viewing; the two largest peaks on each trace overlap each other in raw data.

Some experiments were also performed using a load of catalyst in the reactor. Figure 6.6 shows the results of cracking DPPE with and without a catalyst load, at a catalyst bed temperature of 400 °C. As observed with the catalyst loading of 0 and 200 mg, the types of products produced remain relatively the same. This would suggest that

ZSM-5 cracks the phospholipid in the same spot as thermal decomposition, while the major product is stable enough to avoid further cracking at these retention times.

1-Palmitoyl-2-Hydroxy-sn-Glycero-3-Phosphoethanolamine (LPE)

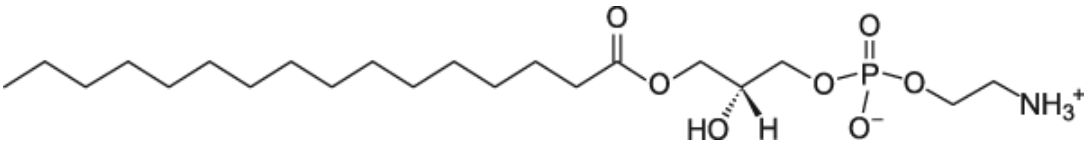

1,2-Dipalmitoyl-*sn*-Glycero-3-Phosphoethanolamine (DPPE)

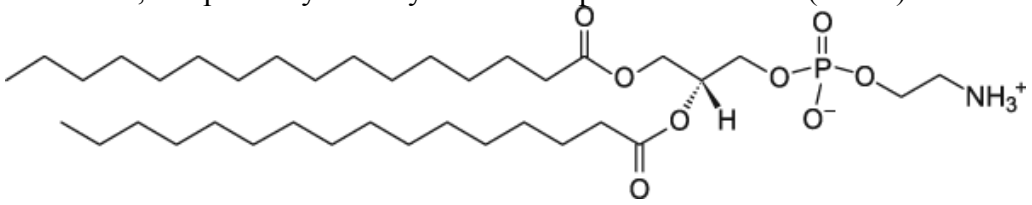

Triethyl Phosphate (TEP)

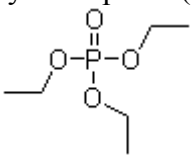

Figure 6.1

Molecular Structure of Phospholipids and Simulant Compound

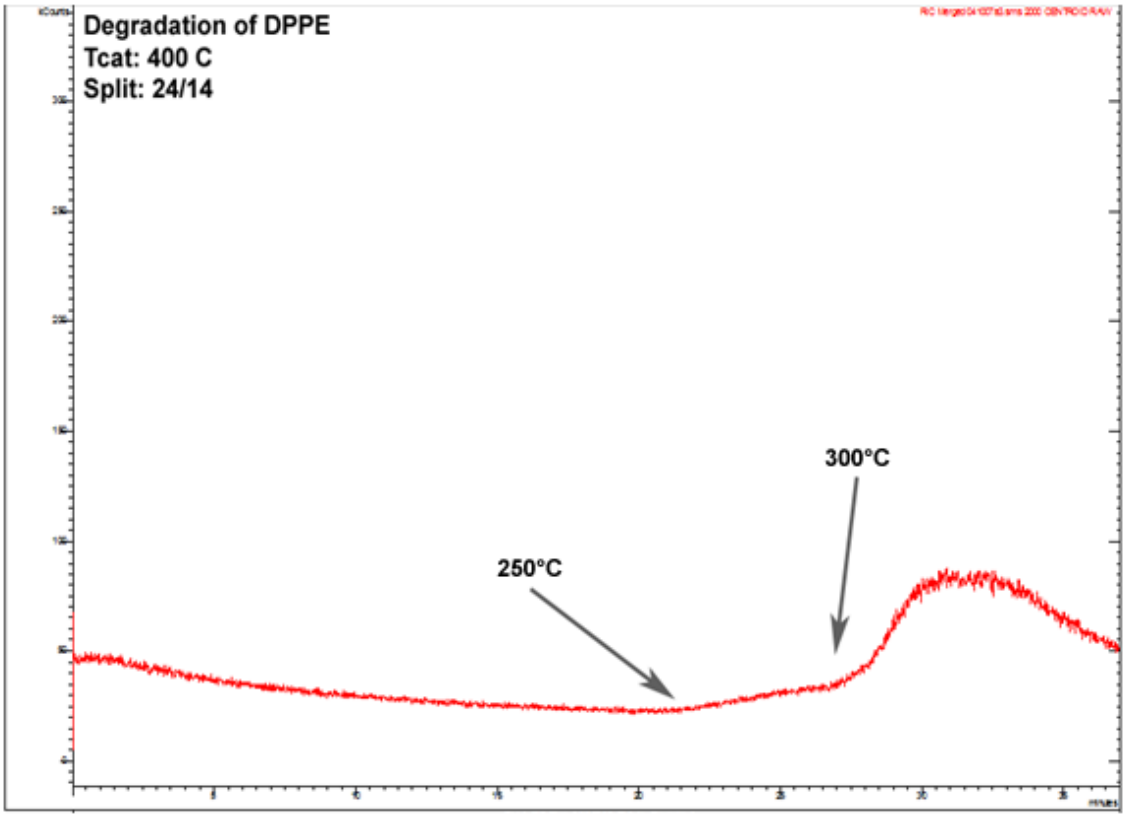

Figure 6.2

Thermal Decomposition of DPPE vs. Temperature
Tcat = 400°C, Inj A Split Flow of 24/14 mL / min

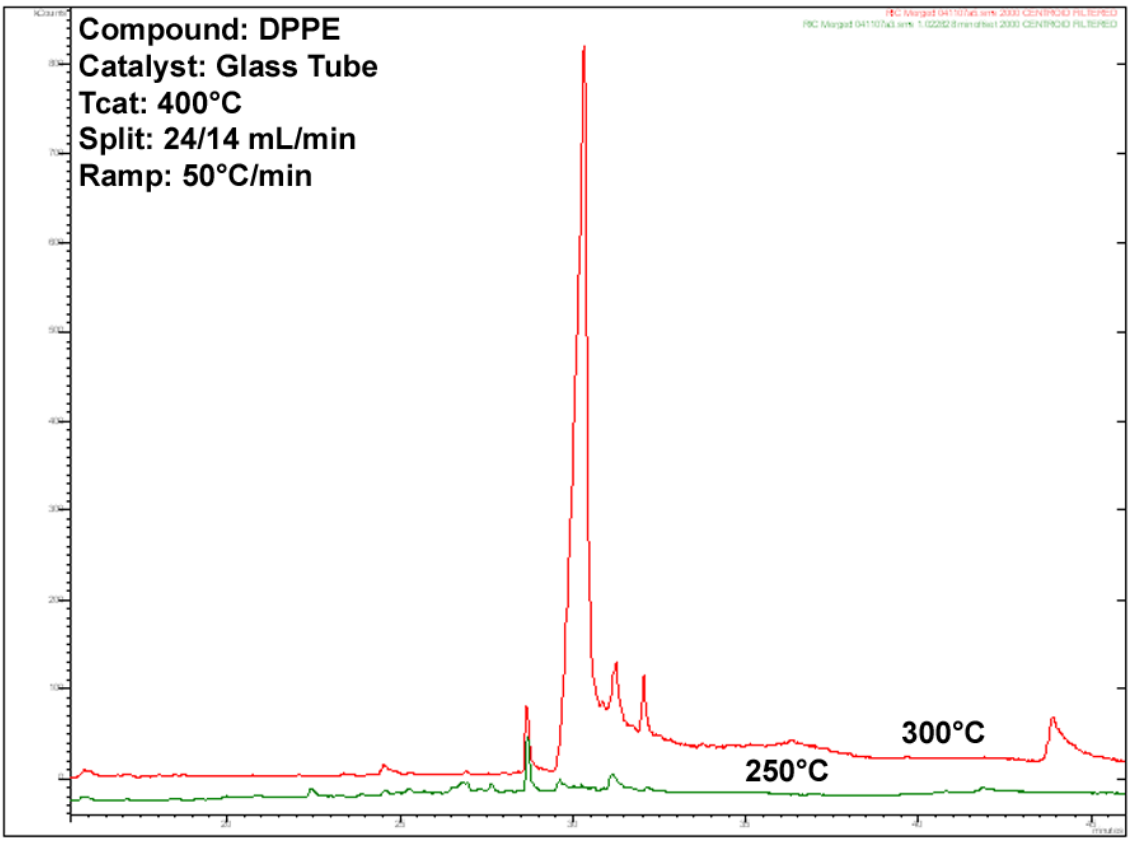

Figure 6.3

Thermal Decomposition of DPPE vs. Final Injector Ramp Temperature
Tcat = 400°C, Inj A Split Flow of 24/14 mL / min
Ramping at 50°C / Minute

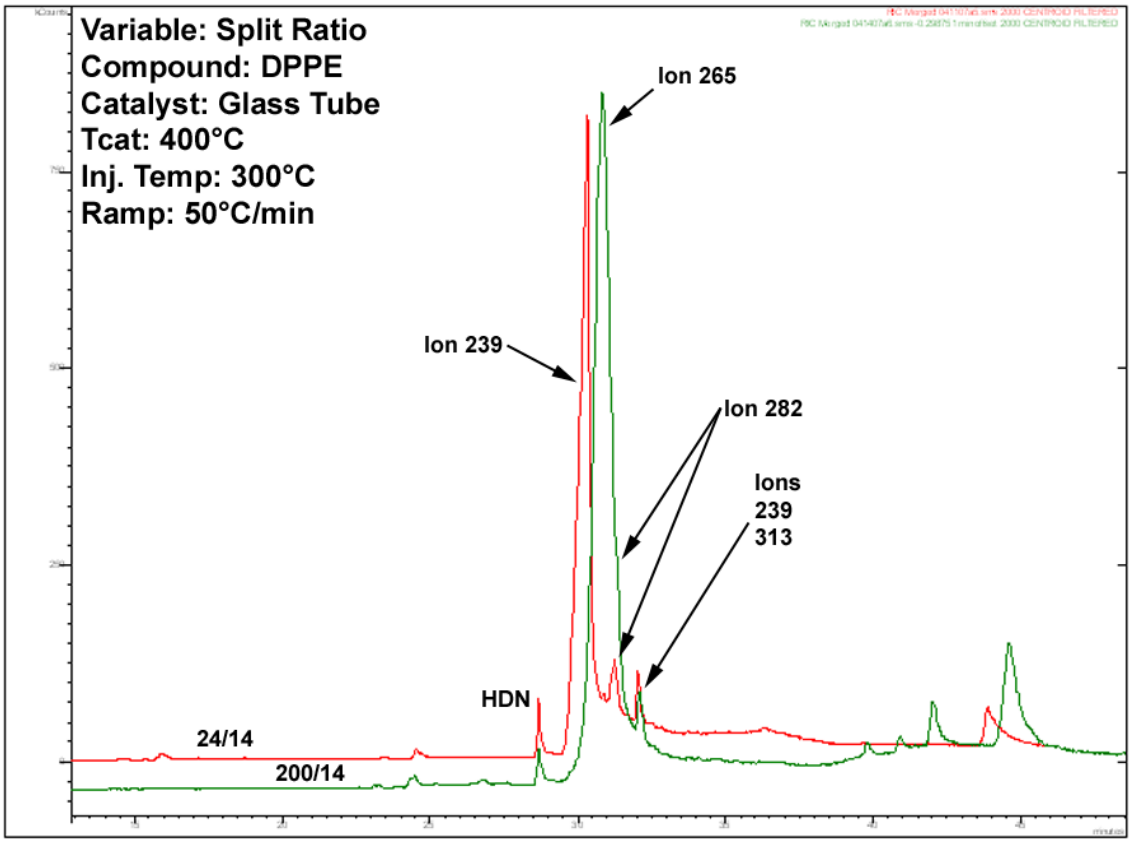

Figure 6.4

Thermal Decomposition of DPPE vs. Injector Split Ratio
Tcat = 400°C, Inj A Temperature 300°C
Ramping at 50°C / Minute

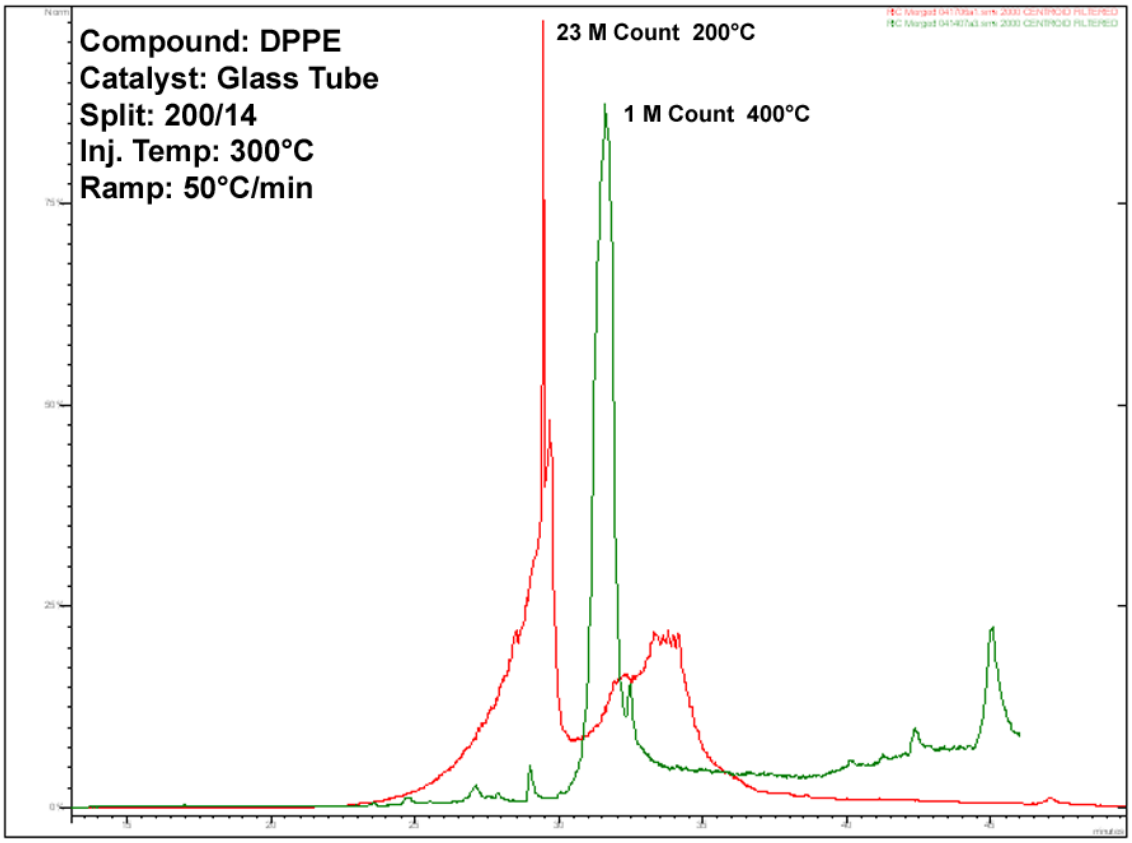

Figure 6.5

Thermal Decomposition of DPPE vs. Catalyst Bed Temperature
200/14 Split Ratio, Inj A Temperature 300°C
Ramping at 50°C / Minute

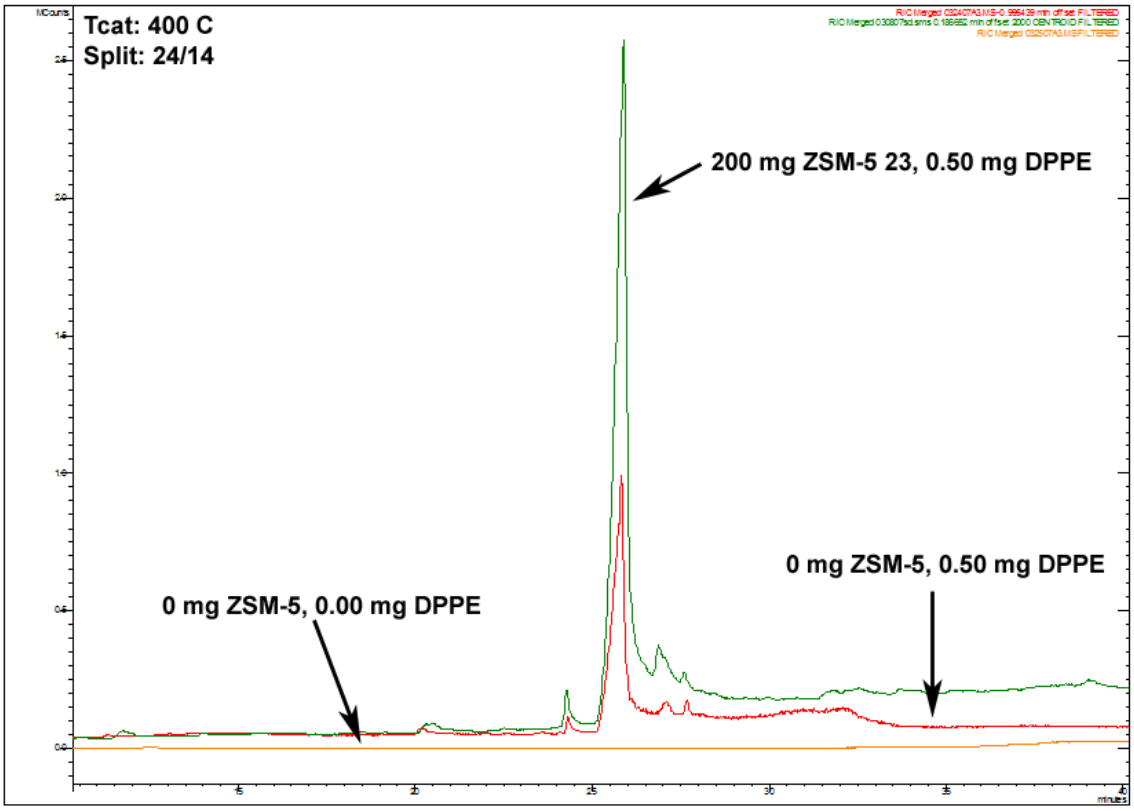

Figure 6.6

Effect of Catalyst on Thermal Decomposition of DPPE
Tcat = 400°C, Inj A Split Flow of 24/14 mL / min
Ramping at 50°C / Minute

6.1.2 Poisoning Through Triethyl Phosphate

Being unable to place intact molecules of phospholipids on the catalyst surface, other methods of phosphorous deposition were investigated. After a search of compounds, it was decided that triethyl phosphate (TEP) would be a good substitute for phospholipids, shown in Figure 6.1. The structure is similar to the bonding arrangement of phosphorous in lipids, raising the possibility of similar cracking effects. TEP also has a boiling point of 216 °C, allowing for vaporization without significant thermal degradation. Initial experiments with blank catalyst tubes showed minimal thermal degradation. It was decided to pass hexane over the catalyst, before and after poisoning with TEP, in order to elucidate the reaction changes. As mentioned in Chapter IV, experiments on the Quatra C can be classified into two major phases, analyses with one column and those with two. Initially, the single column required cooling to sub-ambient conditions in order to capture light gasses produced in the cracking reactions. A second column was added later to split the flow between the original column and one designed for light gases. This negated the need for cryocooling. When two columns were used, the original high boiling-point column was used for calibration of TEP while the low MW column was used for hexane. Both compounds were calibrated to a fit of $R^2 > 0.995$

In order to determine what effect, if any, the cracking of TEP would have on ZSM-5, several experiments were performed on the Quatra C. A catalyst bed was loaded with 50 mg of ZSM-5 23 and placed in InjB. After heating at 400°C until the evolved water subsided, 0.5 µL of TEP were injected through InjA. The split ratio on InjA was 200 / 14, giving a TEP catalyst loading of 0.65 nL per mg catalyst. This was repeated 3

times and the bed allowed to cool. Upon removal of the catalyst bed, it was noticed that the ZSM-5 had turned light gray in color instead of its normal white. This was taken as evidence of TEP cracking over ZSM-5.

6.1.2.1 Poisoning of ZSM-5 23

To record the effect of phosphate poisoning on ZSM-5, a catalyst bed was loaded with ZSM-5 23, placed in the Quatra C, and the bound water allowed to bake out. Hexane was then cracked over the catalyst twice to obtain a replicate and the reaction products recorded. TEP was then injected once, followed again by hexane. The catalyst was kept at 400°C during the cracking reaction. This was repeated several times to study the poisoning effect. Table 6.1 shows the experimental conditions for the initial poisoning of ZSM-5 with TEP, while Figure 6.7 gives the results. For the hexane injections, a vial was purged with helium, followed by addition of hexane. After equilibration, a headspace sample of 0.25 mL was injected into InjA; the TEP was also injected through InjA. As shown in Figure 6.7, the conversion of hexane starts around 11%, but drops to 5% after treatment with TEP. The conversion of hexane then increased, with the jump in conversion becoming successively larger after each treatment of TEP. Analysis of the chromatogram shows that, while the conversion of hexane increased, the mass of products exiting the catalyst bed decreased. Upon removal of the catalyst bed, it was discovered that the ZSM-5 was severely coked, leading to the possibility of autocatalytic coke formation. The rise in conversion could therefore be attributed to hexane forming coke on the catalyst surface, which also explains the

reduction in observed product mass. Analysis of the products, shown in Figure 6.8, shows a decrease in all compounds above three carbons while lower molecular weight compounds increased with phosphorous poisoning. Propane remained relatively constant throughout the experiment. The increase in low molecular weight products with increasing phosphate loading follows data in literature for both phosphate deactivation and coke formation [45,47,98]. Pore blockage in the catalyst results in only the smaller molecules being able to fit in the crystalline structure.

Table 6.1 Experimental Conditions for Initial Poisoning of ZSM-5 with Triethyl Phosphate

Experiment:	05077B					
Catalyst:	05077B		Flow rates at -40°C			
ZSM-5:	10.75	Mg	Inj A Split	0	mL / min	
	10.02	mg Dry Basis	Column Flow	10	mL / min	
Sample Name		Compound	Amount Injected		Amount on Catalyst	
05077B02		Hexane	0.25	mL	0.025	mL
05077B03		Hexane	0.25	mL	0.025	mL
05077B04		TEP	1.0	µL	0.1	µL
05077B05		Hexane	0.25	mL	0.025	mL
05077B06		Hexane	0.25	mL	0.025	mL
05077B07		TEP	1.0	µL	0.1	µL
05077B08		Hexane	0.25	mL	0.025	mL
05077B09		Hexane	0.25	mL	0.025	mL
05077B10		TEP	1.0	µL	0.1	µL
05077B11		Hexane	0.25	mL	0.025	mL
05077B12		Hexane	0.25	mL	0.025	mL
05077B13		TEP	1.0	µL	0.1	µL
05077B14		Hexane	0.25	mL	0.025	mL
05077B15		Hexane	0.25	mL	0.025	mL
05077B16		TEP	1.0	µL	0.1	µL
05077B17		Hexane	0.25	mL	0.025	mL
05077B18		Hexane	0.25	mL	0.025	mL
05077B19		TEP	1.0	µL	0.1	µL
05077B20		Hexane	0.25	mL	0.025	mL
05077B21		Hexane	0.25	mL	0.025	mL

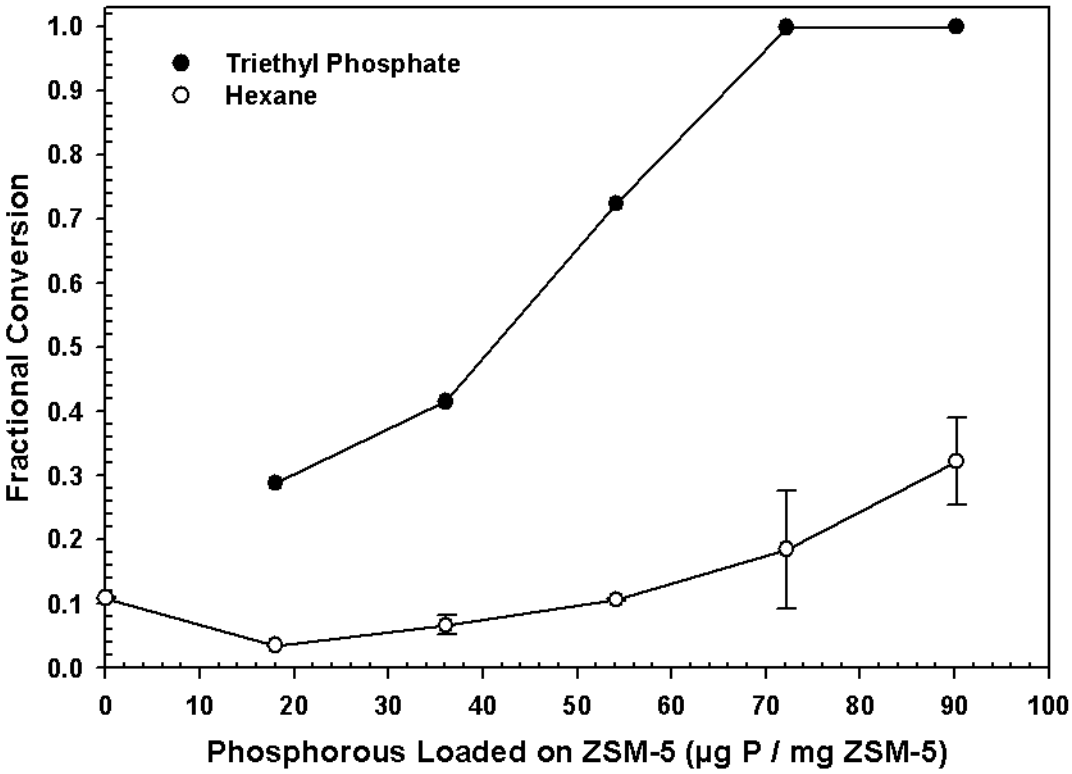

Figure 6.7

Initial Poisoning of ZSM-5 with Triethyl Phosphate
Hexane Conversion vs. Phosphate Poisoning

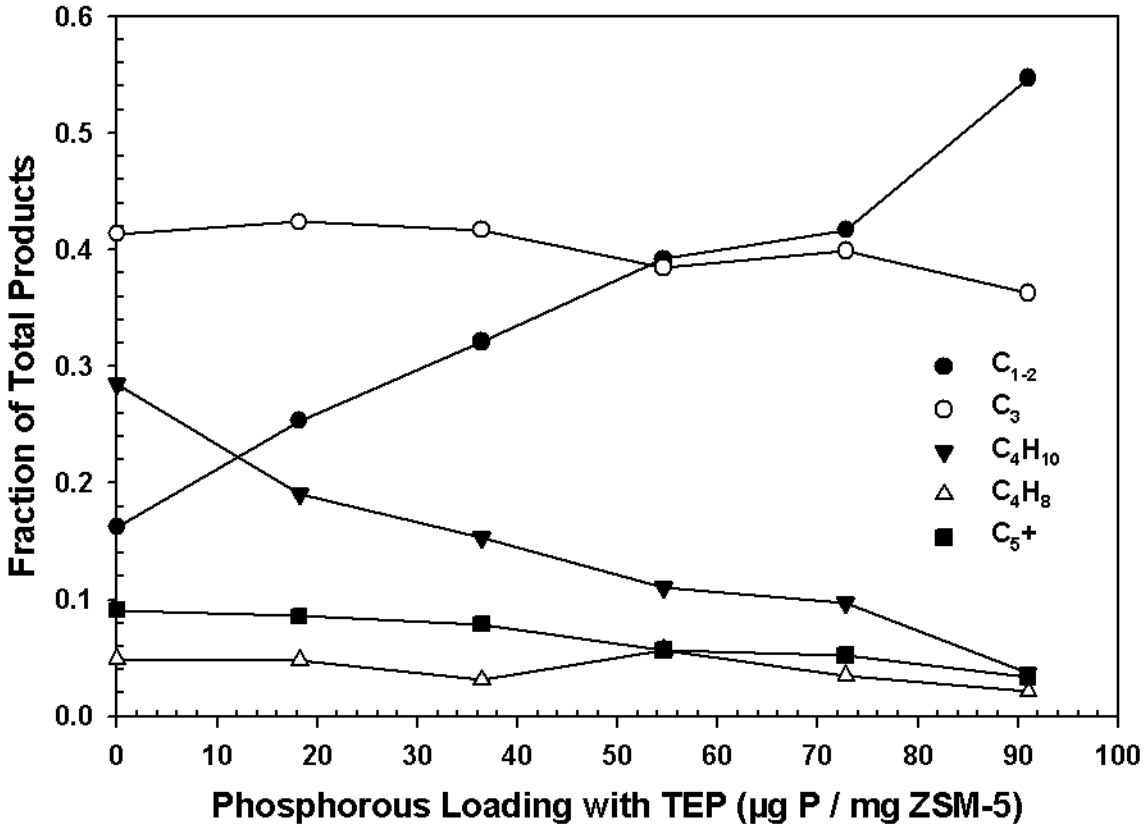

Figure 6.8

Initial Poisoning of ZSM-5 with Triethyl Phosphate
Product Distribution vs. Phosphate Poisoning

It was hypothesized that phosphorous had deactivated the catalyst within the first loading of TEP, since conversion of hexane stopped dropping at that point. To determine this, several experiments were carried out by injecting smaller amounts of phosphorous in an attempt to collect more data points from 0 to 20 µg of phosphorous loading per milligram of ZSM-5. Due to difficultly working with headspace injections the experiments were switched to liquid injections. Figure 6.9 shows that there was a gradual decrease in conversion as more phosphorous was introduced to the system, followed by a rise in conversion after obtaining a minimum. The change in overall conversion from Figure 6.7 is explained by an increase in the mass of catalyst from 10 mg to 20 mg dry catalyst. This was done to enable more accurate loading of the phosphorous onto ZSM-5 as well as giving enough poisoned catalyst per experiment to run other tests such as decoking experiments.

After this series of experiments, the Quatra C benefited from addition of a second GC column, allowing for increased sensitivity of low molecular weight compounds. The oven method was also changed to discontinue the use of cryogenic cooling. Experiments were then performed on small doses of phosphorous to study the effect of poisoning at the onset. A 20 mg load of ZSM-5 23 was placed into InjB and allowed to bake out. The same procedure was followed as before, with two injections of hexane followed by an injection of TEP. The practice of injecting a headspace sample of hexane vapor was also replaced with a standard injection of 1 µL liquid hexane. TEP was injected through the port on InjB, right on top of the catalyst. The results can be seen in Table 6.2.

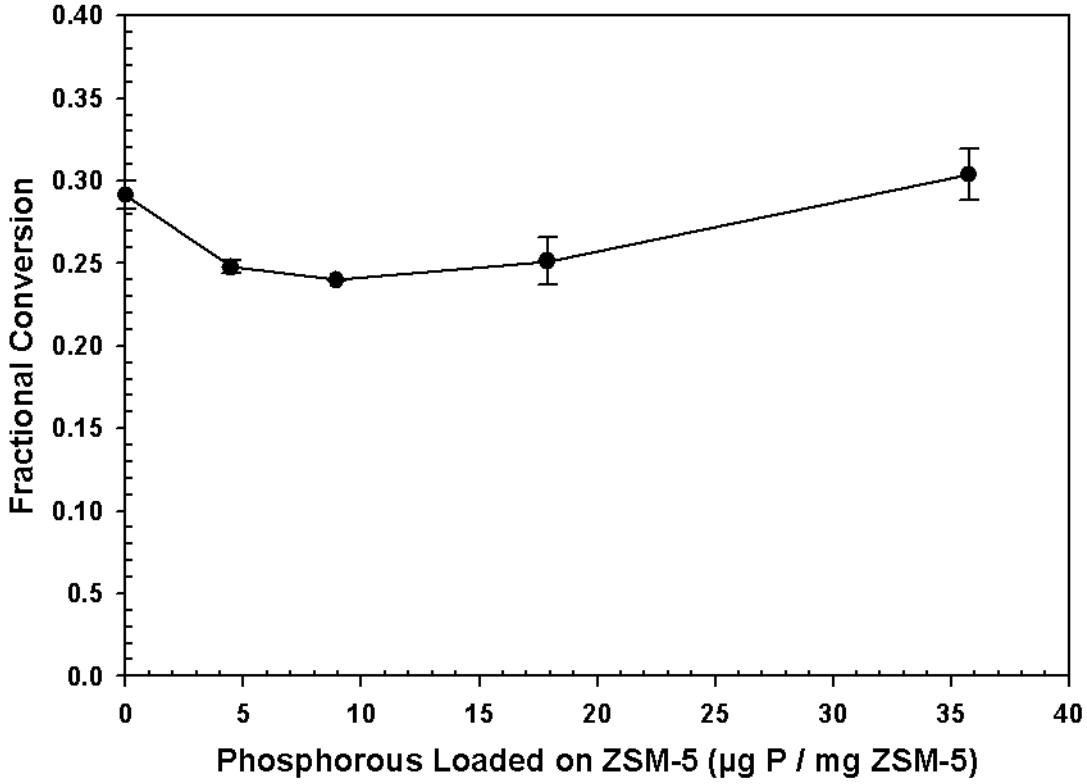

Figure 6.9

Initial Poisoning of ZSM-5 with Triethyl Phosphate
Examination of Low Phosphorous Loading

Table 6.2 Poisoning of ZSM-5 23 with Triethyl Phosphate Examination of Low Phosphorous Loading on Product Distribution

	Phosphorous Loading (µg)		
	0	0.46	1.38
Product Distribution	Mass % Based on Phosphorous Loading[a]		
C_{1-2}	3.87%	3.43%	3.15%
C_3	47.67%	46.37%	45.24%
C_4H_8	3.48%	3.90%	4.17%
C_4H_{10}	31.88%	32.64%	33.22%
C_5H_{10}	1.09%	1.23%	1.34%
C_5H_{12}	7.21%	7.48%	7.98%
C_6+	4.79%	4.96%	4.90%
Total Olefins	8.29%	8.95%	9.46%
Total Paraffins	87.11%	86.29%	85.92%
Total Aromatics	4.23%	4.36%	4.26%
Hexane Conversion	75.54%	73.81%	70.13%

[a]Significant to at least ±0.1%

Table 6.3 Product Distribution on Fresh and Regenerated ZSM-5 23

	Fresh	Regenerated
Product Distribution	Mass % of Total[a]	
C_{1-2}	6.03%	5.92%
C_3	45.51%	45.20%
C_4H_8	9.45%	10.20%
C_4H_{10}	26.61%	25.82%
C_5H_{10}	2.32%	2.98%
C_5H_{12}	7.09%	7.34%
C_6+	2.98%	2.54%
Total Olefins	28.56%	30.81%
Total Paraffins	68.78%	66.89%
Total Aromatics	2.31%	1.88%
Hexane Conversion	29.38%	22.99%

[a]Significant to at least ±0.01%

As before, the conversion of hexane decreased with increasing phosphorous loading. Olefin production also increased during poisoning, followed by a decrease in total paraffins. An increase in olefin production is undesired as it leads to lower octane fuel than paraffins [25]. The composition of aromatics remained about the same. It is also interesting to note that the decrease in conversion was linear with respect to phosphorous loaded on the catalyst, having a correlation coefficient of 0.999. This shows that in the early stages of catalyst poisoning, active sites follow a proportional trend for deactivation. This could be used to predict the lifespan of a catalyst in industrial processes, and used to set limits on the amount of phosphorous allowed in a catalytic cracking feedstock.

6.1.2.2 Catalyst Regeneration

A major concern of catalyst poisoning effects is whether or not the catalyst can be regenerated to a pre-poisoned state. To determine this, ZSM-5 23 was poisoned with TEP to 1.38 µg phosphorous per mg ZSM-5. A sample was then removed from the catalyst bed and regenerated in air at 500°C to remove all coke deposits. The regenerated catalyst was then loaded into a catalyst tube and the cracking activity of hexane measured. Both fresh and regenerated catalyst was used, with a catalyst weight of 4.1 mg and 0.25 µL hexane per injection. The cracking activity of fresh catalyst was measured as 0.1374 µmol hexane per mg of ZSM-5. Activity of the regenerated catalyst was measured at 0.1065 µmol hexane per mg of ZSM-5. This is significant in that it shows, while coke formed during cracking can be removed, the presence of phosphorous in

ZSM-5 still leads to a decreased activity. These results suggest that phosphorous is a permanent poison with regard to active sites of ZSM-5. Table 6.3 shows the product distribution from fresh and regenerated catalyst; as seen before, poisoning of the catalyst resulted in lower overall conversion. Total olefin production was also increased at the expense of paraffins and aromatics.

6.2 Sample Analysis

6.2.1 Coke Removal

Throughout all reactions of hexane and TEP over ZSM-5, there was noticeable deposition of coke on the samples. To study coke buildup on the catalyst samples, ZSM-5 23 was poisoned to the level of 1.38 μg phosphorous per mg ZSM-5. A representative sample of this was then placed in a thermogravimetric analyzer and heated in air at 600 °C. This caused combustion of the organic coke, which exits the TGA as carbon dioxide. The amount of coke present on the catalyst samples was too small for an accurate reading. This precluded quantitative analysis of coke formation.

6.2.2 Activity Determination

In an effort to determine the effects of phosphorous on ZSM-5, the active sites were examined both before and after poisoning. This was determined through use of the Hoffmann reaction performed in a TGA. In this procedure an amine, *n*-propylamine, is passed over a catalyst sample where it undergoes physical and chemical adsorption. The physical adsorption occurs on available pore surfaces while chemical adsorption occurs

on active Brønsted acid sites. The sample temperature is then raised in an inert atmosphere. Since physisorbed molecules are held only by the weak Van der Waals forces they are easily detached with elevated temperatures, leaving only chemisorbed *n*-propylamine above 500K. This temperature was shown to be the cutoff point for physical adsorption in literature [99]. The remaining amine is chemically bound only to the active catalyst sites. As the temperature increases, further chemisorbed *n*-propylamine decomposes into propylene and ammonia, which then exits the sample in gaseous form. The weight loss due to chemically bound amine leaving the catalyst can be used to calculate the moles of *n*-propylamine chemically bound. Since one molecule of amine is adsorbed per acid site, this allows calculation of the total number of active sites in a sample [99]. The Si/Al_2 ratio commonly supplied with zeolites is obtained from elemental analysis and does not reflect the ratio of active aluminum sites to silicon. It was determined that the ZSM-5 23 showed a weight loss during the Hoffmann reaction of 5.22%. This corresponds to an active site ratio of 36, slightly higher than the elemental ratio of 23. The ZSM-5 280 showed an active site ratio of 246. The higher ratio zeolites are more difficult to prepare accurately since the amount of aluminum added becomes very small. Figure 6.10 shows the two periods of weight loss during the Hoffman reaction for a fresh sample of ZSM-5 23. The first is physical desorption of *n*-propylamine followed by chemical desorption of propylene and ammonia. A comparison of Figures 6.10 and 6.11 shows that the chemically bound n-propylamine is a much smaller percentage of the adsorbed total in ZSM-5 280. This could be due to the smaller

number of strong acid sites required for bonding, while the pore volume available for physical adsorption remains relatively constant.

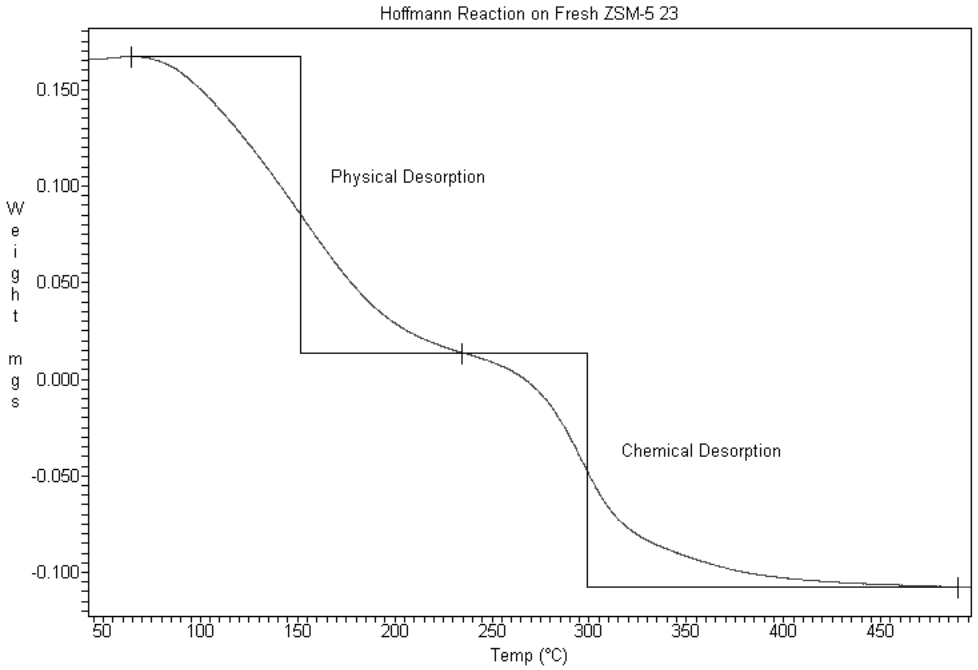

Figure 6.10

Hoffmann Reaction on Fresh ZSM-5 23 Catalyst

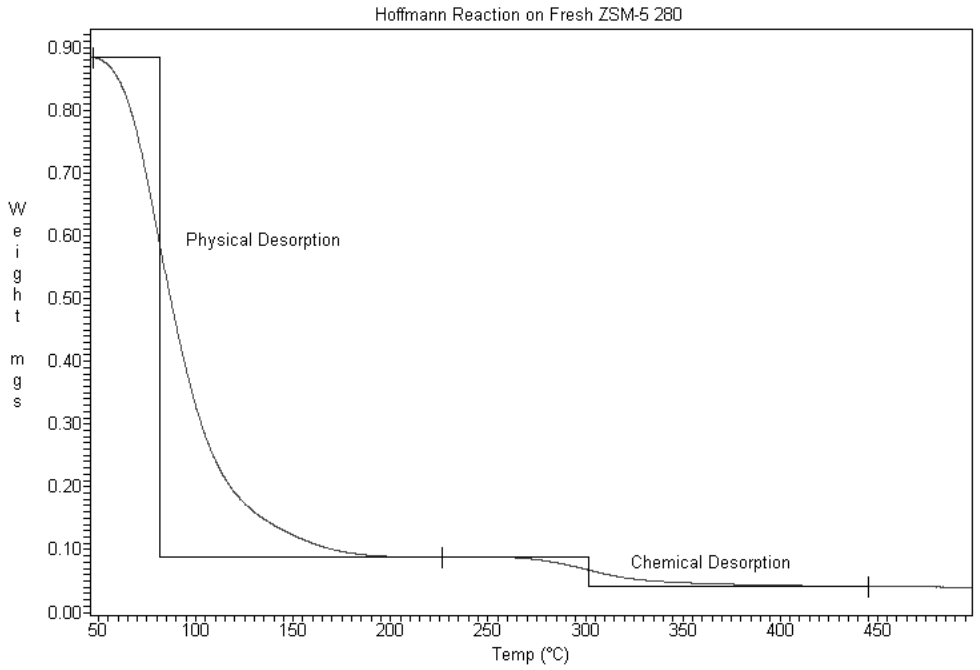

Figure 6.11

Hoffmann Reaction on Fresh ZSM-5 280 Catalyst

To measure how phosphorous poisoning affects the active sites on a zeolite, Hoffmann reaction results were compared for both fresh and poisoned samples. Samples of ZSM-5 23 were poisoned to a phosphorous loading of 1.38 µg phosphorous per mg ZSM-5, followed by decoking in the TGA. A Hoffmann analysis was then performed on the samples to determine the number of acid sites still available. Chemical desorption of the poisoned sample gave a weight loss of 4.92% compared to 5.23% for fresh catalyst, changing the active Si/Al_2 ratio from 35.9 to 38.3. This gives a 6.3% reduction in the number of active sites on the catalyst, agreeing well with the 7.2% decrease in activity of hexane seen in the poisoned sample before decoking. Results suggest that the 7.2% decrease in activity was caused by a combination of both phosphorous-poisoned active

sites and coke buildup. When the coke was removed, the remaining 6.3% reduction in active sites was attributed to phosphorous poisoning. This shows that while both coke formation and phosphorous poisoning are responsible for activity reduction, the majority of deactivation is caused by poisoning of the active sites with phosphorous. In addition, there is only a 15% difference between the moles of phosphorus deposited on the catalyst and the moles of deactivated sites. This suggests that the ratio of phosphorus to active sites is 1:1. The difference may be attributed to the minor deactivation of sites by coking.

6.2.3 NMR Analysis

Samples of fresh and poisoned ZSM-5 were sent to the University of Southern Mississippi where NMR analysis was conducted with ^{27}Al, ^{31}P, and ^{29}Si probes. The use of NMR allows examination of the catalyst atoms environment. Figure 6.12 shows the ^{27}Al NMR spectra for both a fresh and poisoned ZSM-5 23 sample. The NMR reference compound was $Al(NO_3)_3$, set to 0 ppm. The poisoned sample has been loaded with phosphorous to the point that hexane conversion begins to increase due to coke formation. An examination of the chemical shifts shows there is very little difference between the two samples. Integrating under the two peaks shows that the tetrahedral aluminum is 73.4% of the area in fresh catalyst and 76.0% in the poisoned. This gives a value of 4/3 for total Al over framework Al. This suggests that the loss in acidity is not due to aluminum being pulled out of the catalyst framework, as it would lead to different aluminum species not seen in the analysis. The SiO_2/Al_2O_3 ratio based on NMR analysis can then be calculated using the following equation.

$$\text{Framework } SiO_2/Al_2O_3 = \text{Bulk Ratio} \cdot [\text{Total Al}/\text{Framework Al}]$$

This leads to a final value of 30.7. This value is between the ratios obtained by Bulk elemental analysis and the Hoffmann reaction. Possible reasons for the discrepancy may be the low resolution of the NMR used, since it was unable to resolve the pentacoordinate Al peak from tetrahedral Al. The spectra of fresh and poisoned catalyst using a ^{31}P probe are shown in Figure 6.13. As expected, the poisoned sample shows a large composite phosphorous peak. This is indicative of several different phosphorous bonding arrangements. As shown on the plot, possible bond types include three or two non-hydrogen/oxygen bonds (R_3P and R_2PH), phosphorous with double ester bonds ($[RO]_2PHO$), and the initial reactant, triethyl phosphate ($[RO]_3PO$). Figure 6.14 shows the fresh and poisoned NMR spectra for ^{29}Si, where no apparent difference can be seen. This suggests that dealumination of the framework is not responsible for the reduction in acidity.

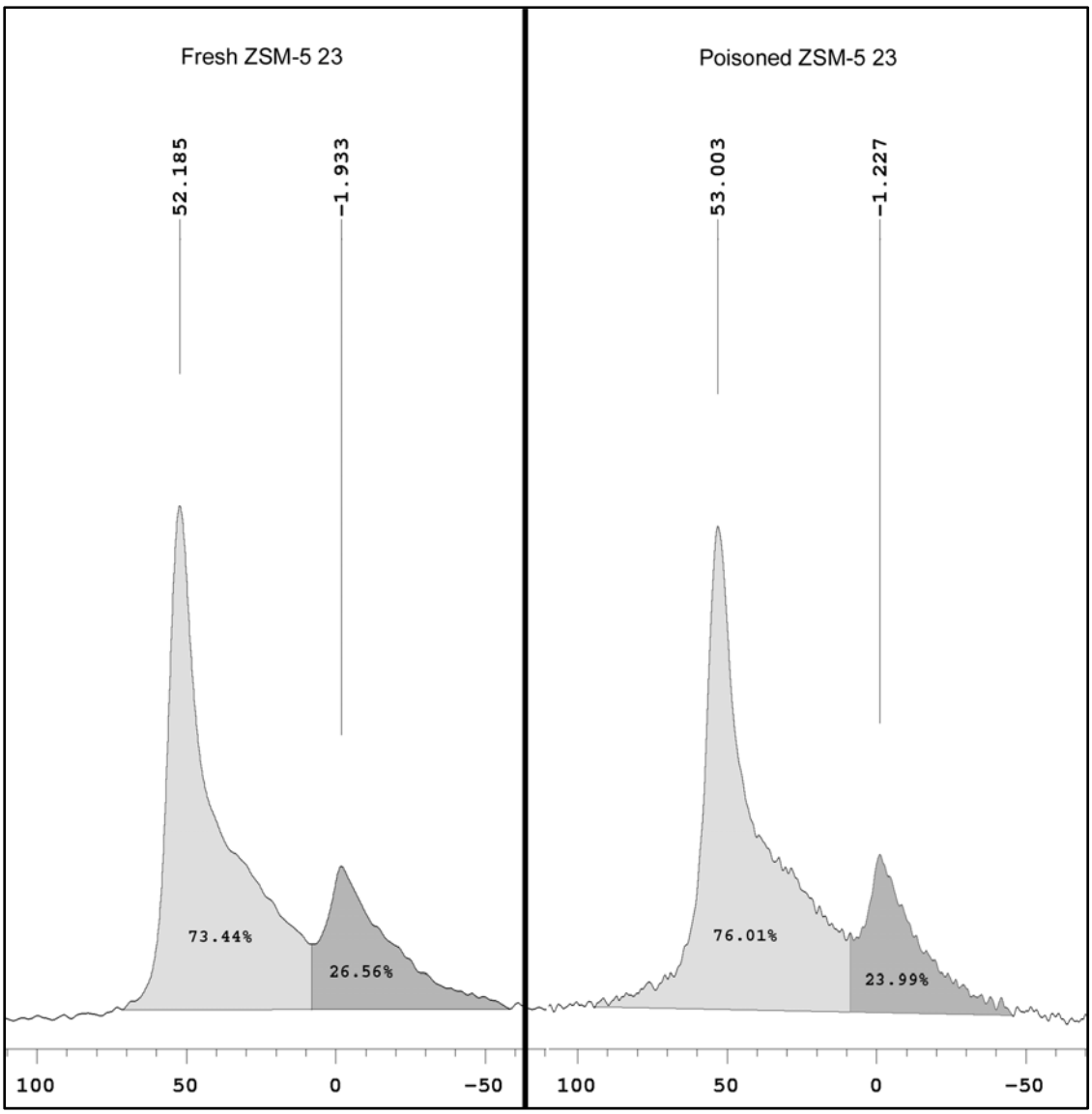

Figure 6.12

^{27}Al NMR Spectra of Fresh and Poisoned ZSM-5 23

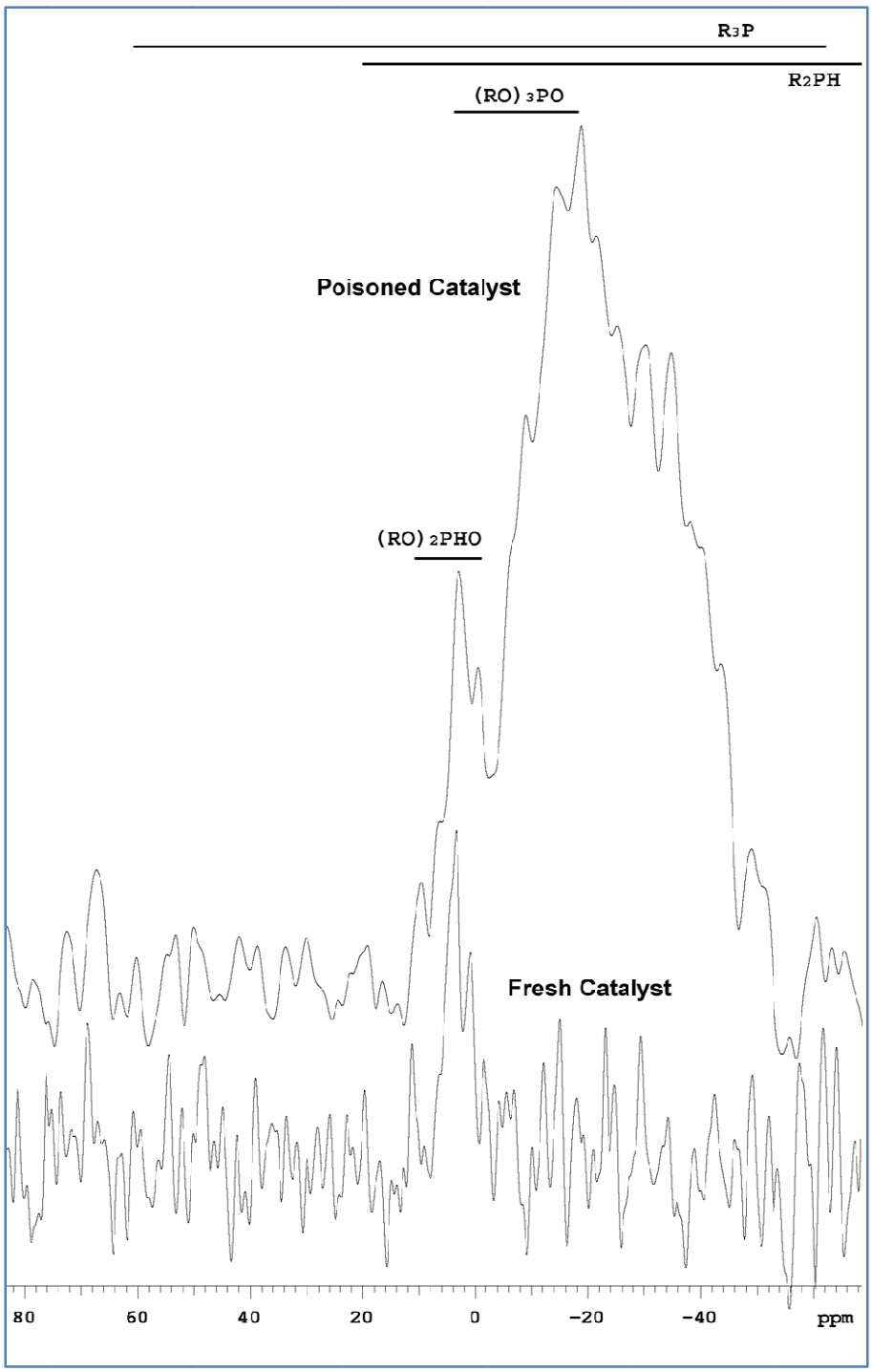

Figure 6.13

^{31}P NMR Spectra of Fresh and Poisoned ZSM-5 23

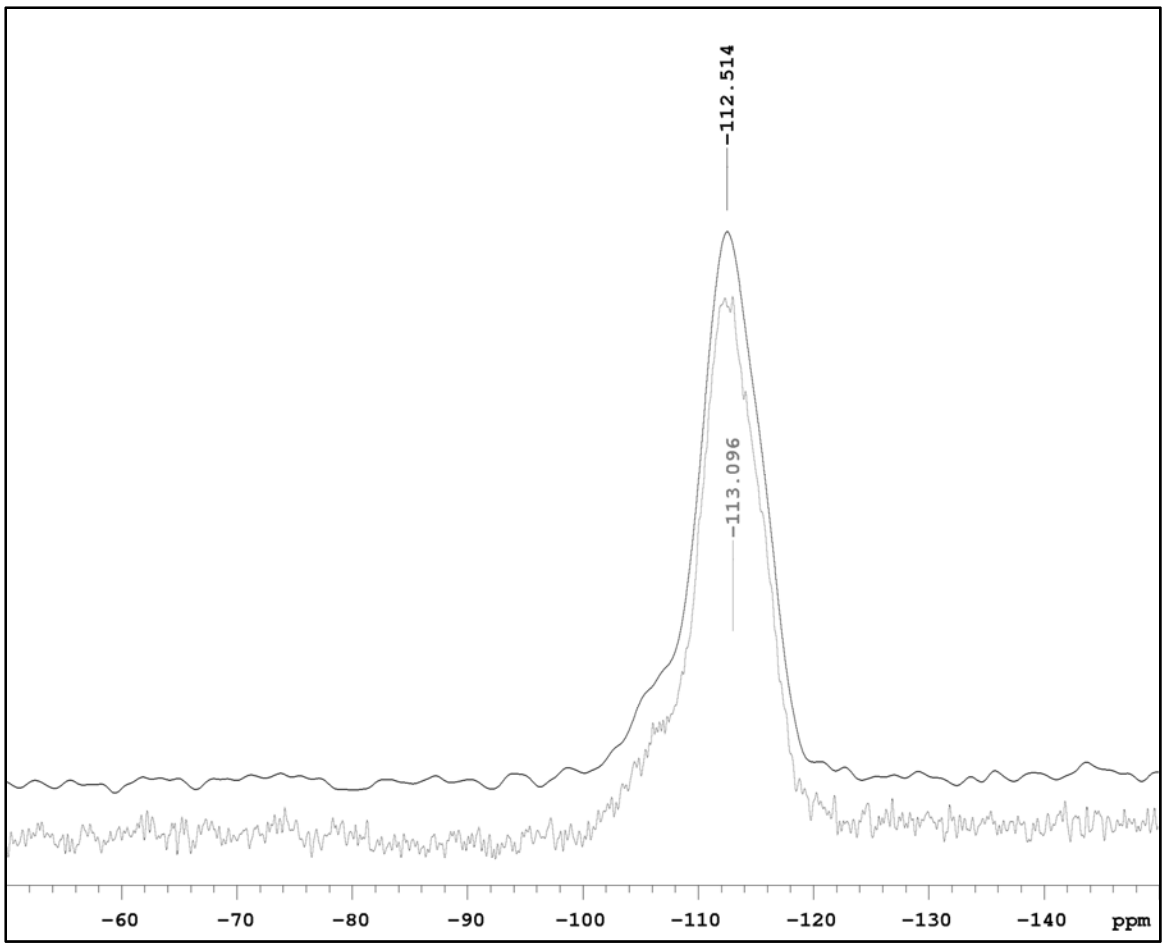

Figure 6.14

^{29}Si NMR Spectra of Fresh and Poisoned ZSM-5 23

6.3 Summary

Although some work has been done on cracking of lipids for fuel production there is a lack of literature regarding how different heteroatoms may affect catalyst performance. Due to phosphorous contained in lipids extracted from microorganisms, it is pertinent to establish what effects the cracking of such compounds will have on the catalyst and overall process in general. The heterogeneous catalyst chosen for this project is ZSM-5.

Triethyl phosphate was chosen as a phospholipid stimulant, able to be catalytically cracked in the vapor phase. Hexane was used as a probe reaction. Poisoning of ZSM-5 with phosphorous was shown to have a negative effect on the conversion of hexane, with deactivation following a liner trend with respect to phosphorous loading. Increases in phosphorous levels corresponded to increased production of olefins and decreases of paraffins.

The ability of the catalyst to be regenerated was tested by thermal regeneration in air at 600º C. It showed that while coke formation was able to be removed, it had no effect on sites poisoned by phosphorous. This lends evidence to the theory that phosphorous is an irreversible poison for the active sites of ZSM-5. The abundance of strong acid sites in both fresh and poisoned catalyst were studied, showing a 6.3% decrease in active sites after poisoning to 1.38 µg phosphorous per mg ZSM-5. This fit well with the 7.2% decrease in activity of hexane seen in the poisoned sample before decoking. NMR analysis conducted with ^{27}Al, and ^{29}Si probes showed no major differences in composition, suggesting that activity reduction was not due to

dealumination of the catalyst framework. Spectra collected for ^{31}P NMR of poisoned catalyst shows a large composite peak of several phosphorous species, although the resolution is too low to definitively identify and compounds.

In conclusion, the poisoning of ZSM-5 with phosphorous compounds has a strong negative effect on both cracking activity and product distribution. Although future methods may be devised to regenerate poisoned catalysts, current procedures point toward the need to remove phosphorous from catalytic cracker feedstock before reaction.

CHAPTER VII

EXTRACTION OF LIPID FEEDSTOCK FROM SEWAGE SLUDGE

One overlooked source for renewable oils is the harvesting of bacteria from municipal wastewater treatment facilities (MWWTF). MWWTF facilities in the USA produce 6.2×10^6 t (dry basis) of sludge annually [19]. This sludge is composed of a variety of organisms which consume organic matter in wastewater. The content of phospholipids in these cells have been estimated at 24% to 25% of dry mass [20,100]. This phosphorous may need to be removed before production of green diesel due to poisoning effects on the catalyst. The most common type of treatment at a MWWTF is the activated sludge process. Activated sludge is the solid or semi-solid produced during biological treatment of industrial and municipal wastewaters. It contains a variety of microorganisms, which utilize the organic and inorganic compounds in the water as a source of energy, carbon, and nutrients. A reactor, settling tank, solid recycle and sludge wasting line comprise the unit operations of the activated sludge process. The waste sludge containing 1% to 2% solids is usually concentrated via gravity thickening or air floatation to approximately 10% solids. In many cases, the concentrated sludge is introduced into an aerobic or anaerobic digester to reduce the level of pathogens and odors (stabilization).

In a wastewater treatment facility, activities associated with sludge treatment represent from 30-80% of electrical power consumed at the plant [19]. Prior to or after stabilization, the sludge may be dewatered and disposed of via incineration, land application, or placement in landfills. However, several environmental health and safety concerns restrict the feasibility of these options.

Research has recently indicated that the lipids of microorganisms contained in sewage sludge are a potential feedstock for lipid based fuels. Literature indicates that sewage sludge contains approximately 20% ether soluble grease and fats [66]. Additionally the cell membrane of microorganisms, a main component of sewage sludge, is composed mostly of phospholipids [101]. Both sources could be converted to renewable fuels. Assuming that cells are 2% phosphorous by dry weight with 50% of phosphorous in the cell membrane, calculations on the estimated mass of phospholipids in cells place them at 24% by dry mass of the cell. This is in agreement with literature values of 25% for *E. Coli* [20].

In this work, lipids were extracted using organic solvents with different polarities or supercritical carbon dioxide. The following text provides results on the lipid and fatty acid methyl ester yields obtained with several extraction strategies.

7.1 Solvent Effects

The amounts of oil, saponifiable material, and the overall yield obtained through different extraction methods can be found in Table 7.1. Different solvents were used during extraction to determine which system gave the best yield. An explanation of the

difference in extraction yield by solvent can be rationalized through use of the Hildebrand Solubility Parameter (δ), which is a measure of the "strength" of the solvent [102]. This can be thought of as the energy required to create a "hole" in the solvent for another molecule to fit in. It can be broken into three parts called the Hansen parameters, which describe forces acting on a molecule. The dispersion force is a measure of London dispersion forces, or non-polar interaction, given by δ_d.

The magnitude of the dipole moment contribution is given by δ_p, and the hydrogen bonding contribution is represented as δ_h. The summed squares of these parameters are equal to the square of the total Hildebrand solubility parameter,

$$\delta^2 = \delta_d^2 + \delta_p^2 + \delta_h^2.$$

Solvents with similar Hildebrand parameters are usually miscible with each other, although the individual Hansen parameters must also be taken into account. The behavior of solutes can also be predicted in the same way [102]. Table 7.2 gives values for the solvents used in extraction of lipids from sludge.

As Table 7.2 shows, all of the solvents have roughly equal contributions from dispersion forces with the exception of SC-CO_2. It is also evident that acetone and methanol are almost equal in strength regarding polarity while *n*-hexane has no polar force at all. The degree of hydrogen bonding is greatest for methanol and is less for acetone. The difference in solvents can thus be summed up as follows. *n*-Hexane contains only dispersion forces and may be considered a standard solvent used for comparison. Acetone and methanol are used to examine the effect of highly polar solvents on extraction and low and high hydrogen bonding strengths. SC-CO_2 has the

smallest dispersion value with a polarity around half that of acetone and methanol and hydrogen bonding near acetone.

Table 7.1 shows that when used in a single solvent extraction, hexane achieves an oil yield of 1.94%. However, the addition of a polar co-solvent results in an increase of extracted oil. Compared to pure hexane, a single extraction using a mixture of hexane, methanol, and acetone increased the oil yield from 1.94% to 21.20%. In addition, the sequential extraction experiment of a hexane, methanol, and acetone mix shows that a significant amount of material is left behind after the first extraction. However, the amount of extractable oil decreases sharply with each subsequent extraction. The increase in yield due to addition of polar co-solvents could be due to high phospholipid levels in the sample. Phospholipids have a polar head and non-polar tail. Secondary sludge is mainly composed of microorganisms whose cell membranes contain phospholipids. Addition of the methanol/acetone mix would expose phospholipids to a solvent with high Hansen values for polarity and hydrogen bonding. It is hypothesized that the solvent mixture helps to disrupt the lipid membrane, which is held together through hydrophobic interactions and is protected by polar head groups. Samples analyzed through thin-layer chromatography indicated the presence of phospholipids but could not give quantitative amounts.

Table 7.1 Extraction and Transesterification Yield of Waste Activated Sludge[a]

Extraction Medium		% Oil Yield[f]		% of Oil Saponifiable[g]		% FAME Yield[h]	
100% Hexane[b]		1.94		19.7		0.38	
100% Methanol[b]		19.39±3.20		14.25±1.66		2.76±0.39	
60% Hexane[c]	Extraction 1	21.20		16.22		3.44	
20% Methanol	Extraction 2	5.37	27.43±0.98	15.57	16.18±3.21	0.84	4.41±0.63
20% Acetone	Extraction 3	0.86		15.92		0.14	
100% Methanol[d]	Extraction 1	19.39	21.96±2.28	14.25	14.21±1.53	2.76	3.07±0.33
100% Hexane	Extraction 2	2.57		12.03		0.31	
In Situ Transesterification[e]		-		-		6.23±0.11	

[a]All extractions carried out at 100°C for 1 hour, solvent to solids ratio 40:1 (wt.)
[b]Sample extracted once
[c]Solvent mixture extracted three times
[d]Sequential extraction using Methanol followed by Hexane
[e]Dried to 95 weight percent solids. Solvent was Methanol with 1% Sulfuric Acid
[f]Gravimetric yield of oil in grams of oil per gram of dry sludge
[g]Percent of extracted oil saponifiable on a mass basis.
[h]Grams of FAME produced per 100 grams of dry sludge
[g,h]Values on left indicate individual extraction yields. Values on the right indicate total yield.

Table 7.2 Solvent Solubility Parameters for Extraction Systems

Solvent	δ_d[a] $MPa^{½}$	δ_p[b] $MPa^{½}$	δ_h[c] $MPa^{½}$	δ[d] $MPa^{½}$
Acetone[e]	15.5	10.4	7.0	20.0
Methanol[e]	15.1	12.3	22.3	29.6
n-Hexane[e]	14.9	0.0	0.0	14.9
HMA[e]	15.1	7.1	10.6	19.8

[a]Magnitude of London Dispersion Forces
[b]Magnitude of Dipole Moment Contribution
[c]Magnitude of Hydrogen Bonding Contribution
[d]Combined Solubility Parameter
[e]Calculated using values from Hansen, C. [103]

If one extracts with a pure polar solvent instead of non-polar the oil yield is much larger. An extraction with pure methanol gives 19.39% yield compared to the 1.94% of pure hexane. This reinforces the idea of polar lipids being extracted more easily with a polar solvent. Following the pure methanol extraction with pure hexane gives a yield for hexane of 2.57%, which is slightly higher than extraction with hexane on a virgin sample. This is intuitive if one considers that hexane extracts mainly non-polar lipids with low values of δ_p and δ_h, while methanol prefers polar lipids with larger values of δ_p and δ_h. Extraction with a polar solvent first may help destroy the cellular membrane and allow a subsequent non-polar extraction access to previously unreachable lipids within the cell.

While polar solvents show a large increase in extractable oil yield, the percent of saponifiable material is lower. Conversion of a pure hexane extract to FAMEs gives 19.70% saponification by weight of the material extracted, while pure methanol only gives 14.25%. Extracting with a mixture of solvents such as the HMA system results in a transesterification yield of 16.22% of material extracted, lower than pure hexane but higher than pure methanol. Repeated extraction with the HMA system shows that the percentage of saponifiable material in extracted oil does not change much with subsequent extractions. The percentage of saponifiable material extracted in the MH system is greater for methanol than for hexane. However, the percent of saponifiable material for hexane on a sample already extracted with methanol is lower than a virgin hexane extraction. This suggests that treatment with a polar solvent will help disrupt cell walls, releasing more extractable material than just non-polar lipids. The trend of decreasing transesterification yield with increasing amounts of polar solvent can also be

rationalized through use of the Hildebrand solubility parameters. Hexane has no Hansen components for polarity or hydrogen bonding, and a low total Hildebrand value. This gives hexane the ability to extract compounds with a similar Hildebrand parameters, including non-polar lipids such as triglycerides. In contrast, methanol is highly polar and has a high degree of hydrogen bonding. This allows for extraction of polar groups such as those found on phospholipids and non-lipid compounds found throughout the bacterial cell. The more polar solvents extract larger amounts of non-lipid material causing a sharp increase in oil yield, which is measured on a weight basis. This is accompanied by a decrease in the percentage of saponifiable material.

7.2 Lipid Extraction

Calculations based on the amount of oil extracted and the percent of saponifiable material in the oil gives an overall yield of saponifiable material extracted from the sludge. This is represented as the mass of biodiesel produced per mass of dry sludge. Although the percent of saponifiable material in a pure hexane extraction was higher than that of a pure methanol extraction, the methanol has a higher overall yield due a much larger amount of oil extracted. This shows that while an extraction with polar solvent will produce oil heavily contaminated with non-saponifiable material, the total amount of saponifiable material is larger. The increase can be contributed to greater extraction of phospholipids with methanol than with hexane. Since phospholipids contain a maximum of two fatty acid groups per molecule the yield of biodiesel is reduced. A comparison of the HMA extraction with MH shows that the first HMA extraction gives a slightly higher

overall yield than the MH. Combining the last two HMA extractions gives the system a significantly larger yield than MH.

The last row in Table 7.1 refers to *In Situ* transesterification of dried sludge. This is a method in which the lipids are converted to FAMEs without extracting them from the sludge. Since the reagents have access to all oil in the sludge instead of just what was extracted the yield should be higher than the other methods. Indeed, the yield of 6.23% is the highest of all methods tried.

An analysis of the fatty acid profile in Figure 7.1 shows differences in lipid composition as a function of various extraction methods. The profile for hexane and methanol shows that hexane extracts a larger ratio of unsaturated fatty acids than methanol for all compounds except the C16s.

Comparison of sludge fatty acid profiles by various extraction methods to a standard soybean sample shows that all sewage sludge samples have a much larger concentration of saturated fatty acids, as seen in Figure 7.2. Although the higher levels of saturated fatty acids may present a problem in cold weather due to gelling, the higher saturated content will produce a better fluidized catalytic cracking feedstock. Feedstocks high in saturated compounds produce less coke and slurry products during the cracking reaction. They are therefore preferred as reactants.

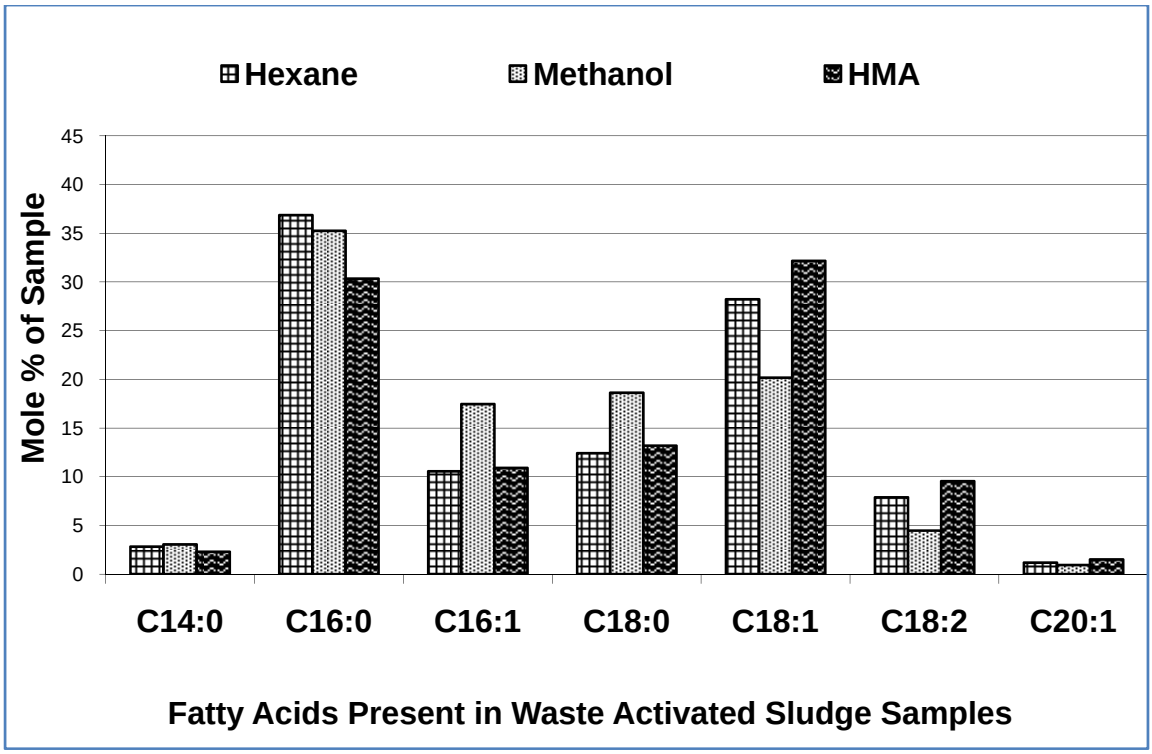

Figure 7.1

Impact of Extraction Medium on Fatty Acid Composition of Oil

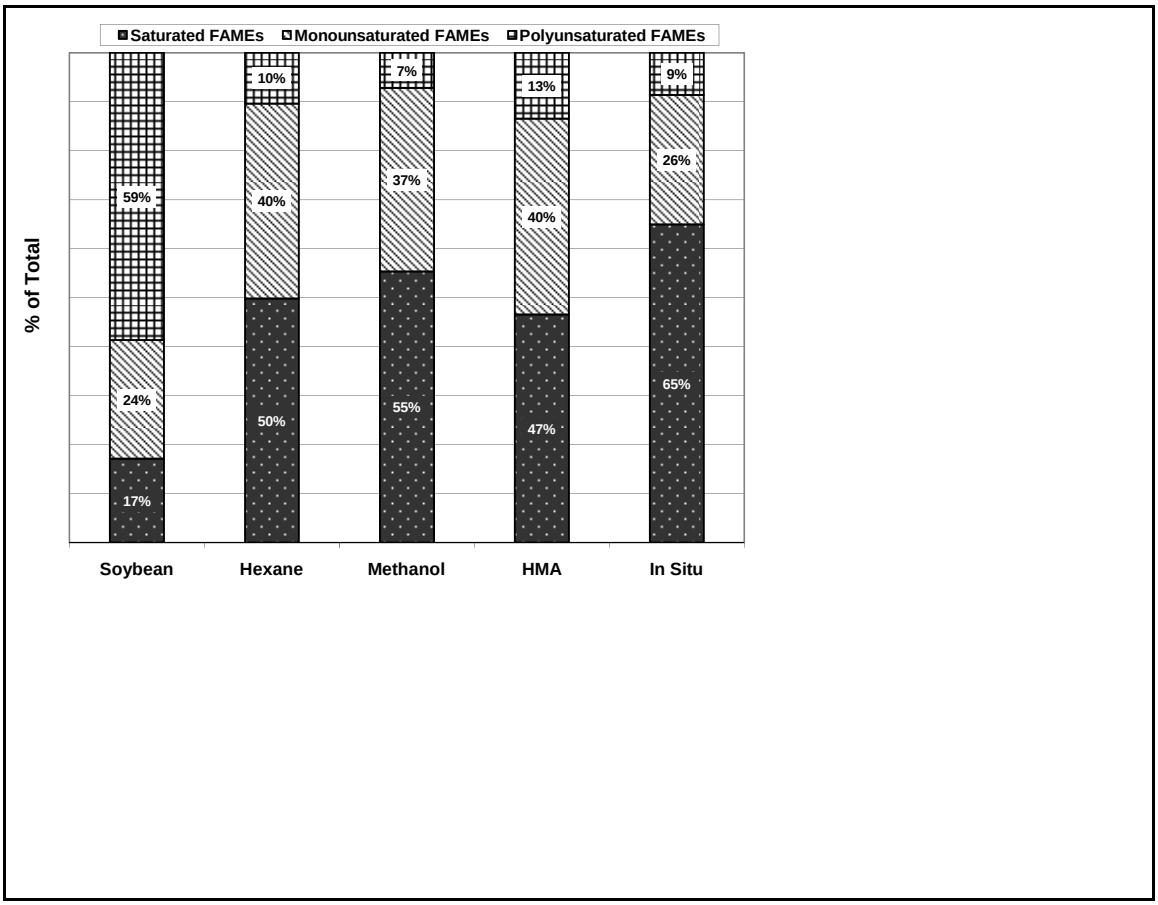

Figure 7.2

Comparison of Saturated vs. Unsaturated Fatty Acids
Present in Waste Activated Sludge Samples

Examination of the various transesterification methods shows that *in situ* conversion of lipids to FAMEs provides the highest overall yield of biodiesel. A breakdown of processing cost is shown in Table 7.3. It is assumed that sludge will be centrifuged to 35% solid content, then dried to 95% solids content via an indirect heat paddle drum. If one then assumes a 7.0% overall yield of FAMEs from dry sewage sludge on a weight basis, the cost per gallon of extracted lipid would be $3.11. Since the lipid is converted to FAMEs, also known as biodiesel, in the *in Situ* extraction process, the product can be used as is for renewable fuel. As transesterification efficiency increases the cost per gallon drops quickly, hitting $2.01 at 15.0% overall yield. An overall yield of 10.0% is required to obtain biodiesel at $2.50 per gallon, allowing it to compete with soybean oil in the marketplace. The extraction of lipids from sewage sludge is possible without a transesterification reaction. This would reduce the overall cost of extraction, although at a tradeoff to total lipid extracted. The use of *in situ* conversion, however, may be beneficial in that phospholipids would be converted to FAMEs. The phosphate head group could then be removed through a water wash process, rendering the feedstock safe for cracking in an industrial catalytic cracker.

Table 7.3 Production Cost Estimate for Sludge Lipids[a]

Centrifuge O&M	$0.43 /gal
Drying O&M	$1.29 /gal
Extraction O&M	$0.34 /gal
Lipid Processing O&M	$0.60 /gal
Labor	$0.10 /gal
Insurance	$0.03 /gal
Tax	$0.02 /gal
Depreciation	$0.12 /gal
Capital P&I Service	$0.18 /gal
Total Cost	$3.11 /gal

[a]Assuming 7.0% overall transesterification yield

7.3 Summary

Municipal wastewater treatment plants in the United States produce over 6.2 million metric tons of dried sewage sludge every year. This microorganism rich sludge is often landfilled or used as fertilizer. Recent restrictions on the use of sewage sludge, however, have resulted in increased disposal problems. Extraction of lipids from sludge yields an untapped source of cheap feedstock for renewable fuel production. Solvents used for extraction in this study include *n*-hexane, methanol, and acetone. Gravimetric yield of oil was low for non-polar solvents but addition of polar solvents gave a considerably increased yield. However, the percent of saponifiable material was less. Extraction of lipids with a mixture of *n*-hexane, methanol, and acetone gave the largest conversion to biodiesel for a solvent system, 4.41% based on total dry weight of sludge. *In Situ* transesterification of dried sludge resulted in a yield of 6.23%. Assuming a 10% dry weight yield of FAMEs the amount of lipid feedstock available for production in the United States is 1.4 million cubic meters per year. Outfitting 50% of municipal wastewater plants for lipid extraction could result in enough production to replace 0.5%

of the national petroleum diesel demand (0.7 million cubic meters). A breakdown of processing cost, assuming 7.0% overall yield of FAMEs from dry sewage sludge on a weight basis places the cost per gallon of extracted lipids at $3.11.

CHAPTER VIII

ENGINEERING SIGNIFICANCE AND FUTURE RESEARCH

This study shows that catalytically cracking phosphorous-containing compounds over ZSM-5 does have a negative impact on lipid cracking and catalyst stability. Although this was suggested by previous research available in literature there were no reports of catalyst poisoning in the gas phase or the effect of phosphorous on the product distribution from lipid cracking. Data obtained on catalyst deactivation caused by phosphorous poisoning is pertinent to the modeling of future industrial processes which produce renewable fuel from lipid feedstocks through catalytic cracking.

The poisoning of active sites by phosphorous precludes the use of raw extracted oil for catalytic cracking feedstock. Common impurities in FCC feedstocks include nitrogen, sulfur, nickel, vanadium, and sodium [25]. These compounds are already heavily monitored, with incoming feed being subjected to a variety of tests. Cracking of oil containing trace amount of phosphorous would cause the catalyst to produce more olefins and coke, similar to poisoning by other metals. While coke may be burned off, it was shown that deactivation of the catalyst by phosphorous is non-reversible. Since the economics of a catalytic cracker depend on the regeneration of equilibrium catalyst, permanent poisoning of active sites would quickly render operation with phosphorous

containing feed unsustainable. If it is desired to use phosphorous-containing oil as a feedstock it must first undergo treatment to remove the phosphorous species. This would add an additional step to the production process, consequently increasing the effective cost of fuel per gallon. Depending on the feedstock profit margin, catalytic cracker operators may elect to not purchase oils high in phosphorous if treatment costs are too high. Possible treatment options include degumming of the oil or other chemical methods to remove the phosphorus.

Data obtained from the cracking of lipid compounds in the liquid phase using a homogeneous superacid catalyst could be used to predict initial cracking mechanisms. The reaction order obtained from data regression shows a complex system with many possible side reactions.

Extraction of lipids from wastewater treatment plant sludge was shown to be a novel source of lipid feedstock. This could serve as a source of plentiful, low-cost, lipids. The largest yield of lipids was realized through use of *In Situ* transesterification of the microbial lipids. Since *In Situ* requires that the entire cell mass be exposed to reaction conditions, a production plant must have equipment large enough to handle the required amount of dried material. Projected costs for an in situ transesterification and lipid extraction process would be $3.11 per gallon if one assumes a 7% yield of total lipid per dry mass of sludge. Although the largest yield of extracted lipids was from an *In Situ* reaction, it adds extra cost to the extraction process since the lipids must undergo a chemical reaction before extraction. Other methods of extraction, such as mixed systems of solvent, may be more economical even though the overall yield of oil is lower.

Production of lipids from sludge using a conventional solvent extraction would cost around $2.50 per gallon of lipid, assuming the same 7% lipid yield. Use of microbial oil in commercial cracking reactions may also lead to a higher value product stream due to the larger amounts of saturated compounds.

Future work would focus on the effect of phosphorous with other widely used commercially used cracking catalysts, including mixed FCC catalysts. Knowledge of how phosphorous changes the process output will allow for increased understanding and control of a system. Research should also be performed on the possibility of regenerating catalyst which has been poisoned by phosphorous. If such a mechanism could be found it would greatly lessen the impact that phosphorous has on cracking performance. This would allow for use of lower quality feedstocks without the expense of removing the phosphorous. Processes which remove the phosphate group from lipids would also be useful as a pretreatment step in commercial cracking operations.

CHAPTER IX

CONCLUSIONS

9.1 Cracking of Lipids via Liquid Superacid

It was shown that lipids can be catalytically cracked by superacids to form organic compounds in the gasoline and diesel range. While cracking of palmitic acid proved to be unobtainable at reaction conditions used, methyl palmitate cracked readily with the addition of triflic acid. This was explained through use of Spartan, a molecular modeling software package. Triflic acid forms an organic acid dimer with palmitic acid, leading to a minimum energy configuration which is resistant to further reaction.

The cracking activity was shown to be linearly dependent on a system's Hammett acidity. This allowed for calculation of kinetic parameters at other levels of acidity. The overall reaction order for cracking of methyl palmitate was found to be three. Linear dependence of cracking kinetics on the acidity of triflic acid, a Brönsted acid, suggests that a similar trend would be seen if comparing different strengths of solid zeolite catalysts. Strong acid sites in ZSM-5, used in this study, are of the Brönsted acid type.

Products from the cracking of methyl palmitate cover a wide range of compounds, including: ethers, ring structures, hydrocarbons, carboxylic acids, and esters. The majority of products formed were ester isomers, with shorter chain lengths than the

starting compound. This suggests that a solid acid catalyst may be needed to decarboxylate the products.

9.2 Catalyst Poisoning by Phosphorous

This study has shown that phosphorous has a negative effect on the cracking performance of ZSM-5. Addition of phosphorous in the gas phase to a catalyst bed will cause deactivation of the active sites due to a combination of phosphorous bonding and coke formation. This will reduce the amount of green diesel able to be produced from feedstocks. Several specific conclusions can be drawn about this data, and are as follows:

- Poisoning of ZSM-5 with phosphorous causes catalyst deactivation and a corresponding drop in conversion. Continued phosphorous loading results in autocatalytic coke formation on the catalyst surface.
- Decrease in conversion of hexane is linear with phosphorous loading for low amounts of phosphorous. This suggests dispersal of phosphorous throughout the catalyst pores.
- Initial poisoning of ZSM-5 with phosphorous gives a increase in olefins and corresponding decrease in paraffins. An increase in C_{1-2} hydrocarbons is seen as phosphorous loading increases to the point of heavy coke formation.
- Thermal regeneration of poisoned catalyst was able to remove accumulated coke formation, but did not restore activity lost due to phosphorous poisoning. This suggests permanent poisoning of the catalyst by phosphorous.
- For a sample of poisoned catalyst with a loading of 1.38 µg phosphorous per mg ZSM-5 the reduction in hexane cracking activity was 7.2%. After decoking, the

same sample showed a 6.3% reduction of strong acid sites through application of the Hoffmann reaction. This shows that a majority of deactivation is caused by phosphorous poisoning as opposed to coke formation.

- Examination of ZSM-5 catalyst by ^{27}Al and ^{29}Si NMR show no major differences between fresh and poisoned samples. The poisoned sample has a large composite peak in the ^{31}P NMR spectra. The resolution is not fine enough to make out individual phosphorous bonding arrangements, but could be a mixture of carbon and ester bonds.

9.3 Extraction of Lipid Feedstock from Wastewater Sludge

Lipids were successfully extracted from microorganisms present in municipal wastewater sludge. This lipid source could provide a significant amount of feedstock for renewable fuel production. It was found that *In Situ* conversion of microbial lipids to fatty acid methyl esters allowed for the highest yield of extractable feedstock. Other methods such as extraction with a cosolvent mixture generated lower yields, but may be more economical depending on the end use of lipids extracted. This is due to the chemical reaction performed during an *In Situ* extraction.

Oil extracted from wastewater plant microorganisms is higher is saturated fatty acids than other commercially available plant oils. In some cases the saturated fatty acid content is more than three times as high as soybean oil, an industrially common feedstock. This could present problems for transportation in cold weather, but the impact depends on end use. For example, most fluidized catalytic cracking feedstocks are solid

or slurries at ambient temperature. Fully saturated feedstocks could also produce a higher quality fuel after catalytic cracking due to the low number of double bonds. Compounds with a high degree of unsaturation, such as olefins, produce larger amounts of coke and slurry during FCC reactions [25]. Any residual phosphorous in the system, however, must be removed prior to cracking. Rapid poisoning of the catalyst will otherwise occur, drastically increasing the use of makeup catalyst to replace destroyed equilibrium catalyst.

Cost estimates for production of lipids from sewage sludge show that the end product is competitive with mainstream lipid feedstocks such as soybean oil. It is therefore a viable alternative to expensive food-grade oil currently used in fuel production.

9.4 Summary

This project showed the feasibility of catalytically cracking lipids to produce green diesel. Cracking in the liquid phase with triflic acid as a catalyst showed linear dependence on acidity of the system, with an overall reaction order of three. Although liquid superacid was able to crack lipid compounds a solid acid catalyst was needed to induce decarboxylation of the products.

Cracking of the products via solid acid catalysis will result in product fractions in the gasoline and diesel range, but is highly sensitive to phosphorous levels of the feedstock. Poisoning by phosphorous was shown to be effective at reducing overall activity of a catalyst, through formation of coke and active site deactivation with

phosphorous. While coke may be regenerated thermally the phosphorous poisoning appears to be permanent. NMR analysis of fresh and poisoned catalyst show little difference in the spectra for aluminum and silica catalyst framework. This suggests that the poisoning effects are not caused by dealumination of the catalyst.

Lipids extracted from microorganisms in municipal wastewater treatment plants could be a viable alternative to currently used lipid feedstocks. Wastewater extracted lipids are currently more economical than common lipids such as soybean oil. While the lipid profile contains several times more saturated fatty acids than phyto-oil, the lower degree of unsaturation may be beneficial in commercial FCC reactions for fuel production.

REFERENCES

1. Skov, A. M. World energy beyond 2050. *JPT, Journal of Petroleum Technology* **55**, 34-37 (2003).

2. DOE. Hydrogen, Fuel Cells & Infrastructure Technologies Program: Multi-Year Research, Development and Demonstration Plan. DOE. 2005.

3. AP. Oil prices fall from record highs. MSNBC . 2005.

4. DOE. U.S. Distillate Fuel Oil Product Supplied (Thousand Barrels). doe.gov . 9-28-2007.

5. DOE. U.S. Finished Motor Gasoline Product Supplied (Thousand Barrels). doe.gov . 9-28-2007.

6. Pinto, A. C. *et al.* Biodiesel: An overview. *Journal of the Brazilian Chemical Society* **16**, 1313-1330 (2005).

7. Mathis, D. A. *Hydrogen Technology for Energy*. Noyes Data Institute, Park Ridge, NJ (1976).

8. Elam, C. C. *et al.* Realizing the hydrogen future: The International Energy Agency's efforts to advance hydrogen energy technologies. *International Journal of Hydrogen Energy* **28**, 601-607 (2003).

9. Nath, K. & Das, D. Improvement of fermentative hydrogen production: various approaches. *Applied Microbiology and Biotechnology* **65**, 520-529 (2004).

10. DOE. Biomass Energy Consumption by Energy Source and Energy Use Sector, 2001-2005. doe.gov . 7-1-2007.

11. Tickell, J. & et al *From the Fryer to the Fuel Tank: The Complete Guide to Using Vegetable Oil as an Alternative Fuel*. Tickell Energy Consultants, (2000).

12. EMA. Use of Raw Vegetable Oil or Animal Fats in Diesel Engines. 3-1-2006.

13. ASTM. D6751-07b Standard Specification for Biodiesel Fuel Blend Stock (B100) for Middle Distillate Fuels. 2007.

14. National Biodiesel Board. National Biodiesel Board Guidance; Use of Biodiesel Blends above 20% Biodiesel. 11-30-2005.

15. EPA. A Comprehensive Analysis of Biodiesel Impacts on Exhaust Emissions. EPA420-P-02-001. 10-1-2002.

16. EPA. A Comprehensive Analysis of Biodiesel Impacts on Exhaust Emissions. EPA420-P-02-001. 10-1-2002.

17. The American Soybean Association. Soy Stats 2005. http://soystats.com/2005/Default-frames.htm . 2005.

18. DOE NREL. A Look Back at the U.S. Department of Energy's Aquatic Species Program: Biodiesel from Algae. NREL/TP-580-24190. 1998. DOE.

19. Water Environment Federation *Activated Sludge MOP OM-9 2nd Edition*. Water Environment Federation, (2002).

20. Nelson, D. & M.Cox *Principles of Biochemistry*. W.H. Freeman and Company, (2005).

21. Stephen Dufreche *et al.* Extraction of Lipids from Municipal Wastewater Plant Microorganisms for Production of Biodiesel. JAOCS . 1-4-2007.

22. Idem, R. O., Katikaneni, S. P. R. & Bakhshi, N. N. Thermal cracking of canola oil: Reaction products in the presence and absence of steam. *Energy & Fuels* **10**, 1150-1162 (1996).

23. Billaud, F., Tran Minh, A. K., Lozano, P. & Pioch, D. Catalytic cracking of octanoic acid. *Journal of Analytical and Applied Pyrolysis* **58-59**, 605-616 (2001).

24. Wilson, N. G. & Williams, P. T. Investigation into the potential of a novel superacid catalyst for the catalytic upgrading of pyrolytic bio-oil. *International Journal of Energy Research* **27**, 131-143 (2003).

25. Sadeghbeigi, R. *Fluid Catayltic Cracking Handbook*. Gulf Publishing Company, (2000).

26. National Biodiesel Board. National Biodiesel Board Guidance; Use of Biodiesel Blends above 20% Biodiesel. 11-30-2005.

27. Adjaye, J. D. & Bakhshi, N. N. Catalytic conversion of a biomass-derived oil to fuels and chemicals I: model compound studies and reaction pathways. *Biomass and Bioenergy* **8**, 131-149 (1995).

28. Katikaneni, S. P. R., Adjaye, J. D., Idem, R. O. & Bakhshi, N. N. Catalytic conversion of canola oil over potassium-impregnated HZSM-5 catalysts: C_2-C_4 olefin production and model reaction studies. *Industrial & Engineering Chemistry Research* **35**, 3332-3346 (1996).

29. Adjaye, J. D. & Bakhshi, N. N. Production of hydrocarbons by catalytic upgrading of a fast pyrolysis bio-oil. Part II: comparative catalyst performance and reaction pathways. *Fuel Processing Technology* **45**, 185-202 (1995).

30. Adjaye, J. D. & Bakhshi, N. N. Production of hydrocarbons by catalytic upgrading of a fast pyrolysis bio-oil. Part I: conversion over various catalysts. *Fuel Processing Technology* **45**, 161-183 (1995).

31. Adjaye, J. D., Katikaneni, S. P. R. & Bakhshi, N. N. Catalytic conversion of a biofuel to hydrocarbons: Effect of mixtures of HZSM-5 and silica-alumina catalysts on product distribution. *Fuel Processing Technology* **48**, 115-143 (1996).

32. Pindoria, R. V., Megaritis, A., Herod, A. A. & Kandiyoti, R. Two-stage fixed-bed reactor for direct hydrotreatment of volatiles from the hydropyrolysis of biomass: Effect of catalyst temperature, pressure and catalyst ageing time on product characteristics. *Fuel* **77**, 1715-1726 (1998).

33. Yadav, G. D. & Nair, J. J. Sulfated zirconia and its modified versions as promising catalysts for industrial processes. *Microporous and Mesoporous Materials* **33**, 1-48 (1999).

34. Weisz, P. B. e. a. Catalytic Production of High-Grade Fuel (Gasoline) from Biomass Compounds by Shape-Selective Catalysis. *Science* **206**, 57-58 (1979).

35. Katikaneni, S. P. R., Adjaye, J. D. & Bakhshi, N. N. Studies on the catalytic conversion of canola oil to hydrocarbons: influence of hybrid catalysts and steam. *Energy & Fuels* **9**, 599-609 (1995).

36. Milne, T. A., Evans, R. J. & Nagle, N. Catalytic conversion of microalgae and vegetable oils to premium gasoline, with shape-selective zeolites. *Biomass* **21**, 219-232 (1990).

37. Prasad, Y. S., Bakhshi, N. N., Mathews, J. F. & Eager, R. L. Catalytic Conversion of Canola Oil to Fuels and Chemical Feedstocks. Part I. Effect of Process Conditions on the Performance of HZSM-5 Catalyst. *Canadian Journal of Chemical Engineering* **64**, 278-284 (1986).

38. Idem, R. O., Katikaneni, S. P. R. & Bakhshi, N. N. Catalytic conversion of canola oil to fuels and chemicals: Roles of catalyst acidity, basicity and shape selectivity on product distribution. *Fuel Processing Technology* **51**, 101-125 (1997).

39. Katikaneni, S. P. R., Adjaye, J. D. & Bakhshi, N. N. Catalytic conversion of canola oil to fuels and chemicals over various cracking catalysts. *Canadian Journal of Chemical Engineering* **73**, 484-497 (1995).

40. Furrer, R. M. & Bakhshi, N. N. Catalytic conversion of tall oil and plant oils to gasoline range hydrocarbons using shape selective catalyst HZSM-5. Energy from Biomass and Wastes XIII, Feb 13-17 1989. 897-914. 1990. New Orleans, LA, USA, Publ by Inst of Gas Technology, Chicago, IL, USA. Symposium Papers - Energy from Biomass and Wastes.

41. Ooi, Y. S., Zakaria, R., Mohamed, A. R. & Bhatia, S. Catalytic conversion of palm oil-based fatty acid mixture to liquid fuel. *Biomass and Bioenergy* **27**, 477-484 (2004).

42. Twaiq, F. A., Zabidi, N. A. M. & Bhatia, S. Catalytic conversion of palm oil to hydrocarbons: Performance of various zeolite catalysts. *Industrial and Engineering Chemistry Research* **38**, 3230-3237 (1999).

43. Dupain, X. e. a. Cracking of a rapeseed vegetable oil under realistic FCC conditions. *Applied Catalysis B: Environmental* **72**, 44-61 (2007).

44. Ren-qing, e. a. The Activity and Theoretical Study of Triethyl Phosphate Modified HZSM-5 Zeolite. *Journal of Molecular Catalysis (China)* **19**, 55-60 (2005).

45. Cabral de Menezes, S. M., Lam, Y. L., Damodaran, K. & Pruski, M. Modification of H-ZSM-5 zeolites with phosphorus. 1. Identification of aluminum species by ²⁷Al solid-state NMR and characterization of their catalytic properties. *Microporous and Mesoporous Materials* **95**, 286-295 (2006).

46. Damodaran, K. *et al.* Modification of H-ZSM-5 zeolites with phosphorus. 2. Interaction between phosphorus and aluminum studied by solid-state NMR spectroscopy. *Microporous and Mesoporous Materials* **95**, 296-305 (2006).

47. Chen, C. S. & Schramm, S. E. Type and catalytic activity of surface acid sites of medium and large pore zeolites. Their deactivation with bulky organophosphorous compounds. *Microporous Materials* **7**, 125-132 (1996).

48. Rahman, A., Adnot, A., Lemay, G., Kaliaguine, S. & Jean, G. Chemical modification of H-ZSM-5 by adsorption of rhodium and phosphorus complexes. *Applied Catalysis* **50**, 131-147 (1989).

49. Nelson, D. L. & Cox, M. M. *Principles of Biochemistry*. W. H. Freeman and Company, New York, NY (2005).

50. Rittmann, B. & P.McCarty *Environmental Biotechnology: Principles and Applications*. McGraw-Hill, New York, NY (2001).

51. Hwu, C. S., Donlon, B. & Lettinga, G. Comparative toxicity of long-chain fatty acid to anaerobic sludges from various origins. *WATER SCIENCE AND TECHNOLOGY* **34**, 351-358 (1996).

52. Rinzema, A., Boone, M., van Knippenberg, K. & Lettinga, G. Bactericidal effect of long chain fatty acids in anaerobic digestion. *Water Environment Reseach* **66**, 40-49 (1994).

53. Liu H, F. H. Extraction of extracellular polymeric substances (EPS) of sludges. JOURNAL OF BIOTECHNOLOGY 95(3), 249-256. 2002.

54. Wagner M, L. A. N. R. P. U. L. N. D. H. Microbial community composition and function in wastewater treatment plants. ANTONIE VAN LEEUWENHOEK INTERNATIONAL JOURNAL OF GENERAL AND MOLECULAR MICROBIOLOGY 81(1-4), 665-680. 2002.

55. Eikelboom DH, G. B. Filamentous micro-organisms observed in industrial activated sludge plants. WATER SCIENCE AND TECHNOLOGY 46(1-2), 535-542. 2001.

56. Barttelbort R.A. Characteristics of waters from apartment buildings. *Public Works* 88 (1966).

57. Farrington, J. W. & Quinn, J. G. Petroleum Hydrocarbons and Fatty Acids In Wastewater Effluents. *Journal Water Pollution Control Federation* **45**, 704-712 (1973).

58. Keefer C.E. & Kratz H. Digestion of garbage with sewage sludge. *Sewage Works Journal* 15 (1934).

59. Mahlie W.S. Oil and Grease in Sewage. *Sewage Works Journal* 527 (1940).

60. Quemeneur, M. & Marty, Y. Fatty acids and sterols in domestic wastewaters. *WATER RESEARCH* **28**, 1217-1226 (1994).

61. Dueholm TE, A. K. N. P. Transformation of lipids in activated sludge. WATER SCIENCE AND TECHNOLOGY 43(1), 165-172. 2001.

62. Conrad, A. *et al.* Fatty Acids of Lipid Fractions in Extracellular Polymeric Substances of Activated Sludge Flocs. *Lipids* **38**, 1093-1105 (2003).

63. Fang H.H. & Jia X.S. Extraction of extracellular polymer from anaerobic sludges. *Biotechnology Technology* **10**, 803-808 (1996).

64. Martinez F, F.-T. E. G. J. Oscillations of exopolymeric composition and sludge volume index in nitrifying flocs. APPLIED BIOCHEMISTRY AND BIOTECHNOLOGY 87(3), 177-188. 2000.

65. Fahmy, G. T. & Hao, O. J. Characterization of activated sludge foams from two plants. *Journal of Environmental Engineering* **116**, 991-997 (1990).

66. Loehr, R. & C.Navarra Jr. Grease Removal at A Municipal Treatment Facility. *Journal WPCF* **41**, 142-154 (1959).

67. Tiehm A, N. K. Z. M. N. U. Ultrasonic waste activated sludge disintegration for improving anaerobic stabilization. WATER RESEARCH 35(8), 2003-2009. 2001.

68. Casado, A. G., Alonso Hernandez, E. J., Espinosa, P. & Vilchez, J. L. Determination of total fatty acids (C8 - C22) in sludges by gas chromatography-mass spectrometry. *Journal of Chromatography A* **826**, 49-56 (1998).

69. Lepage, G. & Roy, C. C. Direct transesterification of all classes of lipids in a one-step reaction. *Journal of Lipid Research* **27**, 114-120 (1986).

70. Previato, e. al. Structural Characterization of a Novel Class of Glycophosphosphingolipids from the Protozoan *Leptomonas samueli*. *Journal of Biological Chemistry* **267**, 24279-24285 (1992).

71. Morita, Y. S. *et al.* Compartmentalization of lipid biosynthesis in mycobacteria. *Journal of Biological Chemistry* **280**, 21645-21652 (2005).

72. Bligh E.G. & Dyer W.J. A rapid method of total lipid extraction and purification. *Can. J. Biochem. Physiol.* **37**, 911-917 (1959).

73. Izard, J. & Limberger, R. Rapid screening method for quantitation of bacterial cell lipids from the whole cells. *Journal of Microbiological Methods* **55**, 411-418 (2003).

74. Lambert M.A., M. C. W. Comparison of the effects of acid and base hydrolyses on hydroxy and cyclopropane fatty acids in bacteria. J.Clin.Microbiol. 18, 1370-1377. 1983.

75. Werker, A. G., Becker, J. & Huitema, C. Assessment of activated sludge microbial community analysis in full-scale biological wastewater treatment plants using patterns of fatty acid isopropyl esters (FAPEs). *WATER RESEARCH* **37**, 2162-2172 (2003).

76. Demirbas, A. Supercritical fluid extraction and chemicals from biomass with supercritical fluids. *Energy Conversion and Management* **42**, 279-294 (2001).

77. Molina Grima, E. *et al.* Comparison between extraction of lipids and fatty acids from microalgal biomass. *JAOCS, Journal of the American Oil Chemists' Society* **71**, 955-959 (1994).

78. Enssani, E. Correlation analysis for the extraction of hydrocarbons from wastewater-grown microalgal biomass. 2, 87-92. 1993. Atlanta, GA, USA, Publ by SAE, Warrendale, PA, USA. Proceedings of the Intersociety Energy Conversion Engineering Conference.

79. Anon Martek Polyunsatuated Fatty Acid Process. *Industrial Bioprocessing* **25**, 2 (2003).

80. Ohr L.M. Nutraceuticals & Functional Foods. *Food Technology* **59**, 63-65 (2005).

81. Gimenez Gimenez, A. *et al.* Downstream processing and purification of eicosapentaenoic (20:5n-3) and arachidonic acids (20:4n-6) from the microalga Porphyridium cruentum. *Bioseparation* **7**, 89-99 (1998).

82. Guil-Guerrero, J. L., Belarbi, E. I. H. & Rebolloso-Fuentes, M. M. Eicosapentaenoic and arachidonic acids purification from the red microalga Porphyridium cruentum. *Bioseparation* **9**, 299-306 (2000).

83. Enssani, E. A method for the extraction of liquid hydrocarbons from microalgal biomass. 6, 250-255. 1990. Reno, NV, USA, Publ by IEEE, Piscataway, NJ, USA. Proceedings of the Intersociety Energy Conversion Engineering Conference.

84. Pernet, F. & Tremblay, R. Effect of Ultrasonication and Grinding on the Determination of Lipid Class Content of Microalgae Harvested on Filters. *Lipids* **38**, 1191-1195 (2003).

85. Rahman, A., Burelle, S., Adnot, A., Lemay, G. & Kaliaguine, S. Characterization of catalysts prepared by adsorption of phosphorus and rhodium complexes on H-ZSM-5 zeolites. *Catalysis Today* **6**, 123-132 (1989).

86. Christie, W. *Lipid Analysis*. The Oily Press, (2003).

87. Kornatowski, J. GROWTH OF LARGE CRYSTALS OF ZSM-5 ZEOLITE. *Zeolites* **8**, 77-78 (1988).

88. Argauer, R. e. a. Crystalline Zeolite ZSM-5 and Method of Preparing The Same. (3,702,886). 11-14-1972.

89. Stahl, K., Gustavsson, E., Jacobsen, C. J. H. & Schmidt, I. Calcination of ZSM-5. An In Situ Synchrotron Powder Diffraction Study. EPDIC 8 Proceedings of the Eighth European Powder Diffraction Conference, May 23-26 2002. 443-444, 319-322. 2004. Uppsala, Sweden, Trans Tech Publications Ltd, Zurich-Ueticon, CH-8707, Switzerland. Materials Science Forum.

90. Haw, J. Zeolite acid strength and reaction mechanisms in catalysis. *Phys. Chem. Chem. Phys.* 5431-5441 (2002).

91. Farcasiu, D., Ghenciu, A., Marino, G. & Rose, K. D. Strength of solid acids and acids in solution. Enhancement of acidity of centers on solid surfaces by anion stabilizing solvents and its consequence for catalysis. *Journal of the American Chemical Society* **119**, 11826-11831 (1997).

92. Howells, R. D. & Mc Cown, J. D. Trifluoromethanesulfonic acid and derivatives. *Chem. Rev.* **77**, 69-92 (1977).

93. Farcasiu, D. & Lukinskas, P. The two modes of reaction of hexane catalyzed by trifluoromethanesulfonic acid. *Journal of the Chemical Society. Perkin Transactions 2* 2715-2718 (1999).

94. Olah, G. A. *et al.* Acidity dependence of the trifluoromethanesulfonic acid catalyzed isobutane-isobutylene alkylation modified with trifluoroacetic acid or water. *Applied Catalysis A: General* **146**, 107-117 (1996).

95. Saito S, Ohwada T & Shudo K The Hammett Acidity Function Ho of Trifluoromethanesulfonic Acid-Trifluoroacetic Acid and Related Acid Systems. A Versatile Nonaqueous Acid System. *Chem. Pharm. Bull.* **39**, 2718-2720 (1991).

96. Farcasiu, D. & Lukinskas, P. The kinetics of isomerization of 3-methylpentane catalyzed by trifluoromethanesulfonic acid. *Journal of the Chemical Society. Perkin Transactions 2* 1609-1613 (1999).

97. Baum, R. ConocoPhillips, Tyson To Make Fuel From Fat. Chemical and Engineering News 85(17), 25. 4-23-0007.

98. Chen, W. H. *et al.* Effects of surface modification on coking, deactivation and para-selectivity of H-ZSM-5 zeolites during ethylbenzene disproportionation. *Journal of Molecular Catalysis A: Chemical* **181**, 41-55 (2002).

99. Parrillo, D. J., Adamo, A. T., Kokotailo, G. T. & Gorte, R. J. Amine adsorption in H-ZSM-5. *Applied Catalysis* **67**, 107-118 (1990).

100. Stephen Dufreche *et al.* Extraction of Lipids from Municipal Wastewater Plant Microorganisms for Production of Biodiesel. JAOCS . 1-4-2007.

101. Rittmann, B. & McCarty, P. *Environmental Biotechnology: Principles and Applications*. McGraw-Hill, New York, NY (2006).

102. Hansen, C. M. *Hansen Solubility Parameters: A User's Handbook*. CRC Press, Boca Raton (2000).

103. Williams, L., J.Rubin & H.Edwards Calculation of Hansen Solubility Parameter Values for a Range of Pressure and Temperature Conditions, Including the Supercritical Fluid Region. *Industrial & Engineering Chemistry Research* **43**, 4967-4972 (2004).